supervising scientist report **165**

Temporal trends in erosion and hydrology for a post-mining landform at Ranger Mine, Northern Territory

DR Moliere, KG Evans, GR Willgoose & MJ Saynor

Environment Australia
Department of the Environment and Heritage

supervising scientist

DR Moliere — Environmental Research Institute of the Supervising Scientist,
GPO Box 461, Darwin NT 0801, Australia.

KG Evans — Environmental Research Institute of the Supervising Scientist,
GPO Box 461, Darwin NT 0801, Australia.

GR Willgoose — Department of Civil, Surveying & Environmental Engineering, University of Newcastle, Callaghan, NSW 2308, Australia.

MJ Saynor — Environmental Research Institute of the Supervising Scientist,
GPO Box 461, Darwin NT 0801, Australia.

This report should be cited as follows:

Moliere DR, Evans KG, Willgoose GR & Saynor MJ 2002. *Temporal trends in erosion and hydrology for a post-mining landform at Ranger Mine, Northern Territory*. Supervising Scientist Report 165, Supervising Scientist, Darwin NT.

The Supervising Scientist is part of Environment Australia, the environmental program of the Commonwealth Department of Environment and Heritage.

Supervising Scientist
Environment Australia
GPO Box 461, Darwin NT 0801 Australia

ISSN 1325-1554

ISBN 0 642 24371 9

e-mail: publications_ssd@ea.gov.au

Internet: www.ea.gov.au/ssd (www.ea.gov.au/ssd/publications)

Printed in Darwin by Copytime; bound by NTUniprint, Darwin

Contents

Figures

Tables

Executive summary

An important part of rehabilitation planning for mines is the design of a stable landform for waste rock dumps or spoil piles, at the completion of mining, which minimise erosion and environmental impact offsite. To successfully incorporate landform designs in planning, there is a need to be able to predict the surface stability of the final landform using erosion and landform evolution modelling techniques.

In the long term, weathering, soil forming processes, ecosystem development and even climate change may affect the surface characteristics, and hence the stability, of the rehabilitated landform. In this study, changes to the surface characteristics of a landform in time can be quantified in terms of erosion parameters. Since a prediction of the stability of the rehabilitated landform is required over the long term, temporal changes in these erosion parameters are incorporated into landform evolution modelling of a post-mining landform.

The landform evolution model SIBERIA was used to predict the stability of the proposed rehabilitated landform at Ranger Mine, Northern Territory. Previous landform evolution modelling at Ranger used input parameter values derived from data collected from areas of the waste rock dump at the mine and these input parameter values were assumed to remain constant throughout the period that was simulated. In this study, natural rainfall event data were collected from various sites considered to be representative of the surface hydrology and erosion characteristics that would exist at Ranger at various stages after rehabilitation. The sites were located on: a batter slope on the waste rock dump at Ranger; the waste rock dump of the abandoned Scinto 6 mine in the South Alligator River valley; a natural, undisturbed area at Tin Camp Creek, Arnhem Land; and a natural area near Pit 1, Ranger Mine. SIBERIA input parameter values were derived for each study site to determine the rate of temporal changes in parameter values under both concentrated flow and sheet flow conditions.

There is a very clear temporal effect on SIBERIA input parameters that reflect the erosion rate likely to occur on the Ranger landform (m_1 and β_1). The change is rapid and occurs within the first 50 years after mining is completed, at which time the parameter values approach that of an old, natural landform. This study has quantified temporal changes of erosion processes in terms of these input parameter values.

SIBERIA landform evolution simulations of the proposed rehabilitated landform at Ranger were conducted incorporating the rate of temporal change in input parameter values due to ecosystem development. The erosion rate and valley development on the simulated landforms with input parameters that change with time decline relatively quickly in the short term, particularly on the landform with sheet flow conditions where sediment movement stabilises almost completely after 50 y of simulation. The incorporation of these temporal changes in parameter values into the SIBERIA model has provided a best estimate of the stability of the landform at Ranger over a 1000 y simulation period.

Acknowledgments

We wish to thank Mr BL Smith and Mr GS Boggs, Erosion and Hydrology Group, ***eriss***, for assistance with field work and data collection at Scinto 6, and assistance with GIS analysis, respectively.

The Jawoyn Association, traditional owners of the land where the Scinto 6 study site is located; Parks Australia North; Northern Land Council; Energy Resources of Australia Ranger Mine; Dr Greg Hancock, Department of Geography and Environmental Science, University of Newcastle; Mr P Waggitt, Office of the Supervising Scientist; and the Corporate Services staff of ***eriss*** are thanked for their cooperation and assistance.

1 Introduction

1.1 Erosion modelling of post-mining landforms

An important part of rehabilitation planning for mines is the design of a stable landform for waste rock dumps or spoil piles, at the completion of mining, which minimise erosion and environmental impact offsite. To successfully incorporate landform designs in planning there is a need to be able to predict the surface stability of the final landform using erosion and landform evolution modelling techniques (Evans et al 1998). It is considered that landform evolution modelling of the stability of post-mining rehabilitated landform designs was first conducted by Willgoose and Riley (1998). Willgoose and Riley (1998) used the landform evolution model, SIBERIA (Willgoose et al 1989; 1991a,b,c; 1992), to simulate the erosional stability of a proposed 'above-grade' rehabilitated landform at Energy Resources of Australia Ranger Mine, Northern Territory, for a period of 1000 y.

The above-grade landform option for rehabilitation at Ranger (fig 1.1) (after Unger & Milnes 1992) encapsulates tailings in two locations within the minesite with a cap of waste rock material. These tailing repositories are the 'above-grade' tailings dam and Pit 1. It is a requirement of the *Code of Practice* (DHA&E 1982) that uranium mill tailings must be contained in structures with 'structural lives' in excess of 1000 y. Stability modelling of the post-mining landform at Ranger, particularly of the areas where extensive erosion of the waste rock material could lead to the exposure of tailings within a certain time frame, is an important part of the design procedure of the final landform for the mine.

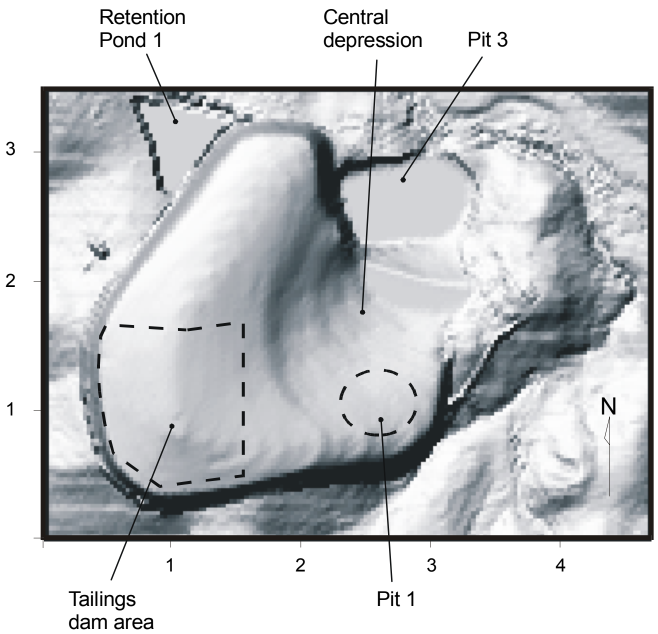

Figure 1.1 3-D representation of the above-grade landform option for rehabilitation at Ranger. Dimensions are in kilometres.

Towards the completion of this study the above-grade rehabilitated landform design became a discarded option by Ranger (Evans 2000). The current plan for rehabilitation of tailings is that they will be stored in Pit 1 and Pit 3 (fig 1.1) below ground level. The final landform design for this option is still being developed.

Many erosion modelling studies, including this one, were undertaken on the above-grade option for rehabilitation at Ranger. The outcomes of these studies, although no longer applicable at Ranger, illustrate the application of modelling technology to assess mine site rehabilitation design for erosion impact. The studies also have relevance to sites where contaminants may need to be stored above ground (Evans 2000).

1.1.1 Previous studies

The erosion modelling studies conducted by the Erosion and Hydrology program at the Environmental Research Institute of the Supervising Scientist (***eriss***) for the overall erosion assessment at Ranger are outlined in figure 1.2. Figure 1.2 also highlights how this study, which focuses on the long-term stability of the landform at Ranger, fits into the overall erosion assessment by ***eriss***. The following is a brief description of previous studies concerned with this aspect — the landform stability in the long term — of the erosion assessment at Ranger.

A prediction of the long-term stability of the final landform was initially determined in Willgoose and Riley (1998) using input parameter values derived from areas of the waste rock dump (WRD) with no vegetation or surface treatment (fig 1.2). The simulations showed that significant erosion will occur on the rehabilitated landform at Ranger in the long term (1000 y) in the central depression area of the above-grade option (fig 1.1).

In later studies the effects of vegetation and surface amelioration on SIBERIA landform evolution simulations were assessed (Evans & Willgoose 1994, 2000; Willgoose 1995; Evans et al 1998; Evans et al 2000). Evans et al (1998) used SIBERIA to predict the stability of the 'above-grade' landform option at Ranger using input parameter values derived from areas of the WRD at Ranger with varying degrees of vegetation and surface treatment (fig 1.2). Evans et al (1998) also analysed the erosion incision into the waste rock material used to cap the areas of tailings containment and discussed possible changes to the landform design as a result of vegetation effects on these areas.

Studies by Hancock et al (2000, 2002) formed part of a collaborative project designed to validate the long-term erosion predictions of the SIBERIA landform evolution model on rehabilitated mine sites. Using parameters derived for a short-term analogue site — an abandoned uranium mine at Scinto 6 (fig 1.2 – Box 5) — Hancock et al (2000) showed that SIBERIA can accurately model gully development on a man-made post-mining landscape over time spans of around 50 y. Hancock et al (2002) also showed that, using parameters derived for a long-term analogue site — a natural, undisturbed site at Tin Camp Creek (fig 1.2 – Box 6) — SIBERIA can accurately model the geomorphology and hydrology of a natural catchment over the long term.

The application of landform evolution modelling for the 'above-grade' option of rehabilitation at Ranger (Willgoose & Riley 1998, Evans et al 1998) has provided a prediction of the stability of the landform design at Ranger after mining has been completed. Landform evolution modelling, using SIBERIA, in these studies was based on input parameter values derived from data collected from areas of the WRD, and these parameter values were assumed to remain constant throughout the period that was simulated. At Ranger in the long term, weathering, soil forming processes, ecosystem development and even climate change may affect the stability of the rehabilitated landform. Therefore there may be a temporal effect of model input parameter values.

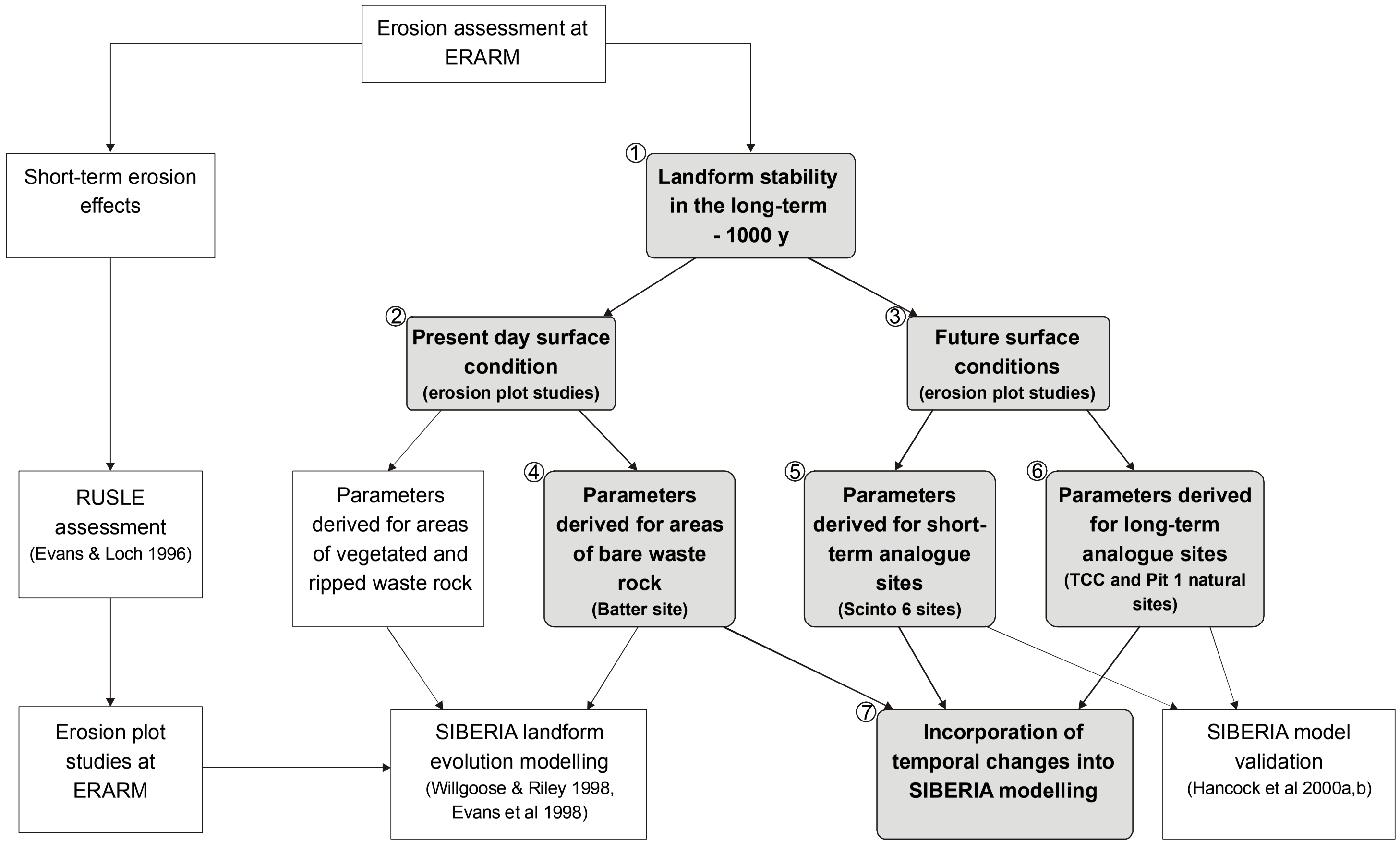

Figure 1.2 Erosion studies conducted by the Erosion and Hydrology program at *eriss* for the erosion assessment at Ranger. The shaded areas (Boxes 1–7) indicate the parts of the work program used in this study.

Elsewhere, studies by Gardner et al (1987) and Jorgensen and Gardner (1987) on reclaimed surface mines in Pennsylvania demonstrated increases in infiltration capacity from less than 0.5 cm hr^{-1} to greater than 5 cm hr^{-1} in just 3 to 4 y. Under natural conditions, changes in infiltration capacity in response to soil genesis or vegetation change may occur over 10^3 to 10^4 y (Birkeland 1984). Ritter (1990) showed that such large changes in infiltration capacity with time on a landform were sufficient to cause changes in the hydrological processes. In turn, discharge characteristics, such as peak and total runoff, could also respond to changes in landform hydrology. The possible changes in erosion rates resulting from these rapid changes in hydrological processes may have important implications for long-term landform evolution models (Ritter 1990).

Loch and Orange (1997) found large improvements in soil properties and soil structure with time on reclaimed mine sites due to revegetation effects. Soil property measurements made on initial surface conditions for the rehabilitated mine site may greatly underestimate the long-term physical productivity of the soil surface used in rehabilitation (Loch & Orange 1997). As a result, erosion rates on a rehabilitated minesite surface in the long term may decline well below those predicted from initial surface conditions (Riley 1992).

The studies of Gardner et al (1987), Jorgensen and Gardner (1987), Ritter (1990) and Loch and Orange (1997) indicate that erosion rates may change with time. The early landform evolution studies at Ranger, such as Willgoose and Riley (1998) and Evans et al (1998), have not considered a change in rate of soil loss with time.

We are not aware of any research that has been conducted on the effect of temporal change in erosion rate, which may occur, on landform evolution modelling of a post-mining landform. This research will attempt to determine whether there is a change in SIBERIA landform evolution model input parameter values with time, and if so, to develop a relationship between SIBERIA model parameter values and time. If erosion and hydrology characteristics of landforms, and hence SIBERIA input parameter values, are effected by temporal change then the long-term erosional stability of the post-mining landform can be reassessed by determining the rate of change of input parameter values and incorporating this rate of change into SIBERIA landform evolution simulations.

The results of this research will further refine the SIBERIA modelling technique. Figure 1.2 graphically demonstrates the original contribution of this study to landform evolution modelling at ***eriss*** and generally.

1.1.2 Study objectives

The primary research objectives of this study were:

- To assess how soil and ecosystem development effect landform evolution model input parameter values, and
- To assess the effect of temporal changes in input parameter values on long-term landform evolution simulations at Ranger.

Rainfall, runoff and sediment loss data were collected from the following sites: a site on a batter slope on the WRD of Ranger; the WRD of the abandoned Scinto 6 mine in the South Alligator River valley; natural undisturbed sites at Tin Camp Creek (TCC), Arnhem Land; and a natural site near Pit 1, Ranger. These data were analysed to achieve the primary objectives. The data collection sites were considered to be representative of the surface hydrology and erosion characteristics that would exist on the WRD at Ranger at various stages after rehabilitation (fig 1.2 – Boxes 2 and 3). That is, the WRD at Ranger parameter values represent the landform at zero years immediately after rehabilitation; the Scinto 6 WRD parameter values represent concentrated flow and sheet flow conditions on the landform 50 y after rehabilitation; and the parameter values for the natural sites at TCC and near Pit 1, Ranger, represent concentrated flow and sheet flow conditions respectively after rehabilitation on the landform in the long term. A description of each of the study sites is given in section 1.3.

The sub-objectives of this study were as follows:

1 Determine a means of predicting missing runoff and sediment data that could be combined with the observed data in order to derive a significant sediment loss-runoff relationship where observed runoff and sediment loss data collected at TCC are insufficient.

2 Determine surface hydrology and soil loss prediction relationships for the sites in this study.

3 Estimate the age of each of the study sites and, in turn, determine the rate of temporal change in parameter values over time under both concentrated flow and sheet flow conditions.

4 Conduct landform evolution simulations, using SIBERIA, of the proposed rehabilitated landform at Ranger to incorporate the rate of temporal change in input parameter values due to ecosystem development.

5 Conduct a sensitivity analysis to determine the reliability of incorporating temporal changes in input parameter values into SIBERIA modelling of the proposed landform at Ranger.

1.2 Study outline

This study advances the knowledge gained by Willgoose and Riley (1998) and Evans et al (1998) and uses measured site data from landforms with hydrology and erosion properties similar to those likely to develop on Ranger at various times after rehabilitation to assess the effect of temporal change on landform evolution model input parameters (fig 1.2).

Section 2 documents the process of SIBERIA input parameter derivation and landform evolution modelling using collected site rainfall, runoff and sediment loss data. This section is based on the detailed descriptions of the process given in Willgoose and Riley (1998) and Evans et al (1998).

In section 3 monitoring data, collected from sites with properties similar to those likely to develop on the proposed above-grade landform at Ranger at various times after rehabilitation under conditions of concentrated flow and sheet flow (fig 1.2 – Boxes 2 and 3), are used to derive (1) hydrology model parameter values using the non-linear software package DISTFW-NLFIT (Willgoose et al 1995), and (2) sediment transport equation parameter values through multiple regression.

In section 4, the DISTFW hydrology model and sediment transport equation parameter values derived in section 3 were used to determine input parameter values for SIBERIA (fig 1.2 – Boxes 4–6). The age of each study site is estimated and the parameter values fitted for each site are compared. A rate of parameter value change is determined and this is incorporated into landform evolution modelling of the proposed rehabilitated landform at Ranger (fig 1.2 – Box 7).

Finally, in section 5, a sensitivity analysis to determine the reliability of incorporating the temporal change in parameter values into SIBERIA was conducted. Using parameter values derived for both present day and future surface conditions, SIBERIA simulations were run over 1000 y for the proposed rehabilitated landform assuming the parameter values to remain constant. The landform evolution modelling results were compared to assess the potential errors on the landform modelling process where temporal changes are incorporated.

1.3 Study sites

Data from the following sites were used in this study (fig 1.3):

1. A batter slope on the WRD at Ranger (WRD_0), which is considered to be zero years after rehabilitation,
2. The WRD at the abandoned Scinto 6 uranium mine which is approximately 50 y old with both channelised flow and sheet flow conditions (WRD_{50C} and WRD_{50S} respectively),
3. Channelised catchments in natural terrain at TCC which are assumed to represent the Ranger surface condition after rehabilitation in the long term (ie > 10^6 years) (Nat_{C1} and Nat_{C2}), and
4. A sheet flow area on the natural surface near Pit 1 at Ranger, which is assumed to represent the surface condition at Ranger after rehabilitation in the very long term (ie >> 10^6 years) (Nat_S).

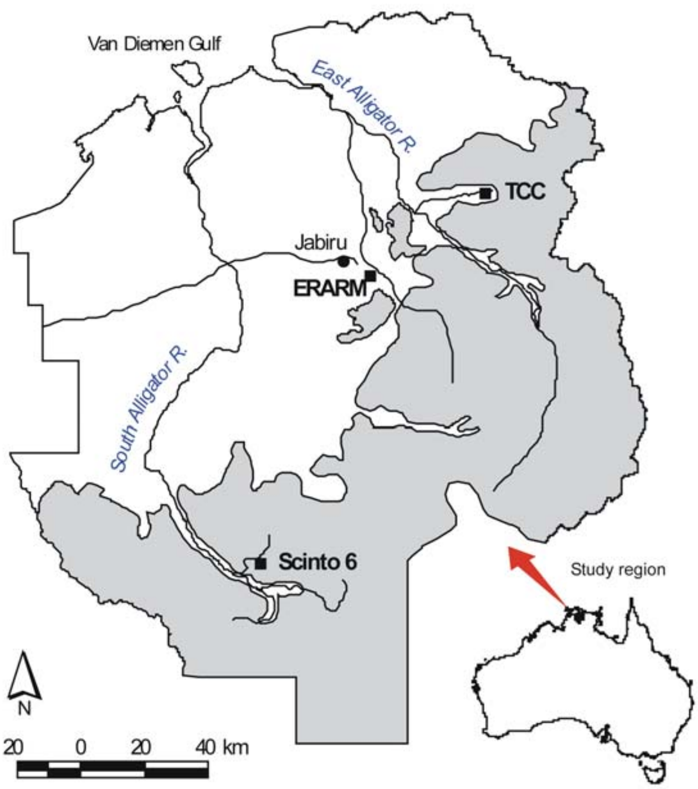

Figure 1.3 Location of the Scinto 6 and TCC field sites and Ranger mine

1.3.1 Batter site (WRD_0)

Ranger Mine is adjacent to the World Heritage Listed Area of Kakadu National Park in the Top End of the Northern Territory. The mine site exploits a stratabound uranium deposit hosted by the lower member of the Early Proterozoic Cahill Formation. The WRD at Ranger consists of rocks from the lower member that comprises carbonates, carbonaceous schists and mica and quartz feldspar schist (Needham 1988). The area receives high-intensity storms and rain depressions between October and April (Wet season) with little rain falling during the remainder of the year (Dry season). The average annual rainfall is 1483 mm (Bureau of Meteorology 1999).

The area on the batter slope of the WRD where the study was conducted (WRD_0) (fig 1.4) rises approximately 12 m above the surrounding land surface and has an average slope of 20.7%. The runoff and erosion plot constructed on the batter slope was 37.7 m long by 15.9 m wide (600 m^2). The site is covered with an armour of coarse material and has negligible vegetation cover. For this study, the surface condition of WRD_0 is assumed to be representative of the proposed final rehabilitated condition immediately after mining is completed.

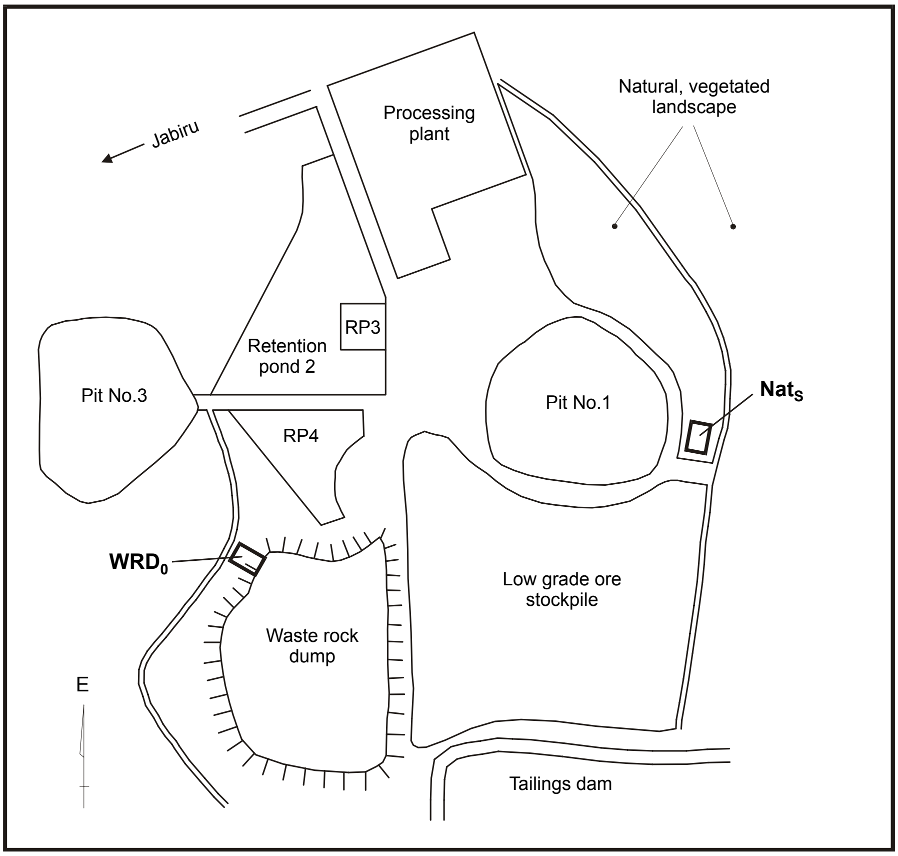

Figure 1.4 Location of the WRD_0 site and the Nat_S site at Ranger (diagram not to scale)

1.3.2 Scinto 6 sites (WRD_{50})

Scinto 6 is an abandoned open cut uranium mine in the South Alligator River Valley within Kakadu National Park (fig 1.3). Mining ceased at Scinto 6 approximately 50 y ago (Waggitt pers comm). The cut was 50 m x 25 m x 20 m deep (DHC 1986) and waste rock was dumped adjacent to the entrance of the cut resulting in a flat topped WRD with angle-of-repose batters and has been undisturbed since mining ceased. The waste rock comprises Precambrian volcanics (Crick et al 1980).

Scinto 6 is approximately 100 km from the town of Jabiru in the north, which has an average annual rainfall of 1483 mm, and approximately 110 km from the town of Katherine in the south, which has an average annual rainfall of 973 mm.

Two areas of the WRD were studied. The first, the gully plot (WRD_{50C}), has an average slope of 0.52 $m.m^{-1}$ (52%). This plot defined a shallow gully on the batter slope that appeared to have formed as water discharged from the low gradient cap area of the WRD to the high gradient batter slope. The surface of WRD_{50C} was armoured with large competent rock fragments. This plot was used to measure gully runoff and sediment loss.

The second area, interrill plot (WRD_{50S}), was on the batter slope and has an average slope of 0.58 $m.m^{-1}$ (58%) in the area studied. The WRD_{50S} surface was armoured with coarse rock fragments. This plot was used to measure interrill runoff and sediment loss.

Both plots had negligible vegetation cover at the beginning of the monitoring season. However, by the end of the monitoring season, both plots had a dense covering of native speargrass (sorghum).

1.3.3 Tin Camp Creek sites (Nat_c)

In terms of weathering and erosion processes, surfaces on the WRD at Ranger are not mature and may not resemble those likely to be present in the long term. Riley (1992) suggested that landforms with geologic and geomorphic properties similar to those likely to develop on Ranger be used as a geomorphic analogue for uranium mine rehabilitation structures. Uren (1992) identified a region within the Tin Camp Creek (TCC) catchment (fig 1.3) as a possible long-term rehabilitation analogue. It was suggested that the TCC catchment could provide information on soil and geomorphic characteristics including 'the probable erosional characteristics of an effectively revegetated rehabilitation structure over the long-term' (Uren 1992).

Two areas within the TCC catchment (Nat_{C1} and Nat_{C2}) (fig 1.5) were studied. Both sites lie within the Myra Falls Inlier, south of Nabarlek. Pockets of exposed Lower Member Cahill Formation material (ie the material that hosts mineralisations at Ranger) were identified in this region, and form strike ridges and dissected hills (Needham 1982 as cited in Uren 1992). Nat_{C1} and Nat_{C2} lie on opposite sides of a ridge, with average slopes of 19% and 22% respectively. The catchment areas of Nat_{C1} and Nat_{C2} are 2032 m^2 and 2947 m^2 respectively. Both sites are in sparse, open woodland and are covered with an armour of small, coarse material and several quartzite outcrops. During the Wet season the surface is covered with speargrass. Both sites are incised and channelised and are assumed to be representative of the characteristics of soils that may develop on weathered waste rock at Ranger under concentrated flow conditions over the long-term (ie > 10^6 years) (Uren 1992).

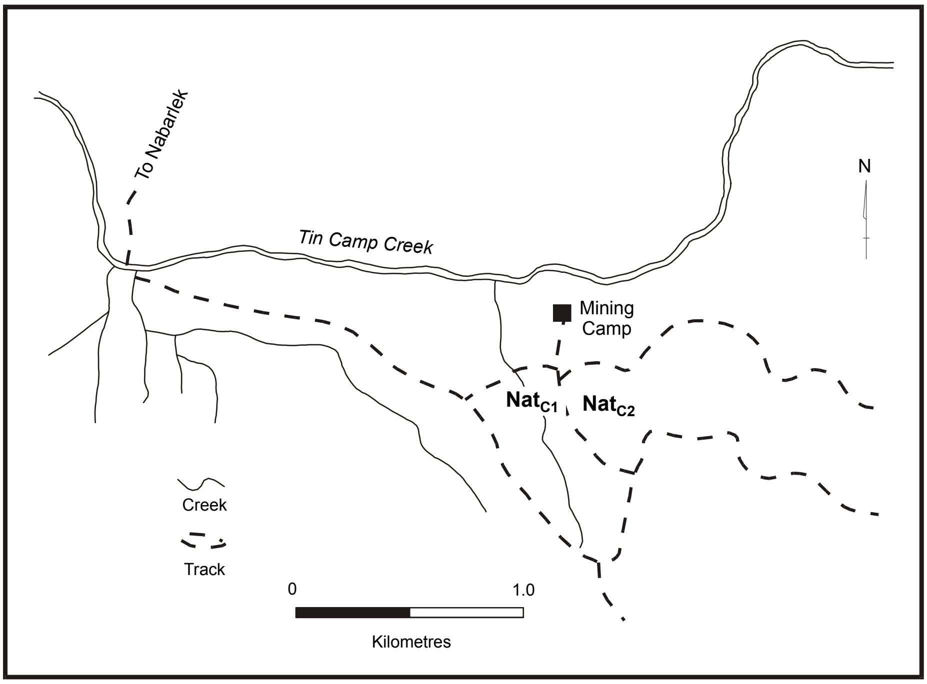

Figure 1.5 Location of Nat$_{C1}$ and Nat$_{C2}$ study sites at TCC

1.3.4 Pit 1 natural site (Nat$_S$)

A natural, undisturbed area of bushland approximately 50 m south of Pit 1, Ranger (Nat$_S$) (fig 1.4) was identified as a possible long-term rehabilitation analogue for sheet flow conditions. Nat$_S$ is located on the Koolpinyah surface, the landform with the highest geomorphological stability in the Alligator Rivers Region (Nanson et al 1990). The Koolpinyah surface was formed during late Tertiary (Pliocene) to early Pleistocene times (Hays 1971 as cited in Nanson et al 1990) and has very low denudation rates (~0.03 mm y^{-1}) (Nanson et al 1990). The runoff and erosion plot constructed on the natural, undisturbed area was 30 m long by 20 m wide (600 m^2), and had an average slope of 2.7%. Nat$_S$ is covered with small trees, low shrubs and, during the Wet season, speargrass. The surface of the site is assumed to be representative of the landscape at Ranger before the commencement of mining operations and may represent the surface of the WRD after revegetation and weathering in the very long term (ie >> 10^6 years) (Bell & Willgoose 1997).

1.3.5 Summary

In summary, each of these sites were assumed to be representative of the surface hydrology and erosion characteristics that would exist on the WRD at Ranger at various stages after rehabilitation. The batter slope on the WRD would initially be constructed during rehabilitation as a planar surface with sheet flow conditions. In time the batter slope could have two evolutionary paths (fig 1.6): (1) the surface will remain planar under sheet flow conditions, and (2) the surface will become incised under concentrated flow conditions.

If, as time passes after rehabilitation, runoff is directed away from the batter slope by constructed drainage and the surface only receives direct rainfall, the site should retain a planar surface with sheet flow conditions. As soil and ecosystem development occurs at

Ranger in the short term, the WRD_0 surface condition will change towards a surface condition that is similar to that of WRD_{50S}. In the long term, the surface condition of the landform at Ranger will become similar to the surface condition of Nat_S (fig 1.6).

If, however, overland flow from the upper WRD surface breaches the bund at the top of the batter slope and flows over the surface then channelised flow will occur and a gully may develop. As soil and ecosystem development occurs at Ranger in the short term under concentrated flow conditions, the WRD_0 surface condition will change towards a surface condition that is similar to that of WRD_{50C}. In the long term, the surface condition of the landform at Ranger will become similar to the surface condition of Nat_C (fig 1.6).

The approximate ages of the natural sites, Nat_C and Nat_S, are discussed further in section 4.

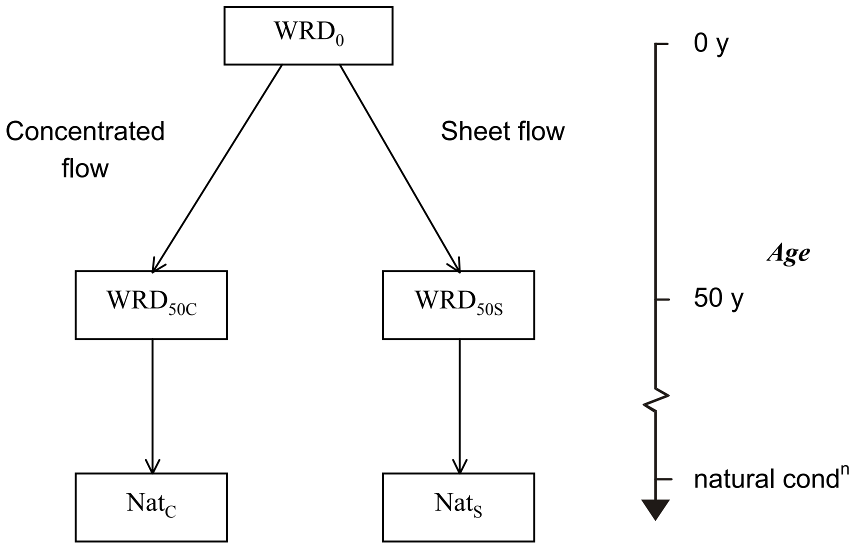

Figure 1.6 A schematic representation of the evolutionary paths of the batter slope at Ranger under concentrated flow and sheet flow conditions

2 SIBERIA landform evolution model

2.1 SIBERIA model parameter derivation

The SIBERIA landform evolution model developed by Willgoose et al (1989, 1991a,b,c) is a physically-based computer model for studying the erosional development of catchments and their channel networks. SIBERIA models long-term changes in elevation with time from the average effect of mass transport processes such as tectonic uplift, fluvial erosion, creep, rainsplash and landsliding. SIBERIA differentiates between diffusive and fluvial erosive processes that primarily act on the hillslopes and in the channels of a landform respectively. The model describes how a catchment will look, on average, at a given time.

The mass transport continuity equation of SIBERIA consists of three terms:

$$Q_s = Q_{sf} + Q_{sd} \tag{2.1}$$

where Q_s is the sediment transport rate per unit width, Q_{sf} is the fluvial sediment transport term and Q_{sd} is the diffusive transport term.

The fluvial sediment transport rate, Q_{sf}, through a point, based on the Einstein-Brown model (Willgoose & Riley 1998), is:

$$Q_{sf} = \beta_1 Q^{m_1} S^{n_1} \tag{2.2}$$

where Q is the discharge ($m^3\ y^{-1}$), S is the slope and β_1, m_1 and n_1 are parameters fixed by flow geometry and erosion physics.

The diffusive term, Q_{sd}, is described as shown:

$$Q_{sd} = DS \tag{2.3}$$

where D is diffusivity.

For large areas, such as the proposed rehabilitated landform at Ranger, the diffusive term becomes relatively less important (Willgoose & Riley 1998). Therefore, in this study the diffusive term is not considered. The sediment transport rate, Q_s (eqn 2.1), determined in SIBERIA can be written as follows:

$$Q_s = \beta_1 Q^{m_1} S^{n_1} \tag{2.4}$$

SIBERIA does not directly model runoff but uses a sub-grid effective parameterisation (Willgoose 1992) which conceptually relates discharge to area (A) draining through a point as follows (Leopold et al 1964):

$$Q = \beta_3 A^{m_3} S^{n_3} \tag{2.5}$$

To run SIBERIA for a field site it is necessary to derive parameter values for β_1, m_1 and n_1 (eqn 2.4) and β_3, m_3 and n_3 (eqn 2.5).

Parameter values used in SIBERIA can be classified as *primary* and *secondary*. The primary parameters in SIBERIA modelling represent the hydrology and erosion characteristics of the site where monitoring data are collected. The secondary parameters are dependent on the primary parameter values fitted for a site and represent the long-term average SIBERIA model parameter values for the landform being modelled.

To obtain the primary parameter values field monitoring data are required to (1) calibrate a hydrology model using rainfall and runoff data from field sites, and (2) fit parameters to a sediment transport equation using sediment loss and runoff data from field sites, as described by Willgoose and Riley (1998) and Evans et al (1998).

Using long-term rainfall data for the region, the calibrated hydrology and erosion models for each study site (primary parameters) are used to derive long-term average SIBERIA model parameter values for the landform being modelled (secondary parameters) which, for this study, is the proposed rehabilitated landform at Ranger. Figure 2.1 shows a flow diagram of this process.

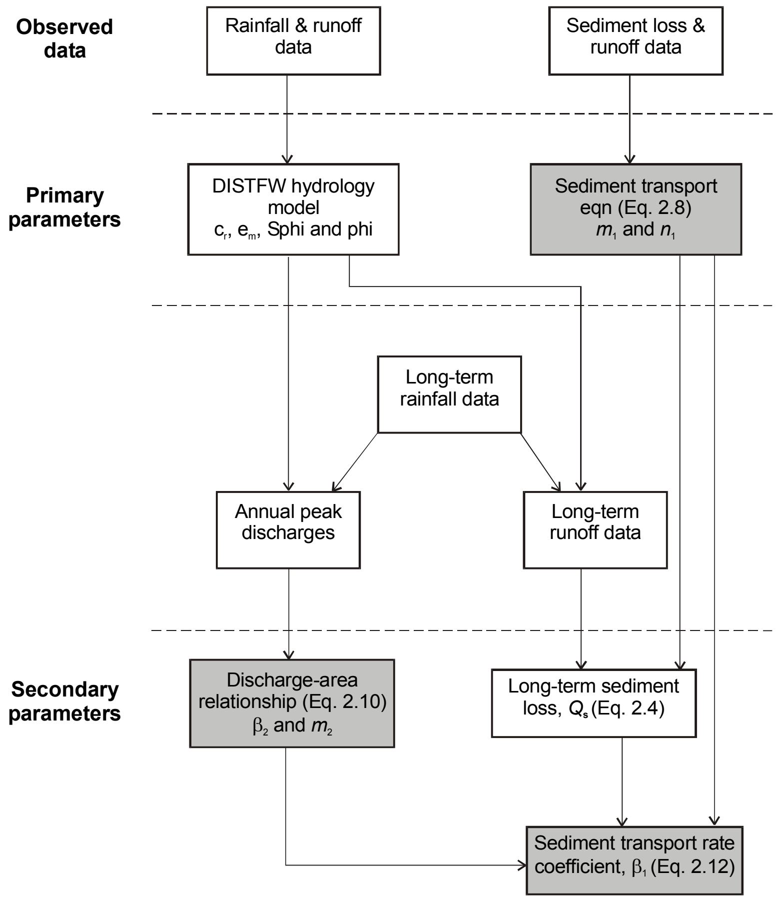

Figure 2.1 Flow diagram representing the SIBERIA input parameter derivation process. The shaded boxes indicate parameters used as input into the model.

2.2 Primary parameters

2.2.1 DISTFW hydrology model

The DISTFW model is a rainfall-runoff model based on the sub-catchment based Field-Williams Generalised Kinematic Wave Model (Field & Williams 1987). The model and its application to mine spoils and waste rock have been described in detail by Willgoose and Riley (1998), Finnegan (1993) and Arkinstal et al (1994). DISTFW divides a catchment into a number of sub-catchments connected together with a channel network draining to a single catchment outlet.

Parameters were fitted using a non-linear regression package, NLFIT version 1.10g (Kuczera 1989, 1994) as provided by The University of Newcastle. Using rainfall data and observed discharge readings as input, parameter values were fitted for the DISTFW model that would produce a predicted hydrograph similar to the observed hydrograph.

The parameters fitted in this study were:

- sorptivity (initial infiltration loss) Sphi,
- long-term infiltration phi, and
- kinematic wave parameters, c_r and e_m.

In this study, NLFIT was used to fit (1) parameters to a single rainfall event for a single site or (2) a number of events at a single site.

2.2.1.1 DISTFW input files

In this study NLFIT uses observed data and prior information on model parameters to fit parameter values to the DISTFW model. For NLFIT to fit parameter values to a rainfall event at a particular site, a data input file (.fw) is required (Willgoose et al 1995). A standard sub-catchment .fw file format (Willgoose et al 1995) was used for the WRD_{50} sites and the Nat_C sites. An example of the .fw file format used as input for DISTFW-NLFIT is shown in appendix A.1 (Nat_{C2}).

Site topographic survey information, rainfall data and observed runoff data are used to determine input for parts of the .fw input file — INCIDENCES, PARAMETERS, CONVEYANCES, RAINFALL and RUNOFF SECTIONS. Each part is described as follows:

- INCIDENCES — Site survey data are used to produce topographic contour maps (figs 2.2 & 2.3). Sub-catchments and flow paths through each sub-catchment mapped on the contour maps are used to determine which sub-catchments drain into other sub-catchments. A flow path matrix is set up describing the sub-catchment INCIDENCES (appendix A.1).
- PARAMETERS — The contour maps showing the sub-catchment analysis (figs 2.2 & 2.3) are used to measure the physical properties of each sub-catchment of the site. These physical properties (tables 2.1 & 2.2) are tabulated in the PARAMETER part of the .fw file (appendix A.1). The sub-catchment physical properties measured using the contour maps are the sub-catchment area, upstream and downstream elevation and flow path length.
- CONVEYANCES — The average sub-catchment width normal to the flow path is also measured and is used to calculate the nominal value for the kinematic wave parameter, c_r, for each catchment. The nominal value for initial model input is determined using the following equation:

$$c_r = 1/w^{2/3} \tag{2.6}$$

where,

w = average sub-catchment width.

The c_r parameter value is included in the CONVEYANCES data of the .fw file (appendix A.1). The catchment widths and corresponding c_r values are also shown in tables 2.1 and 2.2.

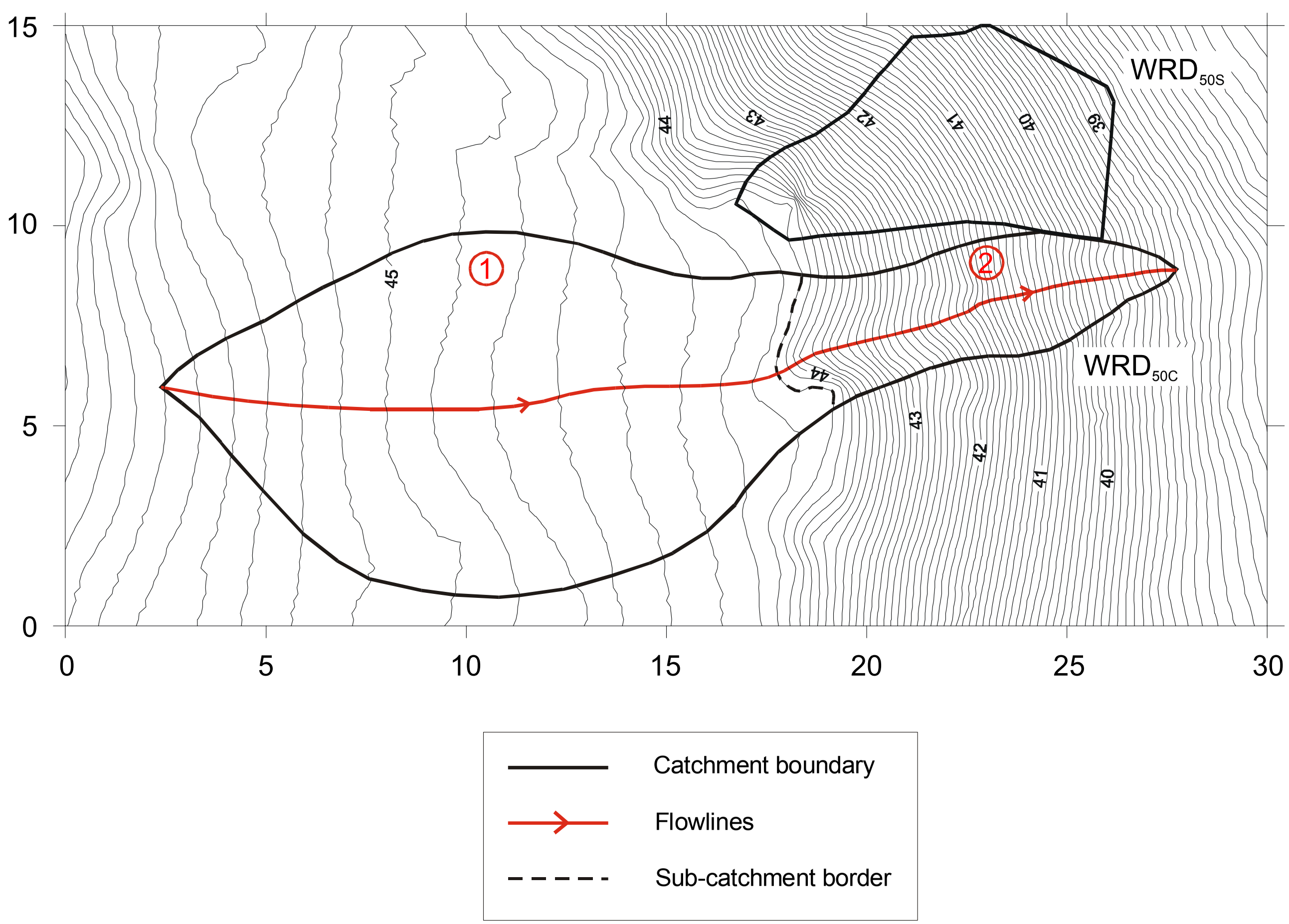

Figure 2.2 Topographic contour map of the WRD_{50} sites. Sub-catchments and flow paths through each sub-catchment are also shown. All dimensions are in metres.

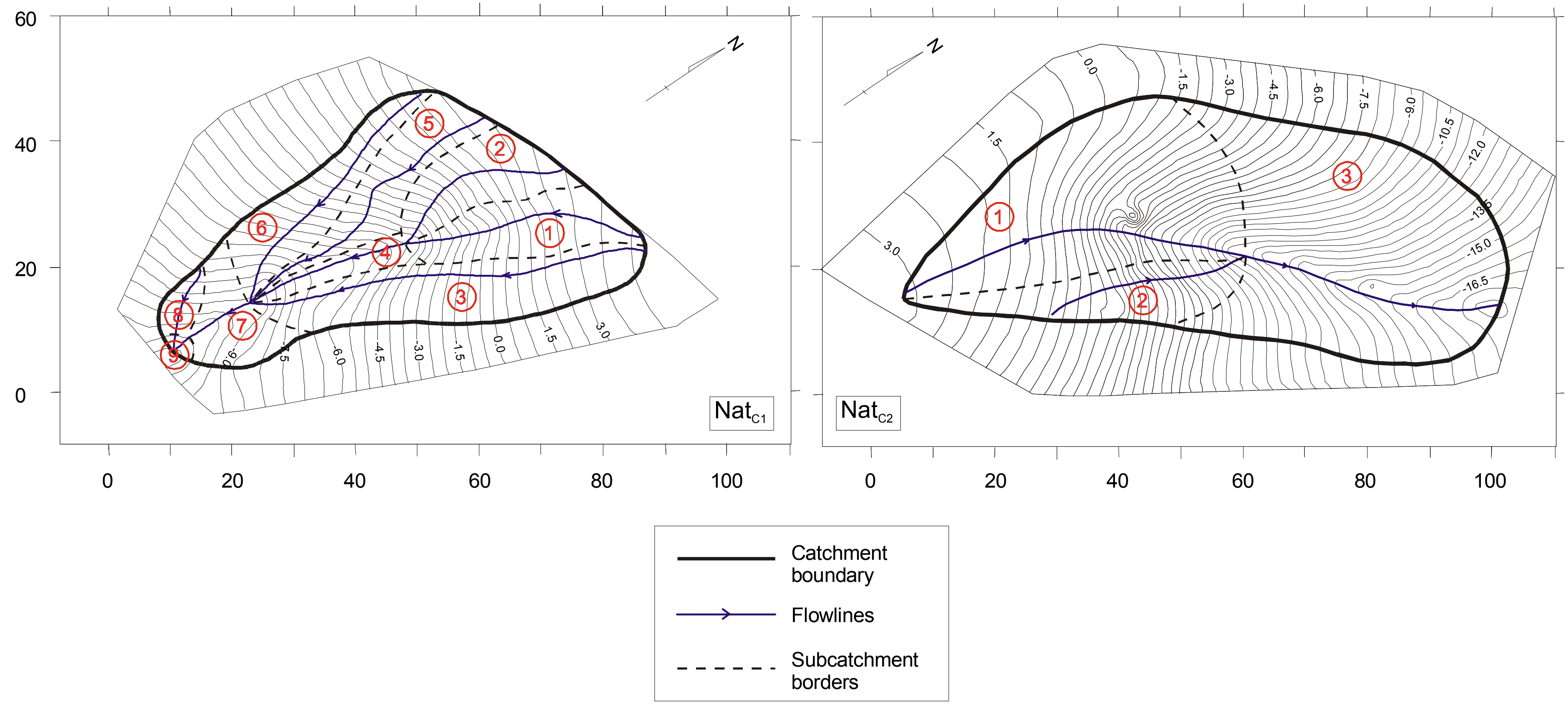

Figure 2.3 Topographic contour map of the Nat$_C$ sites (Riley 1994). Sub-catchments and flow paths through each sub-catchment have been added. All dimensions are in metres.

Table 2.1 Physical properties of the sub-catchments for WRD_{50C} and WRD_{50S}

Site	Sub-catchment no.	Area (m^2)	Length (m)	Slope ($m.m^{-1}$)	Width (m)	c_r (eqn 2.6)
WRD_{50C}	1	101.05	15.665	0.093	6.44	0.289
	2	24.17	9.968	0.517	2.43	0.554
WRD_{50S}	1	34.31	9.796	0.577	3.50	0.434

Table 2.2 Physical properties of the sub-catchments for Nat_{C1} and Nat_{C2}

Site	Sub-catchment no.	Area (m^2)	Length (m)	Slope ($m.m^{-1}$)	Width (m)	c_r (eqn 2.6)
Nat_{C1}	1	283.6	39.91	0.233	7.27	0.266
	2	263.4	31.46	0.257	8.27	0.245
	3	545.3	67.84	0.200	8.10	0.248
	4	101.7	27.46	0.153	3.31	0.450
	5	280.14	50.70	0.221	5.70	0.313
	6	289.12	44.60	0.235	6.24	0.295
	7	203.4	11.27	0.115	15.11	0.167
	8	51.9	11.74	0.273	4.32	0.377
	9	13.2	3.27	0.153	4.46	0.369
	Total area (m^2)	2031.8				
Nat_{C2}	1	1187.9	58.5	0.256	18.93	0.141
	2	273.6	32.7	0.358	7.50	0.261
	3	1484.9	42.0	0.136	32.86	0.097
	Total area (m^2)	2946.4				

- RAINFALL SECTION — Rainfall data are used to generate a .rf (rainfall) file — a two column text file with time (h) and cumulative rainfall (mm) as column one and two respectively for each event. The .rf files are used as input in the .fw file in the CUMPLUVIO section. An example of a .rf file is shown in appendix A.2.
- RUNOFF SECTION — Runoff data are used to generate a .ro (runoff) file — a two column text file with time (h) and observed instantaneous discharge (m^3 s^{-1}) as column one and two respectively for each event. The model will be calibrated to the observed hydrograph using the .ro file as input. The .ro file must have the same start and finish time as the corresponding .rf file. An example of a .ro file is shown in appendix A.3.

The data input file (.fw) is used to fit parameter values to the observed runoff events using the calibration procedure described in Arkinstal et al (1994) and Willgoose et al (1995).

At the completion of parameter fitting, NLFIT output files (.prt and .pmf) are produced. The .prt files are used to generate graphic output of the predictions.

2.2.2 Sediment transport equation

The total sediment loss model used in this study is derived from the equation described in Evans et al (1998) of the form:

$$Q_s = \beta_2 Q^{m_1} S^{n_1} \tag{2.7}$$

where,

Q_s = sediment discharge in a channel, gully or plot (g s^{-1}),

Q = instantaneous discharge (Ls^{-1}), and

S = local slope ($m.m^{-1}$).

β_2, m_1 and n_1 are *parameters* fixed by flow geometry and erosion physics.

Total sediment loss T (g) during a rainfall event can therefore be determined from the following equation:

$$T = \beta_2 S^{n_1} \int Q^{m_1} dt \tag{2.8}$$

where,

$\int Q^{m_1} dt$ = a function of cumulative runoff over the duration of the event.

The parameters β_2, m_1 and n_1 in equation 2.8 can be fitted using log-log linear regression between sediment flux, discharge and slope.

Equation 2.8 above can be expressed as:

$$LogT = Log\beta_2 + n_1 LogS + xLog\left(\int Q^{m_1} dt\right) \tag{2.9}$$

Initially, an arbitrary value of m_1 was selected and used to determine a value for $\int Q^{m}{}_{1}\, dt$ for each event, which was used in equation 2.9 for regression analysis to determine x. The value of m_1 was changed by trial and error and parameter values were fitted to equation 2.9 until the coefficient, x, was equal to 1. The m_1 value for the condition $x = 1$, and the corresponding β_2 parameter and slope exponent, n_1, were selected as the fitted parameters.

2.3 Secondary parameters

The primary parameter values fitted to the DISTFW hydrology model and to the sediment transport equation (eqn 2.8) are used to derive secondary parameter values for the landform to be modelled. The DISTFW hydrology model parameter values and the sediment transport equation (eqn 2.8) characterise the instantaneous values or properties of the landscape. SIBERIA models the long-term erosional behaviour of the landscape (Willgoose & Riley 1998) and therefore the secondary parameters of SIBERIA represent the average properties of the processes shaping the landscape. The instantaneous values represented by the erosion and hydrology parameters are integrated over time to yield the average input values (Evans et al 1998).

In this study the landform used was the proposed 'above-grade' rehabilitated option for Ranger. The secondary parameter derivation process can be considered in two parts, as described below, and is based on the description given by Willgoose and Riley (1998).

2.3.1 Discharge-area relationship

The discharge-area relationship is described by equation 2.5.

The slope dependence of discharge over the landform was ignored (ie n_3=0). Willgoose and Riley (1998) suggested that the slope dependence should only be considered if there are significant changes in the average slope of the catchment over time, which is not the case in this study. Equation 2.5 can be rearranged accordingly to produce a commonly observed relationship between peak discharge and area (ie Strahler 1964).

$$Q = \beta_3 A^{m_3} \tag{2.10}$$

By fitting parameters β_3 and m_3 to equation 2.10 the area dependence of the discharge at Ranger can be determined for a particular soil condition. Equation 2.10 was fitted using the peak discharges and areas for the largest single catchment defined on the 30 m digital terrain map of the proposed above-grade option for Ranger (fig 2.4). This catchment was approximately 1.6 km^2, consisting of 1773 nodes, each 900 m^2 in area, and was assumed to be representative of the hydrologic characteristics of all the catchments (Willgoose & Riley 1998).

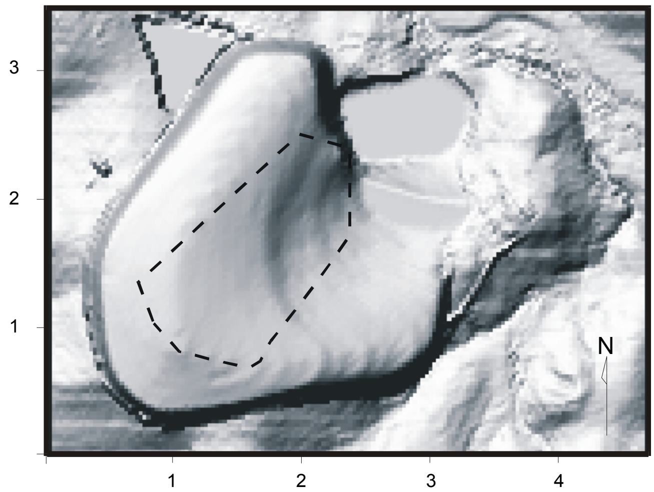

Figure 2.4 The above-grade landform option for rehabilitation at Ranger. The dashed line indicates the approximate boundary for the 1.6 km^2 catchment. Dimensions are in kilometres.

The DTM based version of DISTFW (Willgoose et al 1995) was used to predict the peak discharges of areas within the catchment for mean annual rainfall events (fig 2.1). The rainfall events were selected by Willgoose and Riley (1998) and consisted of storms of various duration for a 1 in 2 year average return interval (ARI).

The step-by-step process to run the DISTFW model to fit β_3 and m_3 (eqn 2.10) for the proposed rehabilitated landform at Ranger is explained in detail in Evans et al (1998).

For each storm duration the peak discharge was predicted at each nodal area within the catchment using the DISTFW model. The maximum peak discharge at every node simulated from the different duration storms was calculated. Log-log linear regression analysis of the maximum peak discharge values for each corresponding area was conducted to fit the SIBERIA input parameters, β_3 and m_3 (eqn 2.10).

2.3.2 Runoff series and long-term average sediment loss rate

A runoff series for the historical rainfall records at Jabiru was created using the DISTFW hydrology model parameter values derived for each site (fig 2.1). This series was used to determine the long-term average sediment loss rate, Q_s (eqn 2.4), for the 1.6 km^2 waste rock dump catchment.

Based on the description given in Willgoose and Riley (1998), the steps were:

1 The DTM based version of DISTFW was used to predict the runoff from the 1.6 km^2 catchment for a single, measured rainfall event. The parameter values used were those fitted to the DISTFW hydrology model derived for the study sites using the method outlined in section 2.2.

2 The subcatchment version of DISTFW with 10 subcatchments was calibrated to simulate the runoff from the DTM output for the single, rainfall event. The rainfall data and the runoff predicted in Step 1 were used as input into the DISTFW model. Only the kinematic wave parameter, c_r, was refitted. The other parameters are independent of whether the DTM or subcatchment version of DISTFW is used (Willgoose & Riley 1998).

3 The calibrated subcatchment based model (Step 2) was used to generate a runoff series for the 1.6 km^2 catchment from the historical rainfall records at Jabiru. The DTM based version of DISTFW (used in section 2.4.1) was not used to predict the runoff series from the annual rainfall data for Jabiru because of the excessive amount of computer processing time required to generate the runoff series (Willgoose & Riley 1998). The calibrated hydrology model parameter values, refitted in Step 2, were used as input into the DISTFW model. The infiltration parameter, Sphi, was fixed at 0.0001 mm hr$^{-0.5}$, indicating a saturated catchment, producing a conservative runoff series (Willgoose & Riley 1998).

4 The runoff series determined in Step 3 above was used to determine an annual sediment loss (Mg y^{-1}) from the 1.6 km^2 catchment using the sediment transport equation (eqn 2.8). The sediment loss was converted to a volumetric loss (m^3 y^{-1}) by dividing the result by the bulk density of the surface material. A long-term average volumetric sediment loss rate, Q_s, was then calculated.

5 The long-term average sediment loss rate, Q_s, was then used to determine the SIBERIA input parameter, β_1 (eqn 2.4), for each of the site conditions. Substituting equation 2.10 into equation 2.4 gives:

$$\beta_1 = \frac{Q_s}{\beta_3^{\,m_1} A^{m_3 m_1} S^{n_1}} \tag{2.11}$$

where S is assumed to be 1 m.m^{-1} and Q_s is the long-term average sediment loss rate. This value, however, is uncorrected for node scale and slope (see section 2.3.3 below).

2.3.3 Slope correction

The average annual sediment losses, Q_s, were calculated for a grid spacing of 1 m x 1 m. Inputting the derived value of the average sediment loss rate, Q_s, into equation 2.11 will produce an erosion rate coefficient, β_1, calculated for an area of 1 m x 1 m. SIBERIA analysis assumes a grid spacing of 1 nodal area (ie. 1 x 1 dimensionless square). In the case of the proposed rehabilitated landform at Ranger, each nodal area is based on a 30 m x 30 m grid. The average annual sediment loss value needs to be adjusted to reflect the sediment loss for a

30 m x 30 m grid spacing. In order to scale down the derived annual sediment loss value, it is not acceptable to simply divide the value by a ratio of 1:30. The value of slope in the long term sediment transport equation (eqn 2.4) is directly related to the grid spacing. The average annual sediment loss values were calibrated for a slope value equal to the change in elevation per unit grid spacing of 1 m. For SIBERIA analysis, the slope value will be a change in elevation per unit grid spacing of 1 node (ie 30 m). As the slope value is raised to the power of the slope exponent, n_1 (eqn 2.4), the scale down ratio of Q_s should also be adjusted to the same power. This correction factor applied to the Q_s term is incorporated into the input parameter calculation (eqn 2.11) as shown:

$$\beta_1 = \frac{Q_s}{\beta_3^{m_1} A^{m_1 m_3}} \times \left(\frac{1}{30} \right)^{n_1} \tag{2.12}$$

The parameters m_1 and n_1 are parameters fitted to the sediment transport equation (eqn 2.8).

3 Derivation of DISTFW hydrology model and sediment transport equation parameter values

3.1 Introduction

Landform evolution modelling using SIBERIA requires input from the DISTFW hydrology model and the sediment transport equation. Monitoring data from rainfall events are required to parameterise the DISTFW hydrology model and the sediment transport equation.

Natural rainfall event data were collected from WRD_0 (Evans et al 1998); WRD_{50C} and WRD_{50S}; Nat_{C1} and Nat_{C2} (Riley 1994); and Nat_S (Bell & Willgoose 1997). These sites are assumed to be representative of the surface conditions that would exist at Ranger at various stages after rehabilitation (fig 1.6).

This section reports the derivation of DISTFW hydrology model and sediment transport equation parameters for use in SIBERIA for each of the study sites. These primary parameter values were compared to assess the effect of temporal change on the DISTFW hydrology model and the sediment transport equation.

3.2 DISTFW hydrology model parameter derivation

Parameter values were fitted to observed rainfall and runoff for the monitored rainfall events at WRD_{50} and Nat_C (Riley 1994) using DISTFW-NLFIT (method described in section 2.2). The DISTFW hydrology model parameter values fitted for events at WRD_0 and Nat_S were derived in Evans et al (1998) and Bell and Willgoose (1997) respectively.

3.2.1 WRD_{50} sites

Runoff/erosion plots were constructed and installed with dimensions of: (1) WRD_{50C} – 24.2 m^2 with a length of 10 m and variable width, and (2) WRD_{50S} – 34.3 m^2 with a variable width and a length of 9.8 m. The plot borders were constructed using wide damp course. At the downslope ends of the plots runoff was channelled through a flume (fig 3.1) where discharge could be measured. A 0.304 m HS flume was placed at the outlet of WRD_{50C} and a ¼ 90° V-notch sharp-crested weir was placed at the outlet of WRD_{50S}. Bedload traps were incorporated in each control structure (fig 3.1). The upslope end of WRD_{50C} was open to the low gradient upper cap surface so that discharge from this area could be included in analysis. However, during monitoring, there was no observed discharge from the upper surface into the gully. The up-slope end of WRD_{50S} had a border in place to prevent flow entering.

Rainfall on each plot was measured using a tipping bucket rain gauge. Stage height in the flumes were measured off the stilling well (fig 3.1) by an observer. Stage (*h*) (m) was then converted to discharge (*Q*) (Ls^{-1}) using the following derived formulas for each particular flume:

$$Q_{WRD_{50C}} = 195.6h^2 + 2.46h + 0.008 \quad (3.1)$$

$$Q_{WRD_{50S}} = 10^{2.41}\, h^{2.31} \quad (3.2)$$

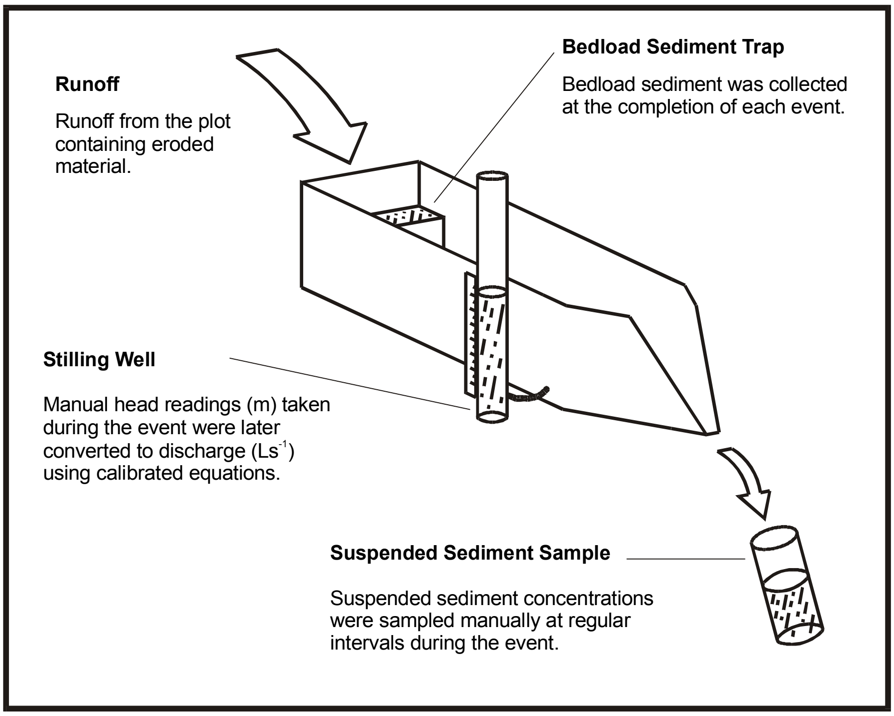

Figure 3.1 Constructed flume at the outlet of the WRD_{50} sites

Sediment loss data were also measured and used for sediment transport equation parameter derivation (section 3.3.3). Runoff water samples were collected during rainfall events for gravimetric analysis of suspended sediment concentrations. Total suspended sediment loss was determined through integration of the sedigraphs. Bedload samples were collected at the conclusion of each event and total bedloads were determined using gravimetric analysis.

The study sites were monitored during natural rainfall events from December 1996 until March 1997. Total rainfall and total runoff for the monitored rainfall events are given in table 3.1. Cumulative rainfall and runoff hydrographs for WRD_{50C} and WRD_{50S} are given in appendices B.1 and B.2 respectively.

The fitted hydrographs and corresponding fitted parameter values for each individual rainfall event are given in appendices B.1 and B.2.

Parameter values were then fitted to observed hydrographs for observed rainfalls by fitting a single parameter set that provided a good fit to four hydrographs for each site simultaneously. Firstly, a single parameter set was fitted to the first four events that occurred on the sites (table 3.1). Secondly, a single parameter set was fitted to the last four events on the sites (table 3.1). Fitted parameter values are given in table 3.2.

Table 3.1 Observed rainfall and runoff data for the rainfall events at WRD_{50C} and WRD_{50S}

Date	Total rainfall (mm)	Total runoff (L) [Peak discharge (Ls^{-1})]	
	Both sites	WRD_{50C}	WRD_{50S}
07/01/97	42.4	261.6 [0.23]	205.9 [0.20]
09/01/97	5.8(1)	29.9 [0.14]	24.9 [0.07]
17/02//97	46.4	677.2 [0.60]	754.6 [0.63]
18/02/97	36.4	351.0 [0.42]	286.0 [0.39]
19/02/97	13.4	88.9 [0.19]	99.5 [0.15]
20/02/97	15.0	79.1 [0.07]	35.4 [0.05]
21/02/97	30.2	200.8 [0.19]	181.8 [0.15]
26/02/97	33.8	316.2 [0.33]	312.7 [0.37]
05/03/97	16.2	174.6 [0.57]	147.4 [0.55]

1 Measured rainfall at WRD_{50S} was 5.2 mm

Table 3.2 Fitted parameter values for 1997 events in parallel on the WRD_{50C} and WRD_{50S} sites. Standard deviations are given in parentheses.

Site	c_r ($m^{(3-2e_m)}s^{-1}$)	e_m	Sphi (mm $h^{-0.5}$)	Phi (mm h^{-1})
WRD_{50C} — 07 Jan, 09 Jan, 17 Feb, 18 Feb	1.330 (1.34)	1.663 (0.24)	1.758 (0.43)	38.22 (1.09)
WRD_{50C} — 20 Feb, 21 Feb, 26 Feb, 05 Mar	2.354 (2.05)	1.761 (0.21)	0.905 (0.54)	18.24 (1.36)
WRD_{50S} — 07 Jan, 09 Jan, 17 Feb, 18 Feb	0.823 (13.37)	1.546 (4.22)	1.464 (10.57)	38.67 (27.97)
WRD_{50S} — 20 Feb, 21 Feb, 26 Feb, 05 Mar	0.359 (0.10)	1.500 (0.07)	2.877 (0.30)	18.84 (0.59)

The parameter values fitted for the first four storms at WRD_{50S} had very large standard deviations and were thus considered unreliable (table 3.2). The parameter values fitted for the first four storms at WRD50C were used to predict hydrographs for all of the events at WRD_{50C}. The predicted hydrographs were similar to observed data for the first four events, however, the last four events were under-predicted and did not fit the observed data well.

The parameter values fitted for the last four storms at WRD_{50C} and WRD_{50S} were used to predict hydrographs for all of the events on those sites (appendices C.1 and C.2 respectively). The predicted hydrographs using parameters for the last four storms were similar to the observed data, although there was some over-prediction. The observed and predicted hydrographs for both sites for the event on 17/02/97 are given in figure 3.2. This event had the greatest rainfall and runoff and it is important that large events are accurately predicted. For WRD_{50S} the rising stage of the hydrograph is generally well predicted but there is some over-prediction in the receding stage of the hydrograph. The peak discharge from both sites was well predicted but there was some over-prediction of rise and fall of secondary peaks in the hydrographs.

The DISTFW hydrology model parameter values fitted for the last four events at both WRD_{50C} and WRD_{50S} (highlighted in table 3.2) will be used to derive SIBERIA input parameter values for the surface condition of these sites in section 4.

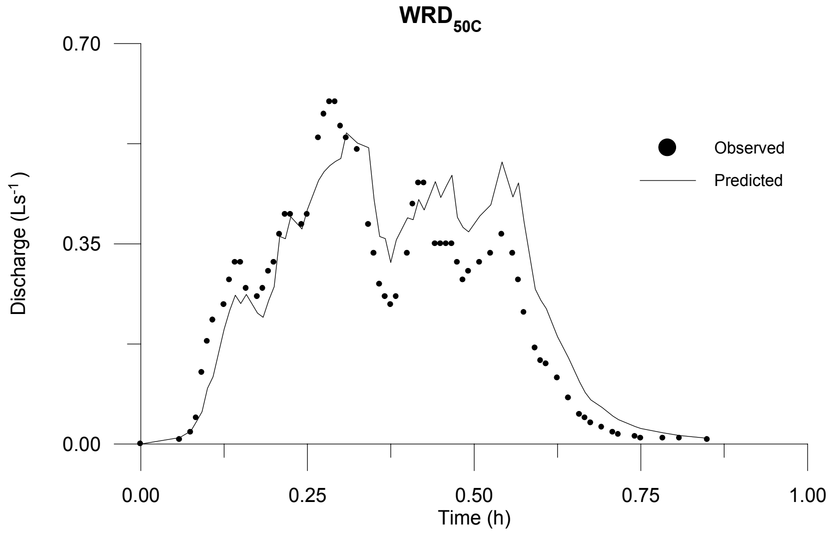

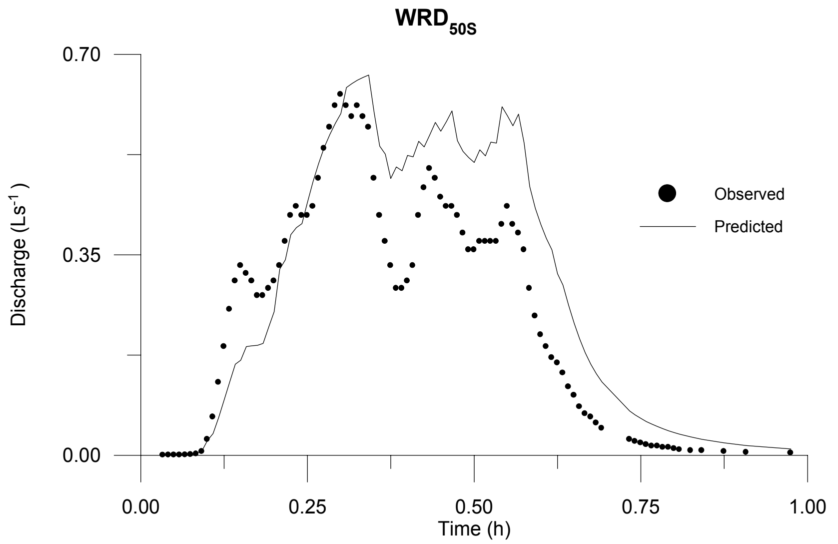

Figure 3.2 Observed and predicted hydrographs using parameter values in table 3.2 for the event on 17/02/97 at WRD_{50C} and WRD_{50S}. WRD_{50C} parameter values are c_r = 2.35, e_m = 1.76, Sphi = 0.91 and phi = 18.2. WRD_{50S} parameter values are c_r = 0.36, e_m = 1.50, Sphi = 2.88 and phi = 18.8.

3.2.2 Nat_C sites

Several discrete periods of rainfall-runoff were observed during a day at Nat_C. In this study, consecutive periods of rainfall-runoff occurring on the same day have been combined in one rainfall record and one discharge hydrograph. These combined records are referred to as daily events.

Total rainfall and total runoff for the monitored daily events are given in table 3.3. Cumulative rainfall and runoff hydrographs for Nat_{C1} and Nat_{C2} are given in appendices B.3 and B.4 respectively.

Initially, parameter values were fitted to each observed daily rainfall-runoff event. The fitted hydrographs for each daily event, and the corresponding fitted parameter values, are given in appendices B.3 and B.4. A single set of parameter values for each site were then fitted to the daily rainfall-runoff events simultaneously. This fitting process is discussed in the following sub-sections.

Table 3.3 Observed rainfall and runoff data for the daily events at Nat_{C1} and Nat_{C2} (Riley 1994)

Site	Date	Total rainfall (mm)	Total Runoff (L) [Peak discharge (Ls^{-1})]
Nat_{C1}	25 Dec	15	3 647 [9.67]
	27 Dec	20	5 459 [6.98]
	29 Dec	23	8 211 [6.84]
	30 Dec	16$^{(1)}$	8 054 [9.96]
Nat_{C2}	25 Dec	12.6	5 440 [6.48]
	27 Dec	24	6 836 [9.13]
	29 Dec	24.8	11 209 [9.32]
	30 Dec	35.4$^{(1)}$	25 465 [28.71]

(1) For the first part of this daily event at Nat_{C1} rainfall and runoff data were not collected. The rainfall and runoff shown for Nat_{C1} corresponds to only the second part of the daily event at Nat_{C2}.

3.2.2.1 Nat_{C1} site

A single set of parameter values was fitted simultaneously to all four daily hydrographs for Nat_{C1}. However, the observed daily hydrograph for 30 December was considerably under-predicted using this single set of parameter values. This has been attributed to the fact that runoff data for the early part of the day were missing for 30 December at Nat_{C1}. The soil at Nat_{C1} may have been saturated when the later rainfall period on 30 December occurred. Therefore, the predicted daily hydrograph for this second rainfall period on 30 December may represent unrealistically dry conditions.

As a result, a single set of parameter values was fitted simultaneously to the daily events on 25, 27 and 29 December only. This set of parameter values was then used to predict the daily hydrograph for 30 December. To more accurately predict the daily hydrograph for 30 December an antecedent soil moisture parameter, initial wetness, was also fitted. This parameter value is normally fixed at 0.001 m (ie very low soil moisture content) unless otherwise indicated by wet conditions prior to the event.

The single set of parameter values fitted to the daily events on 25, 27 and 29 December simultaneously are given in table 3.4. The fitted initial wetness value for the daily event on 30 December was 43.2 mm. The predicted hydrographs using the fitted parameter values (table 3.4) were reasonably similar to the observed hydrographs for each of the daily events at Nat_{C1} (appendix C.3). The observed and predicted hydrograph for Nat_{C1} for the event on 30 December, the event with the greatest peak discharge, is given in figure 3.3. The predicted hydrograph compares well to observed data for this event (fig 3.3) despite the lack of antecedent wetness information.

Table 3.4 Mean DISTFW model parameter values fitted to WRD_0 (Evans et al 1998), WRD_{50} sites, Nat_C sites and Nat_S (Bell & Willgoose 1997). Standard deviations are given in parentheses.

Site	c_r ($m^{(3-2e_m)}s^{-1}$)	e_m	Sphi (mm $h^{-0.5}$)	Phi (mm h^{-1})
WRD_0	6.711 (0.65)	1.541 (0.03)	5.476 (0.36)	16.305 (0.93)
WRD_{50C}	2.354 (2.05)	1.761 (0.21)	0.905 (0.54)	18.24 (1.36)
WRD_{50S}	0.359 (0.10)	1.500 (0.07)	2.877 (0.30)	18.84 (0.59)
Nat_{C1}	4.545 (1.06)	1.375 (0.07)	10.321 (0.28)	0.164 (0.38)
Nat_{C2}	6.475 (0.56)	1.242 (0.03)	8.645 (0.12)	5.238 (0.26)
Nat_S	4.98	1.82	1.67	14.55

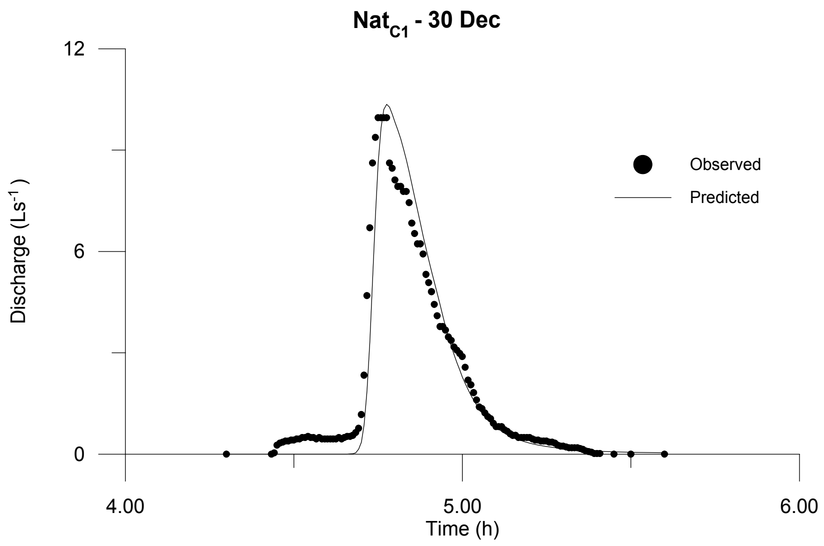

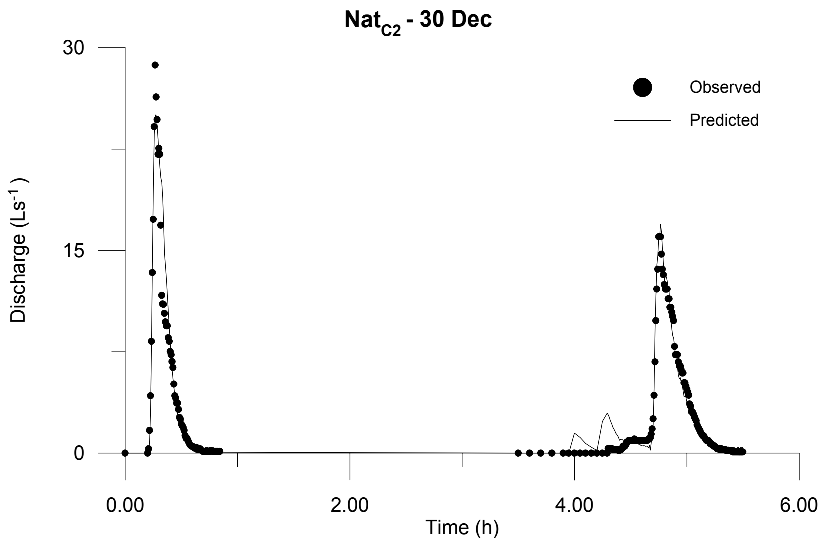

Figure 3.3 Observed and predicted hydrographs using parameter values in table 3.4 for the event on 30 December at Nat$_{C1}$ and Nat$_{C2}$. Nat$_{C1}$ parameter values are c_r = 4.55, e_m = 1.38, Sphi = 10.32 and phi = 0.16. Nat$_{C2}$ parameter values are c_r = 6.48, e_m = 1.24, Sphi = 8.65 and phi = 5.24.

3.2.2.2 Nat$_{C2}$ site

A single set of parameter values was fitted simultaneously to all four daily hydrographs for Nat$_{C2}$ (table 3.4). The predicted hydrographs using the fitted parameter values (table 3.4) were reasonably similar to the observed hydrographs for each of the daily events at Nat$_{C2}$ (appendix C.4). Figure 3.3 shows that the predicted hydrograph compares well to the observed data for the event on 30 December, the event with the greatest rainfall and runoff, at Nat$_{C2}$.

3.2.2.3 Deriving DISTFW kinematic wave parameter values from plot survey data

The kinematic wave parameter values are influenced by factors such as surface roughness, flow geometry and surface treatments (Willgoose & Kuczera 1995). In addition to using DISTFW-NLFIT, the kinematic wave parameters, c_r and e_m, can also be determined from a combination of analysis of flow geometry and surface flow resistance. In this section the kinematic wave parameter values fitted simultaneously to the observed hydrographs for the daily events at the Nat$_C$ sites using NLFIT (table 3.4) were compared with the kinematic wave parameter values determined from flow geometry and surface conditions at the Nat_C sites. A similar result for the two methods indicates that the rainfall-runoff data can be reliably used to estimate the surface roughness and flow geometry for the Nat_C sites.

The following method of kinematic wave parameter determination is described in Willgoose and Kuczera (1995).

Using the site survey data and constructed contour maps (fig 2.3) cross-sections of the surface topography of the two sites are taken normal to the flowpath along the catchment area (fig 3.4). Cross-sections of the surface are taken at equal distances apart along the flowpath. Measurements taken from the cross sections for both sites were used to fit the following equations (Willgoose & Kuczera 1995):

$$Nat_{C1}: \quad A_{cs} = 0.045P^{2.046} \tag{3.3}$$

$$Nat_{C2}: \quad A_{cs} = 0.041P^{2.204} \tag{3.4}$$

where,

A_{cs} is the flow cross-sectional area per unit width, and

P is the wetted perimeter per unit width.

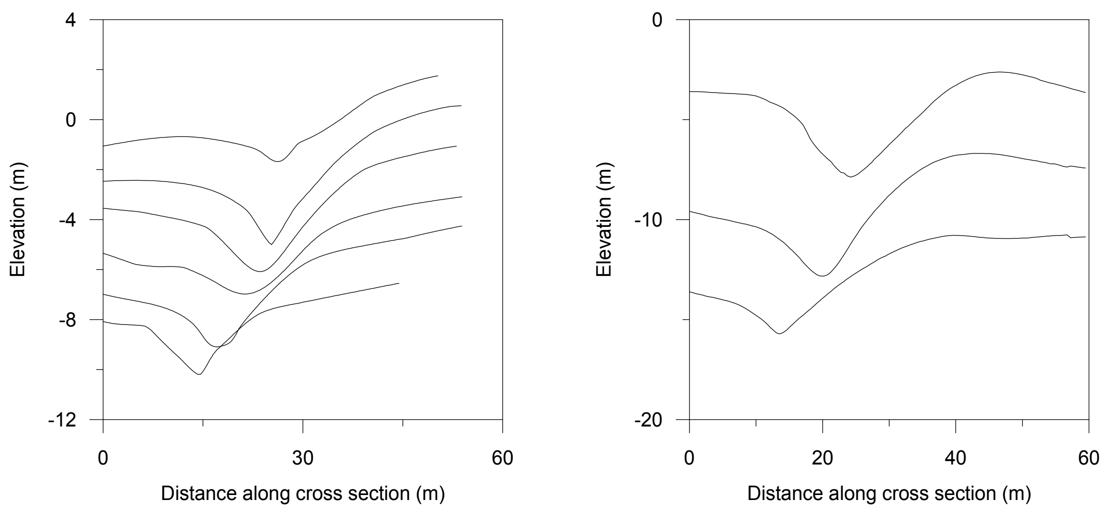

Figure 3.4 Cross sections taken from Nat_{C1} (left) and Nat_{C2} (right) catchments based on data from Riley (1994)

Letting the coefficient and exponent of P from equations 3.3 and 3.4 be K and a respectively, the kinematic wave parameters, c_r and e_m, can be calculated using the following equations derived from Willgoose and Kuczera (1995):

$$e_m = \left(\tfrac{5}{3}a - \tfrac{2}{3}\right)/\, a \tag{3.5}$$

$$c_r = K^{(1.67 - e_m)} / n \tag{3.6}$$

where n is Manning's roughness.

Using the exponent a derived in equations 3.3 and 3.4, e_m values of 1.34 and 1.36 were calculated for Nat_{C1} and Nat_{C2} catchments respectively (table 3.5).

Table 3.5 Comparison between kinematic wave parameter values calculated from flow geometry (Willgoose & Kuczera 1995) and those fitted using the DISTFW-NLFIT model

Site	Parameter	Calculated from flow geometry and surface conditions	Derived from DISTFW-NLFIT model
Nat_{C1}	e_m	1.34	1.375
	c_r	6.53	4.545
Nat_{C2}	e_m	1.36	1.242
	c_r	6.75	6.475

In order to establish c_r parameter values for each site, a value for Manning's roughness, *n*, is required. A procedure for estimating *n* was developed by Cowan (1956) (as cited by Dingman 1984) and can be represented using the equation:

$$n = (n_0 + n_1 + n_2 + n_3 + n_4)m \tag{3.7}$$

The values of n_0 to n_4 take into account the runoff resistance added by the type of material involved; surface roughness; slope and size of channel cross section; flow obstructions; and vegetation, respectively. The value of *m* is determined by the degree of channel meandering (Dingman 1984).

A table of values to estimate each component of equation 3.7 given a set of corresponding channel conditions (Chow 1959 as cited by Dingman 1984) was applied to the surface conditions at Nat_{C1} and Nat_{C2}. Manning's roughness, *n*, was estimated to be 0.055 for both sites. The kinematic wave parameter, c_r, for each site was determined by substituting the values of e_m, *K* and *n* into equation 3.6 (table 3.5).

Table 3.5 compares the sets of kinematic wave parameter values estimated from flow geometry with those derived using the DISTFW-NLFIT model. The kinematic wave parameter values derived by fitting multiple daily events at the Nat_C sites using NLFIT are similar to those estimated from flow geometry and surface conditions.

Moreover, predicted hydrographs, using the kinematic wave parameter values calculated from flow geometry and surface conditions (table 3.5), were similar to the observed hydrographs for each of the daily events at Nat_{C1} and Nat_{C2} (appendix D). The infiltration parameter values used were those previously fitted above (table 3.4). The fitted daily hydrographs using 'NLFIT' kinematic wave parameter values are also shown (appendix D). Figure 3.5 shows that the predicted hydrograph, using the 'geometric' kinematic wave parameter values, compares well with the observed data for the daily event on 30 December, the event with the greatest peak discharge, at Nat_{C1} and Nat_{C2}. As mentioned previously, the runoff event at Nat_{C1} corresponds to the second part of the discharge event at Nat_{C2}.

For each event the predicted peak discharge, using the 'NLFIT' kinematic wave parameter values, is generally:

- lower than the predicted peak discharge using the 'geometric' kinematic wave parameter values at Nat_{C1} (fig 3.5 and appendix D), and
- higher than the predicted peak discharge using the 'geometric' kinematic wave parameter values at Nat_{C2} (fig 3.5 and appendix D).

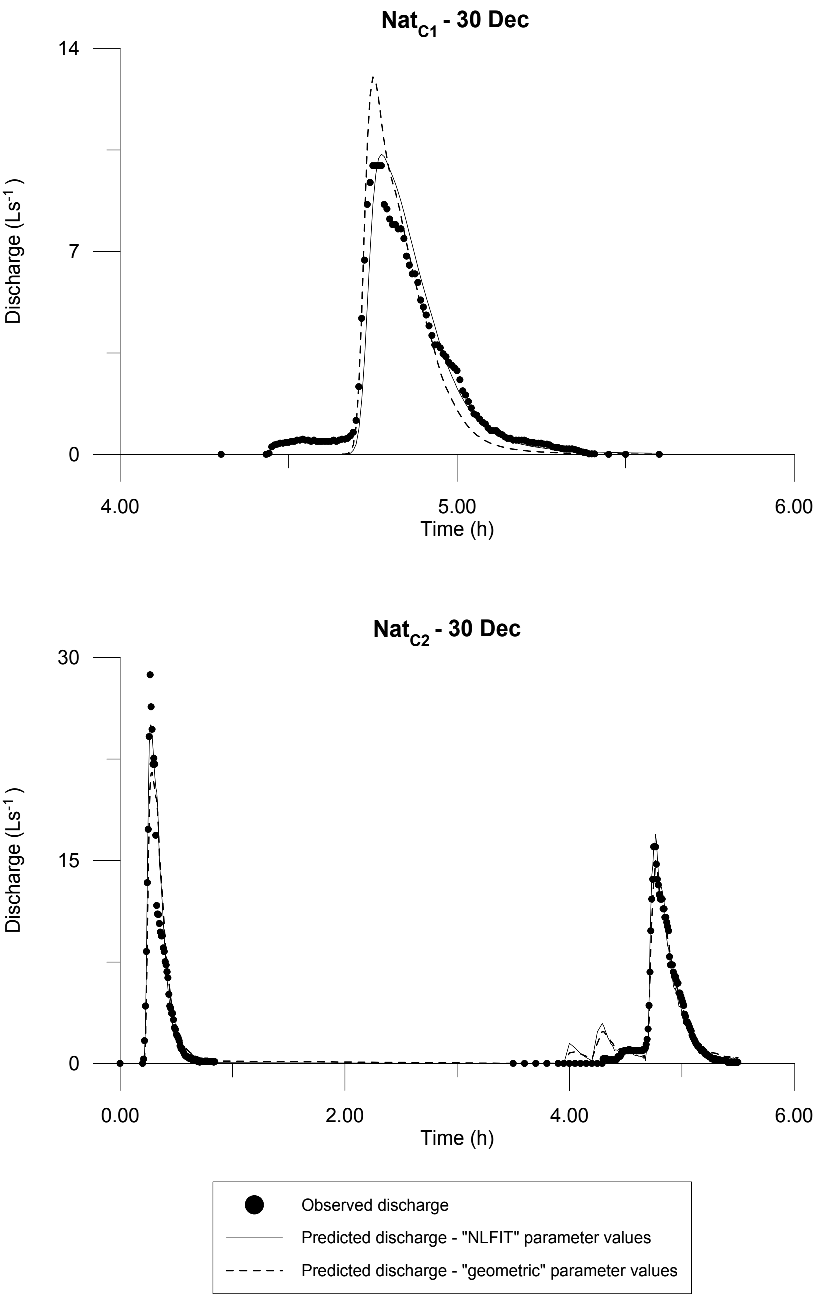

Figure 3.5 Predicted hydrographs for the events at Nat$_{C1}$ and Nat$_{C2}$ on 30 December using DISTFW model kinematic wave parameter values fitted using NLFIT and calculated using flow geometry and surface conditions (table 3.5). The infiltration parameter values used were those previously fitted using NLFIT (table 3.4). Observed hydrographs are also shown.

Total predicted runoff volumes, using both 'NLFIT' and 'geometric' kinematic wave parameter values, for each daily event at Nat$_{C1}$ and Nat$_{C2}$ were determined. A *t*-test showed that the total predicted runoff volume for each of these events, using 'NLFIT' parameter values, were not statistically different from (1) the total predicted runoff using 'geometric' kinematic wave parameter values, and (2) the total observed runoff (table 3.3).

The results show that the kinematic wave parameter values fitted using DISTFW-NLFIT for the Nat$_C$ sites reflect the surface conditions at the Nat$_C$ sites and that the rainfall-runoff data can be reliably used to predict the surface roughness and flow geometry for both sites.

3.2.3 WRD_0 and Nat_S sites

The DISTFW hydrology model parameter values for the WRD_0 and Nat_S sites were derived by Evans et al (1998) and Bell and Willgoose (1997) respectively (table 3.4). The hydrology parameter derivation method used by Bell and Willgoose (1997) and Evans et al (1998) is similar to that used in this study, described above in sections 3.2.1 and 3.2.2.

3.3 Sediment transport equation parameter derivation

Monitoring data collected at WRD_0 (Evans et al 1998), WRD_{50} and Nat_C (Riley 1994) were used to fit the relationship between total sediment loss and runoff from rainfall events (eqn 2.8) (see section 2.3). Bell and Willgoose (1997) fitted a total sediment loss relationship for Nat_S.

3.3.1 Data

To parameterise the sediment transport equation (eqn 2.8) complete data sets of sediment loss, rainfall and runoff are required from a discrete rainfall event. Thirty-two rainfall events were monitored at WRD_0 (Evans et al 1998); 9 rainfall events were monitored at the WRD_{50} sites; and 19 rainfall events were monitored at the Nat_C sites (Riley 1994). Of these discrete rainfall events, 4 complete data sets were obtained at WRD_0, 9 complete data sets were obtained at the WRD_{50} sites and 3 complete data sets were obtained at the Nat_C sites. The remaining events at WRD_0 and Nat_C were incomplete because either sediment (suspended sediment concentration and/or bedload) data or discharge data were not collected. Rainfall, runoff and sediment loss data for the discrete rainfall events where complete data sets were obtained are given in tables 3.6, 3.7 and 3.8 for the WRD_0, WRD_{50} and Nat_C sites respectively.

Table 3.6 Complete data sets for rainfall events monitored at WRD_0 (Evans et al 1998)

Site	Date	Total rainfall (mm)	Total runoff (L)	Runoff Coefficient	Suspended sediment loss (g) [Loss per unit runoff (g L^{-1})]	Bedload loss (g) [Loss per unit runoff (g L^{-1})]	Total sediment loss (g) [Loss per unit runoff (g L^{-1})]
WRD_0	22/02/93	7	2194	0.52	97 [0.04]	388 [0.18]	485 [0.22]
	18/03/93	16	4375	0.46	3041 [0.70]	12000 [2.74]	15041 [3.44]
	16/11/93	20	2021	0.19	263 [0.13]	1079 [0.53]	1341 [0.66]
	09/12/93	50	14328	0.48	8881 [0.62]	36017 [2.51]	44898 [3.13]

Table 3.7 Complete data sets for rainfall events monitored at WRD_{50C} and WRD_{50S}

Site	Date	Total rainfall (mm)	Total runoff (L) [Peak discharge (Ls^{-1})]	Runoff Coefficient	Suspended sediment loss (g) [Loss per unit runoff ($g L^{-1}$)]	Bedload loss (g) [Loss per unit runoff ($g L^{-1}$)]	Total sediment loss (g) [Loss per unit runoff ($g L^{-1}$)]
WRD_{50C}	07/01/97	42.4	261.6 [0.23]	0.25	117.71 [0.45]	328.19 [1.25]	445.90 [1.70]
	09/01/97	5.8	29.9 [0.14]	0.21	13.99 [0.47]	33.52 [1.12]	47.51 [1.59]
	17/02//97	46.4	677.2 [0.60]	0.60	419.43 [0.62]	853.09 [1.26]	1272.52 [1.88]
	18/02/97	36.4	351.0 [0.42]	0.40	118.99 [0.34]	229.24 [0.65]	348.23 [0.99]
	19/02/97	13.4	88.9 [0.19]	0.27	16.41 [0.18]	42.83 [0.48]	59.24 [0.67]
	20/02/97	15.0	79.1 [0.07]	0.22	8.89 [0.11]	16.44 [0.21]	25.33 [0.32]
	21/02/97	30.2	200.8 [0.19]	0.27	40.33 [0.20]	39.12 [0.19]	79.45 [0.40]
	26/02/97	33.8	316.2 [0.33]	0.39	100.07 [0.32]	72.54 [0.23]	172.61 [0.55]
	05/03/97	16.2	174.6 [0.57]	0.45	57.56 [0.33]	91.41 [0.52]	148.97 [0.85]
WRD_{50S}	07/01/97	42.4	205.9 [0.20]	0.14	30.60 [0.15]	320.87 [1.56]	351.47 [1.71]
	09/01/97	5.2	24.9 [0.07]	0.14	1.00 [0.04]	55.02 [2.21]	56.02 [2.25]
	17/02//97	46.4	754.6 [0.63]	0.47	208.44 [0.28]	292.12 [0.39]	500.56 [0.66]
	18/02/97	36.4	286.0 [0.39]	0.23	48.60 [0.17]	107.54 [0.38]	156.14 [0.55]
	19/02/97	13.4	99.5 [0.15]	0.22	8.25 [0.08]	30.82 [0.31]	39.08 [0.39]
	20/02/97	15.0	35.4 [0.05]	0.07	3.96 [0.11]	10.70 [0.30]	14.66 [0.41]
	21/02/97	30.2	181.8 [0.15]	0.18	36.23 [0.20]	23.08 [0.13]	59.31 [0.33]
	26/02/97	33.8	312.7 [0.37]	0.27	38.58 [0.12]	51.87 [0.17]	90.45 [0.29]
	05/03/97	16.2	147.4 [0.55]	0.27	35.91 [0.24]	41.13 [0.28]	77.04 [0.52]

Table 3.8 Complete data sets for rainfall events monitored at Nat_{C1} and Nat_{C2}

Site	Date	Rainfall period No.	Total rainfall (mm)	Total runoff (L) Peak discharge (Ls^{-1})]	Runoff Coefficient	Suspended sediment loss (g) [Loss per unit runoff ($g L^{-1}$)]	Bedload loss (g) [Loss per unit runoff ($g L^{-1}$)]	Total sediment loss (g) [Loss per unit runoff ($g L^{-1}$)]
Nat_{C1}	30/12/93	2	16	8054 [9.96]	0.25	2628 [0.33]	2936 [0.36]	5565 [0.69]
Nat_{C2}	30/12/93	1	15.6	11995 [28.7]	0.26	18071 [1.51]	7516 [0.63]	25588 [2.13]
Nat_{C2}	30/12/93	2	19.8	13470 [16.0]	0.23	2383 [0.18]	3108 [0.23]	5855 [0.41]

3.3.2 WRD_0 sediment transport equation parameter values

The monitoring data at WRD_0 (table 3.6) were used to fit parameter values to the sediment transport equation (eqn 2.8). However, the slope exponent, n_1 (eqn 2.8), cannot be fitted to data for one site as there is no slope variation. As a result, parameter values were fitted to the sediment transport equation with a 'lumped' coefficient (eqn 3.8).

$$T = K\int Q^{m_1}\,dt \tag{3.8}$$

where,

$$K = \beta_2 S^{n_1}$$

The resultant sediment loss-discharge relationship for the WRD_0 site was:

$$T_{WRD_0} = 0.146\int Q^{2.52}\,dt \quad (r^2 = 0.97;\ \text{no. of obs} = 4;\ df = 2;\ p < 0.02) \tag{3.9}$$

This relationship is significant at the 98% level. Figure 3.6 shows that the observed sediment losses compare well with the predicted sediment losses using equation 3.9 for events at WRD_0. Equation 3.9 is a reliable sediment loss-discharge relationship for WRD_0.

Willgoose and Riley (1998) derived an n_1 value of 0.69 for the Ranger WRD using a combination of monitoring data and rainfall simulation data. Based on this, n_1 was fixed at 0.69 and equation 3.9 was refitted to give the following sediment transport equation for the WRD_0 site:

$$T_{WRD_0} = 0.432S^{0.69}\int Q^{2.52}\,dt \tag{3.10}$$

For wide-channel geometry, such as WRD_0, Willgoose et al (1989) determined a m_1 value mathematically assuming the surface to be a flat plain with sheet flow conditions. This produced a value for m_1 of 1.8. Henderson (1966) considered that sediment discharge is proportional to the square of the runoff (ie $T \propto \int Q^2 dt$). The m_1 value fitted to the sediment transport equation for WRD_0 (eqn 3.10) is high compared with studies by Henderson (1966) and Willgoose et al (1989).

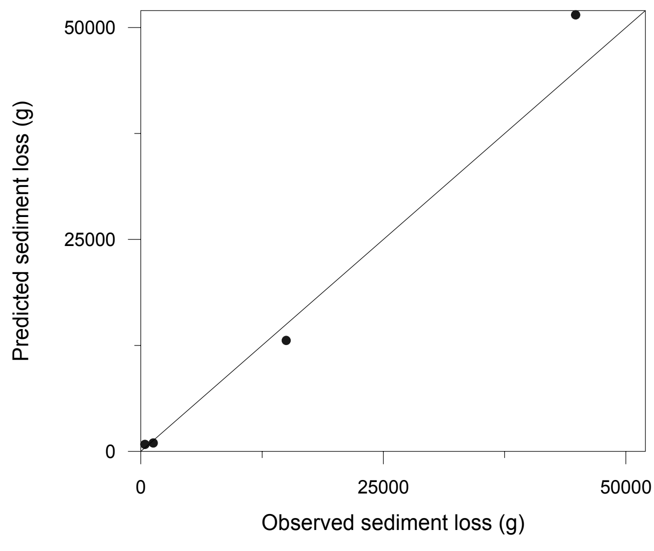

Figure 3.6 Predicted sediment loss (eqn 3.9) against observed sediment loss for the WRD_0 site using the observed data (table 3.6)

3.3.3 WRD_{50} sediment transport equation parameter values

The monitoring data (table 3.7) were used to fit parameter values to the sediment transport equation (eqn 2.8). However, similar to WRD_0 (section 3.3.2), the slope exponent, n_1 (eqn 2.8), can not be fitted to data for one site. As a result, event data were used to fit parameter values to equation 3.8 for WRD_{50C} and WRD_{50S} (eqns 3.11 and 3.12 respectively).

$$T_{WRD_{50C}} = 1.618\int Q^{1.29}dt \qquad (r^2 = 0.80;\ \text{no. of obs} = 9;\ df = 7;\ p < 0.01) \quad (3.11)$$

$$T_{WRD_{50S}} = 0.294\int Q^{0.74}dt \qquad (r^2 = 0.58;\ \text{no. of obs} = 9;\ df = 7;\ p < 0.02) \quad (3.12)$$

The relationship between predicted and observed soil loss (fig 3.7) indicates that equations 3.11 and 3.12 under-predict total sediment loss for the events occurring on 07/01/97 and 17/02/97 by approximately 50% at both sites. Both of these events occurred early in the Wet season and were observed to cause the most sediment loss. Equations 3.11 and 3.12 do not accurately predict these early, low frequency, large events.

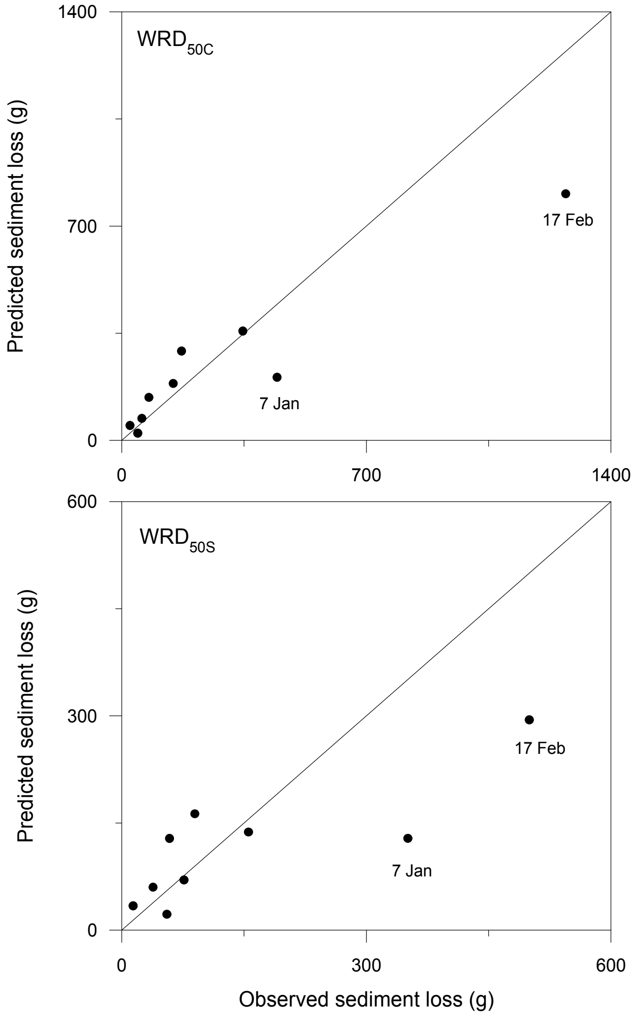

Figure 3.7 Relationship between predicted and observed sediment loss at WRD_{50C} and WRD_{50S} using equations 3.11 and 3.12 respectively

The high intensity events at WRD_{50C} on 07/01/97 and 17/01/97 removed 66% of the total sediment removed by the nine reported events (table 3.7). Similarly, the same events at WRD_{50S} removed 63% of the total sediment removed by the nine reported events.

Other studies have shown a similar dominance of large events. Edwards (1987) found that 10% of runoff events produced 90% of the total soil loss at long-term sites throughout the cropping regions of New South Wales. Wockner and Freebairn (1991) found that, out of 81 rainfall events that produced runoff at study sites on the eastern Darling Downs of Queensland, six storms caused 70% of the total soil erosion. A 28 year study of hilly farmland in Ohio, USA, showed that the five largest erosion events on the studied watersheds were responsible for 66% of the total erosion (Edwards & Owens 1991). Similarly, one event on the batter site removed 73% of the total sediment removed by the four reported events (table 3.6).

Therefore it is important that high sediment loss storms are accurately predicted, as one or two high intensity storms in a Wet season will remove a much greater amount of sediment than a number of low sediment loss events. Evans et al (1998) considered that, based on practical knowledge of the local natural system, representative storm events should be selected from a site to parameterise an equation that accurately predicts the low frequency high sediment loss events.

The relatively high number of data points representing the low sediment loss events (fig 3.7) may have biased the relationships fitted for the WRD_{50} sites (eqns 3.11 and 3.12). Two events that were observed to have low rainfall intensities, total runoff and peak discharges (09/01/97 and 20/02/97) were omitted from the parameter fitting process. The fitted equations using the amended data sets were:

$$T_{\mathrm{WRD}_{50C}} = 3.00\int Q^{1.64}dt \quad (r^2 = 0.78;\ \text{no. of obs} = 7;\ df = 5;\ p < 0.01) \qquad (3.13)$$

$$T_{\mathrm{WRD}_{50S}} = 0.696\int Q^{1.14}dt \quad (r^2 = 0.59;\ \text{no. of obs} = 7;\ df = 5;\ p < 0.05) \qquad (3.14)$$

Equations 3.13 and 3.14 better predict the large event on 17/02/97 but still under-predict sediment losses on 07/01/97 (fig 3.8).

The rainfall event on 07/01/97 was the first storm monitored and one of the first major storms of the season. It was been observed in other studies conducted by the authors in the region that these early large storms are responsible for initial removal of sediment loosened during the Dry season resulting in high sediment losses. For each sediment transport model fitted in this study the sediment loss from this event has been under-predicted. It is difficult to accurately predict the high sediment loss caused by large events which occur early in the Wet season.

As mentioned above, the slope exponent, n_1 (eqn 2.8), could not be fitted for the WRD_{50} site data. As discussed in section 3.3.2, Willgoose and Riley (1998) derived an n_1 value of 0.69 using combined rainfall simulation and monitoring data from the Ranger WRD. Evans et al (1997), using a laboratory rainfall simulator and mine spoil samples from Central Queensland, found that for one mine site the CREAMS (Knisel 1980) erodibility parameter (K) was inversely proportional to $S^{0.624}$ (ie $K \propto 1/S^{0.624}$). Other researchers (Foster 1982, Watson & Laflen 1986, Guy et al 1987) derived slope exponents ranging from 0.26 to 0.8. It appears that the value of 0.69 derived by Willgoose and Riley (1998) may be a realistic value to use in equation 2.8. Based on this, n_1 was fixed at 0.69 and equations 3.13 and 3.14 were refitted to give the following equations for the two sites:

$$T_{\mathrm{WRD}_{50C}} = 4.732S^{0.69}\int Q^{1.64}dt \qquad (3.15)$$

$$T_{\mathrm{WRD}_{50S}} = 1.014S^{0.69}\int Q^{1.14}dt \qquad (3.16)$$

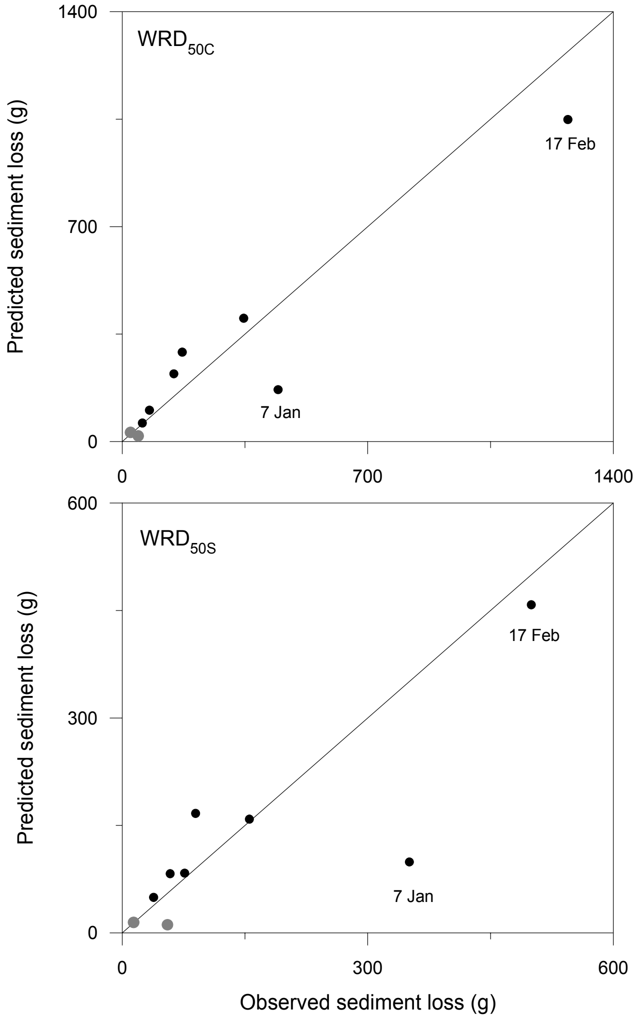

Figure 3.8 Relationship between predicted and observed sediment loss at WRD_{50C} and WRD_{50S} using equations 3.13 and 3.14 respectively. Events indicated by a black circle were used to parameterise the sediment transport equation (eqn 3.8); events indicated by a grey circle were omitted from the parameter fitting process.

3.3.4 Nat_C sediment transport equation parameter values

The monitoring data (table 3.8) were used to fit parameter values to the sediment transport equation (eqn 2.8). However, since the slope values for Nat_{C1} and Nat_{C2} are similar (19% and 22% slope respectively), the fitted value for the slope parameter, n_1, is unreliable. As a result, event data were used to fit parameter values to equation 3.8 for the Nat_C sites (eqn 3.17).

$$T_{Nat_C} = 0.107\int Q^{1.92}dt \quad (r^2 = 0.55;\ \text{no. of obs} = 3;\ df = 1;\ p > 0.4) \qquad (3.17)$$

Equation 3.17 is not significant at the 95% level (p is not <0.05). More event data were required to develop a significant relationship.

However, only a small number of monitored events had a complete set of rainfall, runoff and sediment data. To overcome this deficiency, methods for infilling missing data in the runoff and sediment record are developed below. This more comprehensive data set was then used for the sediment transport equation calibration.

3.3.4.1 Predicting suspended sediment data

A sediment concentration-discharge relationship was used to predict suspended sediment concentration data for the rainfall-runoff periods where suspended sediment data were missing. Willgoose and Riley (1998) used observed suspended sediment concentration data from natural rainfall events on areas of the WRD at Ranger to fit a sediment concentration-discharge relationship of the form:

$$c = \beta_2 Q^{m_2} S^{n_1} \tag{3.18}$$

where c is suspended sediment concentration (g L^{-1}), Q the discharge (Ls^{-1}) and S the local slope. The parameters β_2, m_2 and n_1 are fixed by flow geometry and erosion physics.

Willgoose and Riley (1998) noted that the c-Q relationship (eqn 3.18) fitted to the monitored data was poor. Within a rainfall-runoff event it was observed that the ratio c/Q at a given discharge was greater on the rising limb of the hydrograph than the ratio on the falling limb of the hydrograph. In other words, there was a temporal effect on the c data within a hydrograph that was not considered in the relationship (eqn 3.18). This temporal effect within the monitored data may have led to the poor fit of this equation (Willgoose & Riley 1998).

Figure 3.9 shows a plot of observed c against Q at Nat_{C1} and Nat_{C2} from a discrete rainfall event. The ratio c/Q at any chosen time on the rising limb of the hydrograph is greater than that for the same discharge on the falling limb. The 'clockwise loop' fitted for the c-Q data has been attributed to sediment depletion or the formation of an armoured layer before the runoff has peaked (Williams 1989).

Therefore, in this study it is important to incorporate a temporal component into the c-Q relationship in order to more accurately predict suspended sediment concentration where data were missing (eqn 3.19).

$$c = \beta_2' Q^{m_2'} S^{n_1'} t^b \tag{3.19}$$

where t is the time since start of runoff.

The constants β_2', m_2', n_1' and b were fitted to equation 3.19 using log-log multiple regression. Equation 3.19 can be expressed as follows:

$$Logc = Log\beta_2' + m_2' Log(Q) + n_1' Log(S) + bLog(t) \tag{3.20}$$

Equation 3.21 describes the fitted equation for the observed data collected at Nat_{C1} and Nat_{C2} combined:

$$c = 2.306 Q^{0.598} S^{1.19} t^{-0.523} \quad (r^2 = 0.814,\ p<0.001) \tag{3.21}$$

Percentage errors of parameters β_2', m_2', n_1' and b were calculated using the number of data points and the standard deviations provided by the regression analysis output. The parameters m_2' and b have a relative error of 0.3% and 0.4% respectively. The parameters β_2' and n_1' have a relative error of 5.7% and 2.5% respectively, comparatively higher than the relative errors for the first two parameters. The high relative errors associated with β_2' and the slope parameter n_1' may be due to only two values for slope being used to fit parameter values to equation 3.19. For this reason, the fitted slope parameter, n_1', is unreliable. Therefore, observed suspended sediment data were used to derive a c-Q relationship with a 'lumped' coefficient (eqn 3.22).

$$c = K' Q^{m_2'} t^b \tag{3.22}$$

where,

$$K' = \beta_2' S^{n_1'}$$

The resultant *c-Q* relationship for the Nat_C sites was:

$$c = 0.336 Q^{0.629} t^{-0.52} \quad (r^2 = 0.806,\ p<0.001) \tag{3.23}$$

The relative errors associated with the three parameters, β_3', m_3' and b_1, are 0.47%, 0.27% and 0.4% respectively. Overall, the errors associated with parameter values fitted to equation 3.22 are less than those fitted to equation 3.19. Therefore, equation 3.23 will be used to predict suspended sediment concentration data for the rainfall-runoff periods where suspended sediment data were missing.

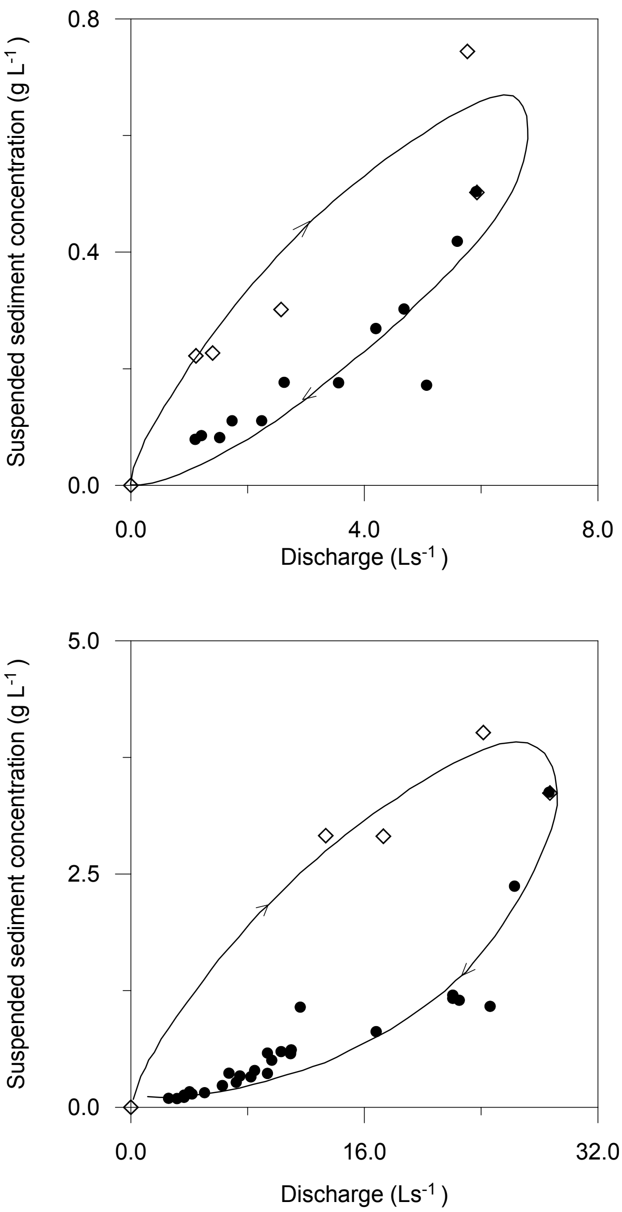

Figure 3.9 Suspended sediment concentration against discharge using monitored data from a discrete rainfall event at Nat_{C1} on 27 December (Top) and Nat_{C2} on 30 December (Bottom). Data are collected during the event on the rising limb of the hydrograph (indicated by ◊) and the falling limb of the hydrograph (●).

Three discrete rainfall-runoff periods were observed on 27 December and suspended sediment data were missing for one of these three rainfall-runoff periods at both Nat_{C1} and Nat_{C2} (appendix E). Suspended sediment data were also missing on part of the second rainfall-runoff period on 30 December at Nat_{C2}.

Using equation 3.23 suspended sediment concentration data was predicted for the above rainfall-runoff periods and combined with the observed data to calculate the total suspended sediment loss for these events, and hence provide a complete data set for these events. The rainfall, runoff and sediment loss data for the events on 27 December at both sites and on 30 December at Nat_{C2} are given in table 3.9.

Complete sedigraphs showing observed and predicted sediment discharge for events at Nat_{C1} and Nat_{C2} are shown in appendices B.3 and B.4 respectively.

3.3.4.2 Parameter fitting using a combination of observed and predicted suspended sediment data

Using all of the data in table 3.9, and excluding the event on 31 December at Nat_{C1} (which is discussed later), parameter values were fitted to the sediment transport equation (eqn 3.8) for both Nat_C sites (eqn 3.24).

$$T_{Nat_C} = 0.359\int Q^{1.43}dt \quad (r^2 = 0.65;\ \text{no. of obs} = 5;\ df = 3;\ p < 0.1) \qquad (3.24)$$

Equation 3.24 is not significant at the 95% level ($p > 0.05$).

Figure 3.10 shows that the derived sediment transport equation (eqn 3.24) is not a good predictor of total sediment loss for the first rainfall-runoff period on 30 December at Nat_{C2}. This may be because the number of rainfall events with complete data sets are still insufficient to establish an accurate prediction model.

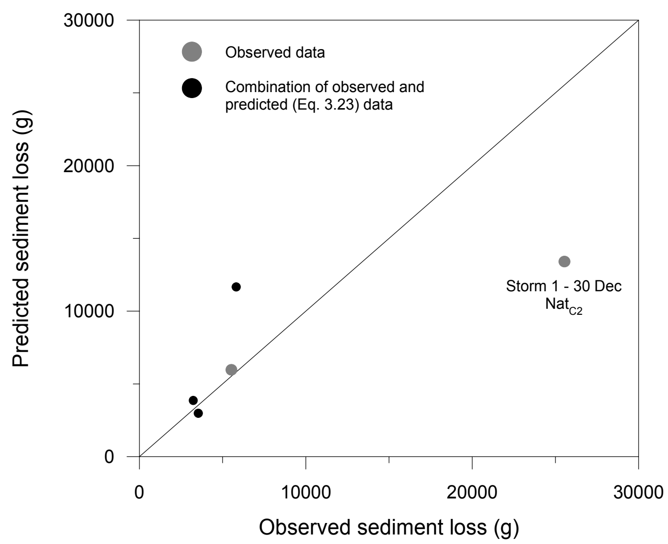

Figure 3.10 Predicted sediment loss (eqn 3.24) against sediment loss using a combination of observed and predicted (eqn 3.23) data for Nat_C sites (table 3.9)

Table 3.9 Complete data sets, using a combination of observed and predicted suspended sediment data, for rainfall events monitored at Nat_{C1} and Nat_{C2}.

Site	Date	Storm no.	Total rainfall (mm)	Total runoff (L) [Peak discharge (Ls^{-1})]	Runoff Coefficient	Suspended sediment loss (g) [Loss per unit runoff ($g\ L^{-1}$)]	Bedload loss (g) [Loss per unit runoff ($g\ L^{-1}$)]	Total sediment loss (g) [Loss per unit runoff ($g\ L^{-1}$)]
Nat_{C1}	27/12/93[(a)]	1, 2 & 3	20	5459 [6.98]	0.13	1624 [0.30]	1957 [0.36]	3581 [0.66]
	30/12/93	2	16	8054 [9.96]	0.25	2628 [0.33]	2936 [0.36]	5565 [0.69]
	31/12/93[(b)]	1	22	18204 [56.0]	0.41	31578 [1.73]	12824 [0.70]	44402 [2.44]
Nat_{C2}	27/12/93[(a)]	1, 2 & 3	24	6836 [9.13]	0.10	2516 [0.37]	756 [0.11]	3272 [0.48]
	30/12/93	1	15.6	11995 [28.7]	0.26	18071 [1.51]	7516 [0.63]	25588 [2.13]
	30/12/93[(a)]	2	19.8	13470 [16.0]	0.23	2747 [0.20]	3108 [0.23]	5855 [0.43]

a Total suspended sediment loss was partially predicted using eqn (3.23)

b DISTFW model parameters were used to predict the runoff.

Riley (1994) collected sediment data (suspended sediment and bedload) for two other rainfall-runoff events at Nat_{C1}, the first rainfall-runoff period on 30 December and a rainfall event on 31 December (appendix E). Complete runoff data, however, were not collected for these two rainfall events.

The rainfall event on 31 December at Nat_{C1} had eight observed discharge readings taken during the event (Riley 1994), all collected on the falling limb of the hydrograph. However, there were no runoff data for the rising stage of the hydrograph. To infill the missing part of the runoff record for this event, the fitted DISTFW model parameters for Nat_{C1} (table 3.4) were used to predict runoff data for the rising stage of the hydrograph. Rainfall data for this event on 31 December was used as input into the DISTFW rainfall-runoff model. The predicted runoff data for the rising stage of the hydrograph were combined with the observed data on the falling limb of the hydrograph to establish a complete runoff record for this rainfall event (appendix F). The combined observed and predicted runoff data were then used to calculate the total suspended sediment loss for the rainfall event on 31 December.

The first rainfall-runoff period on 30 December at Nat_{C1}, however, had no observed runoff data. Thus, runoff data predicted using the fitted DISTFW model parameters for Nat_{C1} could not be reliably used to derive parameter values for the sediment transport equation.

All of the data in table 3.9, including the event on 31 December at Nat_{C1}, were used to fit parameter values to the sediment transport equation (eqn 3.8). The resultant sediment loss-runoff relationship for the Nat_C sites is as follows:

$$T_{Nat_C} = 0.264\int Q^{1.61}dt \quad (r^2 = 0.84;\ \text{no. of obs} = 6;\ df = 4;\ p < 0.01) \quad (3.25)$$

Equation 3.25 better predicts total sediment loss for the first rainfall-runoff period on 30 December at Nat_{C2}, compared with that predicted using equation 3.24 (figs 3.11 and 3.10 respectively). However, equation 3.25 still under-predicts the total sediment loss for the larger rainfall events (fig 3.11).

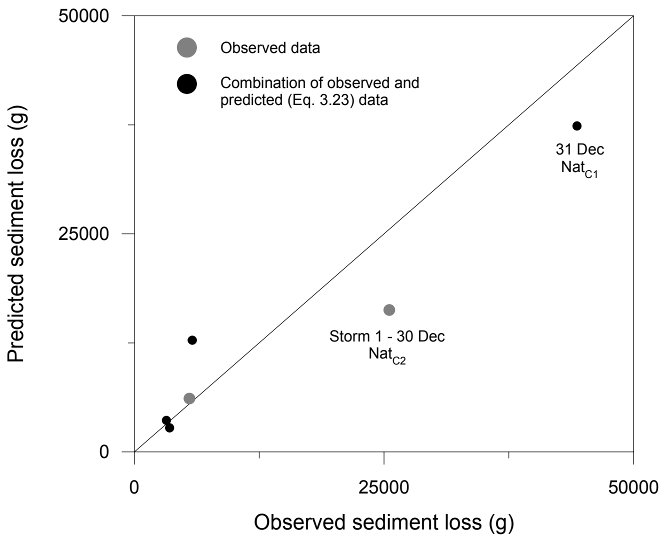

Figure 3.11 Predicted sediment loss (eqn 3.25) against sediment loss using a combination of observed and predicted (eqn 3.23) data for Nat_C sites (table 3.9)

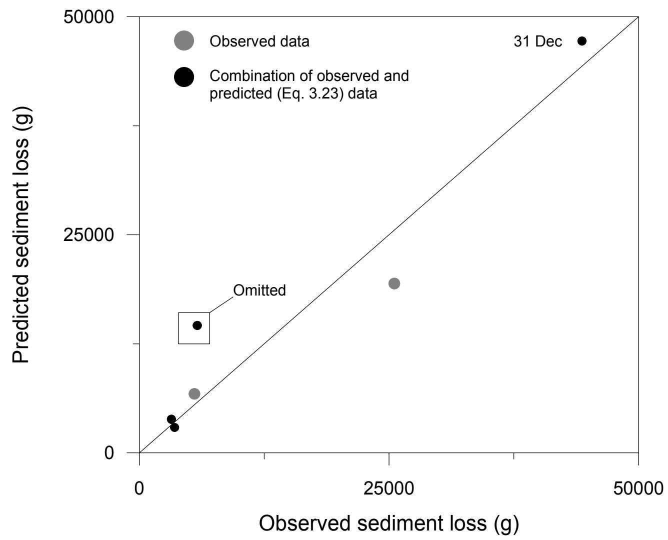

Figure 3.12 Predicted sediment loss (eqn 3.26) against sediment loss using a combination of observed and predicted (eqn 3.23) data for the Nat_C sites (table 3.9), omitting the second rainfall event on 30 December at Nat_{C2}

The two high intensity events at the Nat_C sites removed 80% of the total sediment removed by the six reported events (table 3.9). As discussed in section 3.3.3, it is important that high sediment loss storms are accurately predicted, and that representative storm events should be selected from a site to parameterise an equation that accurately predicts these low frequency high sediment loss events (Evans et al 1998). On this basis, equation 3.25 is still not an adequate sediment loss-runoff relationship for the Nat_C sites.

The second rainfall period on 30 December at Nat_{C2} had a low sediment loss per unit runoff value (table 3.9) and the sediment loss was over-predicted by more than 100% using equation 3.25. This rainfall event was considered to be a possible outlier and was therefore omitted from the parameter fitting process. The fitted equation using the amended data set is:

$$T_{Nat_C} = 0.251\int Q^{1.69}\,dt \quad (r^2 = 0.97;\ \text{no. of obs} = 5;\ df = 3;\ p < 0.003) \qquad (3.26)$$

Equation 3.26 is significant at the 99.7% level and better predicts the sediment losses of the larger rainfall events (fig 3.12).

The derived discharge exponent, m_1, value of 1.69 is within the range of m_1 = 1.45 to 1.71 found by Willgoose (1994) for the Pokolbin field catchment, New South Wales. The value here is also within the range of m_1 = 1.3 to 1.7 for a concave surface profile with fluvial erosion processes dominant (Kirkby 1971).

Multiplying discharge (Q) to the c-Q relationship (eqn 3.18) and then combining the result with the sediment transport equation (eqn 2.7), yields a relationship between the corresponding discharge exponents as shown:

$$m_1 = m_2 + 1$$

In putting the values of m_1 (1.69) and m_2 (0.63) fitted for the Nat_C sites into the above discharge exponent relationship indicates that the derived discharge exponent, m_1, value (eqn 3.26) correlates well with the discharge exponent, m_2, value fitted to the c-Q relationship (eqn 3.23).

As mentioned previously, the slope exponent, n_1 (eqn 2.8), could not be fitted for the Nat_C data. Willgoose and Riley (1998) derived an n_1 value of 0.69 for the Ranger WRD using a combination of monitoring data and rainfall simulation data. The slope exponent, n_1, value of 0.69, which is less than that derived in experimental studies (n_1~2.1) (Hancock 1997), implies that erosion increases with slope gradient at a decreasing rate. Kinnell and Cummings (1993) suggested that this can occur for soils that become armoured by large stable aggregates, a condition that exists at the Nat_C sites. The value of 0.69 was also used in further studies on the WRD at Ranger (Evans et al 1998) as a realistic value for the slope exponent. The lithology of the rocks at the Nat_C sites closely resemble the rocks found on the WRD at Ranger (Riley 1994). Therefore, although other studies have, in the absence of field data, generally assumed the n_1 value to be greater than one (Kirkby 1971, Willgoose et al 1989, Willgoose 1994), it could be reasonably assumed that the slope exponent at Nat_{C1} and Nat_{C2} is the same as the one derived by Willgoose and Riley (1998) for the WRD at Ranger.

Based on this, n_1 was fixed at 0.69 and equation 3.26 was refitted to give the following sediment transport equations for Nat_{C1} and Nat_{C2}:

$$T_{Nat_{C1}} = 0.791 S^{0.69} \int Q^{1.69} dt \quad (r^2 = 0.97;\ p < 0.003) \tag{3.27}$$

$$T_{Nat_{C2}} = 0.718 S^{0.69} \int Q^{1.69} dt \quad (r^2 = 0.97;\ p < 0.003) \tag{3.28}$$

The sediment transport model constant, β_2 (eqn 2.8), reflects differences in surface characteristics between sites, such as surface cover and erodibility (Evans et al 1998). A qualitative assessment by inspection of Nat_{C1} and Nat_{C2} suggests that vegetation cover and stone-cover is similar on the two sites. Furthermore, the runoff coefficients and sediment loss per unit runoff values at each site are similar for corresponding events (table 3.6). The β_2 values for Nat_{C1} and Nat_{C2} are very similar (eqns 3.27 & 3.28 respectively) which is consistent with these other similarities between the two sites and their surface characteristics.

3.3.5 Nat_S sediment transport equation parameter values

Complete data sets were obtained from rainfall events monitored at Nat_S (Bell & Willgoose 1997). These monitoring data were used to fit parameter values to the sediment transport equation (eqn 3.8) to give the following sediment loss-discharge relationship for Nat_S (Bell & Willgoose 1997):

$$T_{Nat_S} = 0.068 \int Q^{1.12} dt \quad (r^2 = 0.99;\ \text{no. of obs} = 6;\ df = 4;\ p < 0.001) \tag{3.29}$$

Assuming the exponent on the slope term, n_1, was 0.69 (see previous sections) the equation was refitted as follows:

$$T_{Nat_S} = 0.817 S^{0.69} \int Q^{1.12} dt \tag{3.30}$$

3.4 Discussion

Rainfall-runoff data collected at the study sites were used to fit parameter values for the DISTFW hydrology model (table 3.4). Two sets of parameter values were fitted to the DISTFW hydrology model using NLFIT–kinematic wave parameters (c_r and e_m) and infiltration parameters (Sphi & phi).

The fitted e_m parameter values for the Nat_C sites (table 3.4) are typical of triangular rill flow and the fitted e_m parameter values for the WRD_0, WRD_{50} and Nat_S sites (table 3.4) are more typical of constant depth sheet flow (Willgoose & Kuczera 1995). By inspection the e_m

parameter values fitted in this study appear to represent the flow geometry that exists at these sites.

Differences in the c_r value may be attributed to different conveyance properties such as surface roughness or surface treatments on the sites (Willgoose & Kuczera 1995). The fitted c_r values in this study (table 3.4) suggest that the conveyance properties on each of the study site surfaces are similar.

The long-term infiltration parameter value, phi, fitted for the sites on the waste rock dumps (WRD_0 and WRD_{50}) are greater than that fitted for the natural sites (Nat_C and Nat_S) (table 3.4). And the sorptivity value, Sphi, fitted for WRD_0 is similar to that fitted for Nat_C and Nat_S (table 3.4).

The relatively high infiltration parameter values fitted to the sites on the waste rock dumps may reflect (1) the increased level of stone cover at WRD_0 and WRD_{50} (Agassi & Levy 1991), and (2) the unconsolidated nature of the batter slopes at WRD_0 and WRD_{50}.

The long-term temporal changes in the DISTFW hydrology model parameter values are discussed in section 4.

The sediment transport equation (eqn 2.8) fitted for each of the study sites is shown below (fig 3.13). These equations will be used to derive the fluvial sediment transport rate in the landform evolution model, SIBERIA.

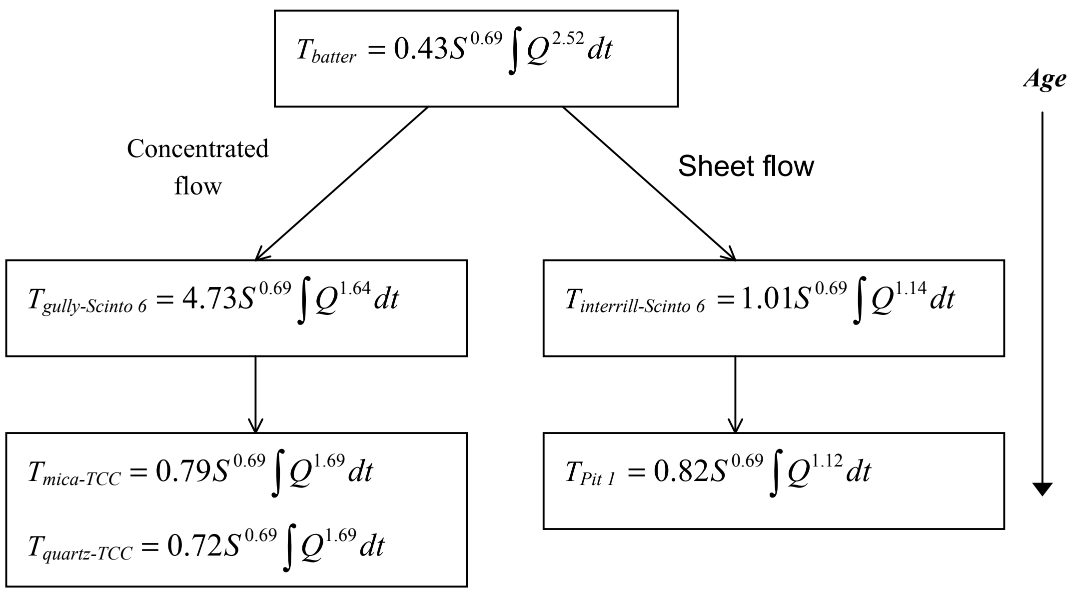

Figure 3.13 A schematic representation showing the age and the sediment transport equations derived for each of the study sites

The relatively high m_1 value fitted to the sediment transport equation for WRD_0 (fig 3.13) indicates that flow from this site has a high sediment carrying capacity or that there may be more sediment available for transport at WRD_0 than at the other sites (Rickenmann 1997).

The lower m_1 value fitted to both of the WRD_{50} sites, relative to WRD_0 (fig 3.13), may be due to factors such as compaction, surface armouring and soil and ecosystem development WRD_{50}. As a result, there may be less fine sediment available for transport giving detachment-limited conditions (Howard 1994). This result indicates that there is a short-term temporal effect on the m_1 parameter value under both concentrated flow and sheet flow conditions. The drop in the m_1 value in the short term suggests that the erosion rate on a rehabilitated site surface may decline rapidly in the early years, which supports studies by Graf (1977), Riley (1992) and Loch and Orange (1997).

Figure 3.13 also shows that the m_1 values fitted for the WRD_{50} sites are similar to those fitted for Nat_C and Nat_S for concentrated flow and sheet flow conditions respectively. That is, after the initial 50 year period after rehabilitation, there is very little change in the m_1 value in the long term. The trend in m_1 parameter values, both during the short term and the long term, will be discussed further in section 4.

For a given rainfall event the total sediment loss from a site, with surface conditions described by each of the derived DISTFW parameter values and sediment transport equations, could be estimated to range in descending order between each of the study sites as shown below.

Concentrated flow conditions: $T_{\mathrm{WRD}_0} > T_{\mathrm{WRD}_{50C}} \approx T_{TCC}$

Sheet flow conditions: $T_{\mathrm{WRD}_0} > T_{\mathrm{WRD}_{50S}} \approx T_{\mathrm{Nat}_S}$

3.5 Conclusions

Sediment loss-runoff relationships were parameterised for the WRD_0, WRD_{50} and Nat_C sites. Initially, runoff and sediment loss data collected at Nat_C were found to be insufficient to establish a statistically significant sediment loss-runoff relationship. A *c-Q* relationship, incorporating a temporal component, was used to predict suspended sediment concentration data for the rainfall-runoff periods where data were missing. This ‘time’ parameter in the relationship accounted for the observed hysteresis effect in individual sedigraphs, where suspended sediment concentration was higher on the rising limb of the hydrograph than the falling limb.

The hydrology model parameter values fitted for Nat_{C1} using DISTFW–NLFIT were used to predict the runoff data for part of a hydrograph for a rainfall event monitored at Nat_{C1} where data were missing.

As a result of this infilling of missing runoff and sediment data, all rainfall events at Nat_C, including the events consisting of predicted runoff and sediment loss data, were able to be used to obtain a statistically significant sediment loss-runoff relationship.

The parameterised sediment loss-runoff relationships for each of the study sites showed:

- that because n_1 parameter values could not be determined with the available data, no temporal trend in n_1 could be determined, and
- that there is a rapid change in the m_1 parameter values in the short term (50 years) for concentrated flow and sheet flow conditions, after which the m_1 value changes little over the long term. This temporal change is discussed further in section 4.

4 The effect of ecosystem development on landform evolution modelling

4.1 Introduction

An important part of the design of a rehabilitated post-mining landform is to be able to predict the surface stability of the final landform. Previous studies by Willgoose and Riley (1998) and Evans et al (1998) have used the landform evolution model, SIBERIA, to model the proposed 'above-grade' rehabilitated landform at Ranger. Landform evolution modelling, using SIBERIA, in these studies was based on input parameter values derived from data collected from areas of the WRD at Ranger. However, these input parameter values were assumed to remain constant throughout the period that was simulated and hence the possible effect of weathering and ecosystem development on the landforms during the 1000 y period were not considered.

The aim of this section is to assess how erosion and hydrology characteristics of landforms, and hence SIBERIA input parameter values, are affected by temporal change. To more accurately predict the stability of the proposed rehabilitated landform at Ranger the temporal effects, which may occur, on the SIBERIA input parameter values should be incorporated into the landform evolution modelling at Ranger. In order to achieve this, the rate of change in SIBERIA input parameter values, due to temporal effects such as weathering and ecosystem development on the surface of the proposed rehabilitated landform at Ranger, is required.

In this section the DISTFW hydrology model and the sediment transport equation, parameterised in section 3 using monitoring data from rainfall events on the each of the study sites, were used to derive input parameter values for the SIBERIA model. The approximate age of each of the study sites is estimated and, in turn, the rate of change in each of the SIBERIA input parameter values is predicted. Finally, the rate of change of input parameter values is incorporated into SIBERIA modelling of the rehabilitated landform at Ranger.

4.2 Age of the study sites

Each study site represents the surface properties likely to develop at Ranger at various times after rehabilitation. The following sub-sections discuss the estimation of the approximate age of the WRD_0, WRD_{50}, Nat_C and Nat_S sites.

4.2.1 WRD_0 site

The surface condition of the WRD_0 site is assumed to be representative of the proposed final rehabilitated condition immediately after mining is completed. Therefore, in this study, the WRD_0 parameter values are considered to represent the landform at zero years after rehabilitation.

As discussed in section 1 (section 1.3.5) the batter slope on the waste rock dump at Ranger, in time, could have two evolutionary paths: (1) the surface will remain planar under sheet flow conditions, and (2) the surface will become incised under concentrated flow conditions (fig 1.6).

4.2.2 WRD_{50} site

The surface condition at WRD_{50} is assumed to be representative of the surface characteristics that may develop on the WRD at Ranger in the short term. In this study parameter values were derived for two areas — WRD_{50C} and WRD_{50S} — which represent the landform at 50 y after rehabilitation under concentrated flow and sheet flow conditions respectively.

4.2.3 Nat_S site

The Nat_S site is representative of the surface condition at Ranger after revegetation and weathering under sheet flow conditions in the very long term (Bell & Willgoose 1997). Nat_S is located on the Koolpinyah surface, the most mature and erosionally stable landform in the Alligator Rivers Region (Nanson et al 1990). The Koolpinyah surface was formed during late Tertiary (Pliocene) to early Pleistocene times (Hays 1971 as cited in Nanson et al 1990) and, according to Nanson et al (1990), is probably > 1.3 Ma.

The location of Nat_S on the Koolpinyah surface, surrounded by sandstone escarpment, is shown in figure 4.1. The escarpment comprises resistant quartz sandstone of the Kambolgie formation, and overlies less resistant Cahill formation metamorphics (Needham 1988). As erosion attacks the less stable underlying rocks the more resistant sandstone is undermined and collapses, causing the escarpment to gradually retreat across the landscape at a rate of approximately 1 m per 1000 y (Galloway 1976).

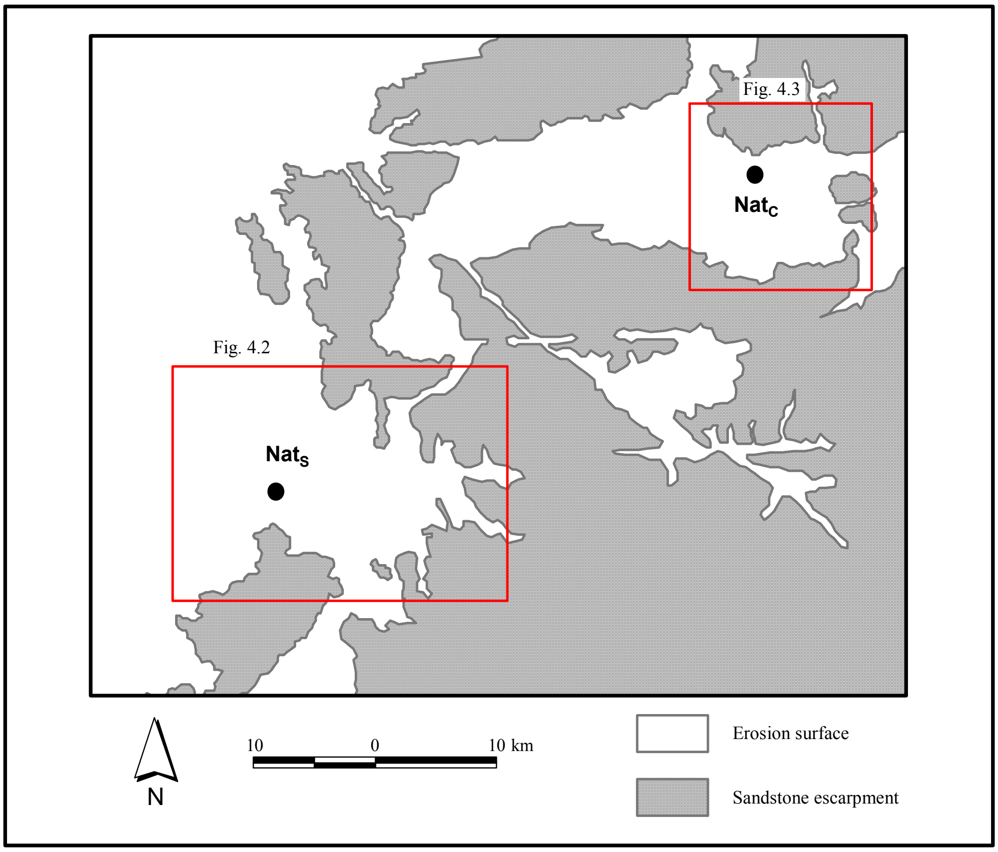

Figure 4.1 Location of Nat_C and Nat_S analogue study sites relative to the sandstone escarpment. The two outlined areas represent the close-up of the two study sites as shown in figures 4.2 and 4.3.

In this study it is assumed that tributaries of Magela Creek have eroded the sandstone escarpment in the area shown in figure 4.2. Therefore, it is also assumed that the escarpment has retreated in an approximate southerly direction from Nat_S. The average line of escarpment retreat from Nat_S is shown in figure 4.2. The average measured distance from Nat_S to several points along the line of escarpment retreat was approximately 3.2 km. Assuming the rate of escarpment retreat is 1 m per 1000 years, the age of the Nat_S surface is estimated to be 3.2 Ma. This value is in agreement with the age estimate for the Koolpinyah surface given in previous studies such as Nanson et al (1990).

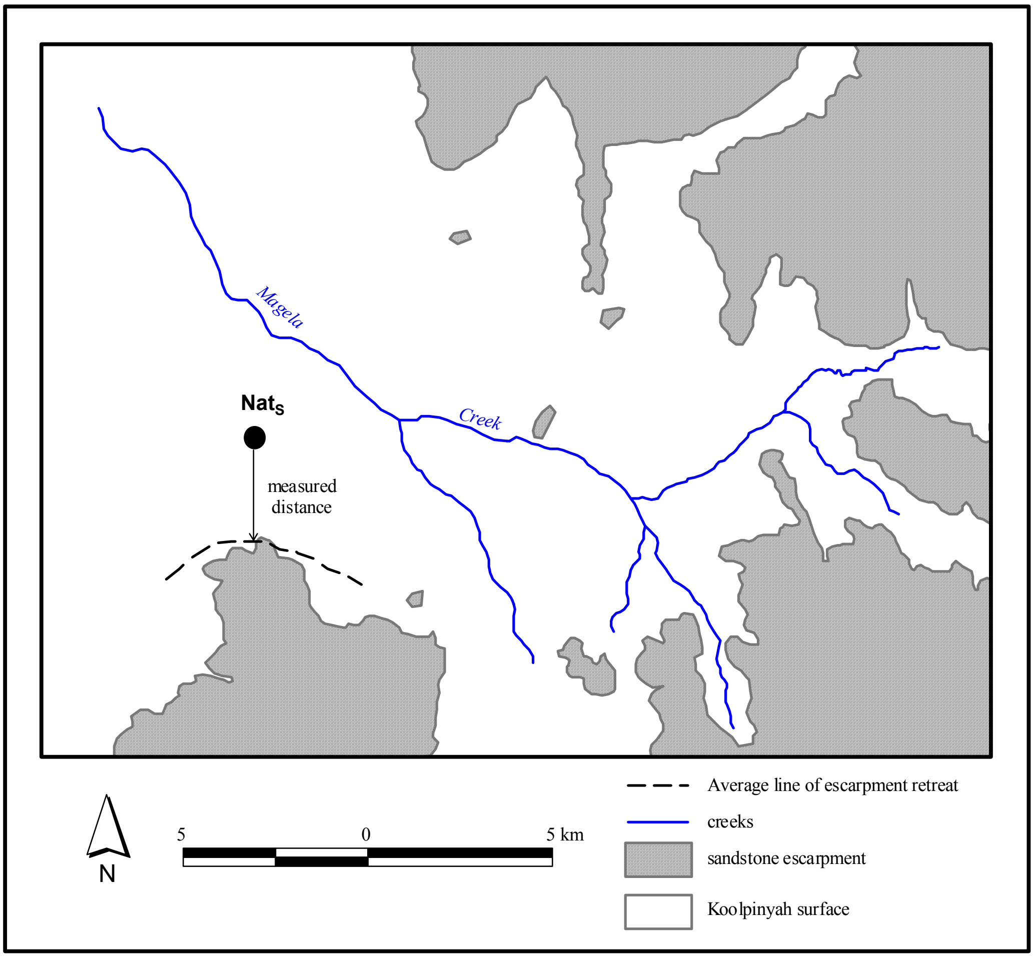

Figure 4.2 Escarpment retreat from Nat_S on the Koolpinyah surface. Distances were measured from Nat_S to various positions along the average line of escarpment retreat and the average distance was determined.

4.2.4 Nat_C sites

The Nat_C sites are assumed to be representative of the characteristics of soils that may develop on weathered waste rock at Ranger under concentrated flow conditions over the long term (Uren 1992).

The location of Nat_C surrounded by the sandstone escarpment is shown in figure 4.1.

Figure 4.1 indicates that Nat_C is located closer to the retreating escarpment than Nat_S and so it can be reasonable to assume that the Nat_C site surface is younger than the Nat_S surface.

Tin Camp Creek (TCC) flows on both sides of three small sandstone outliers located between the main areas of sandstone escarpment (fig 4.3). In this study it is assumed that the TCC tributaries have eroded the sandstone on both sides to leave these remaining outliers of sandstone that form a catchment boundary. Therefore, it is also assumed that the escarpment has retreated in an approximate southerly direction from Nat_C. The average line of escarpment retreat from Nat_C is shown in figure 4.3. The average measured distance from Nat_C to several points along the line of escarpment retreat was approximately 2.1 km. Assuming the rate of escarpment retreat is 1 m per 1000 y, the age of the Nat_C site surface is estimated to be 2.1 Ma.

The age of the Nat_C site surface is younger than the Nat_S site surface. The topography of the sites would support this result. Nat_S is on a peneplain and the Nat_C sites comprise dambos on rounded hills that have not reached the peneplain stage.

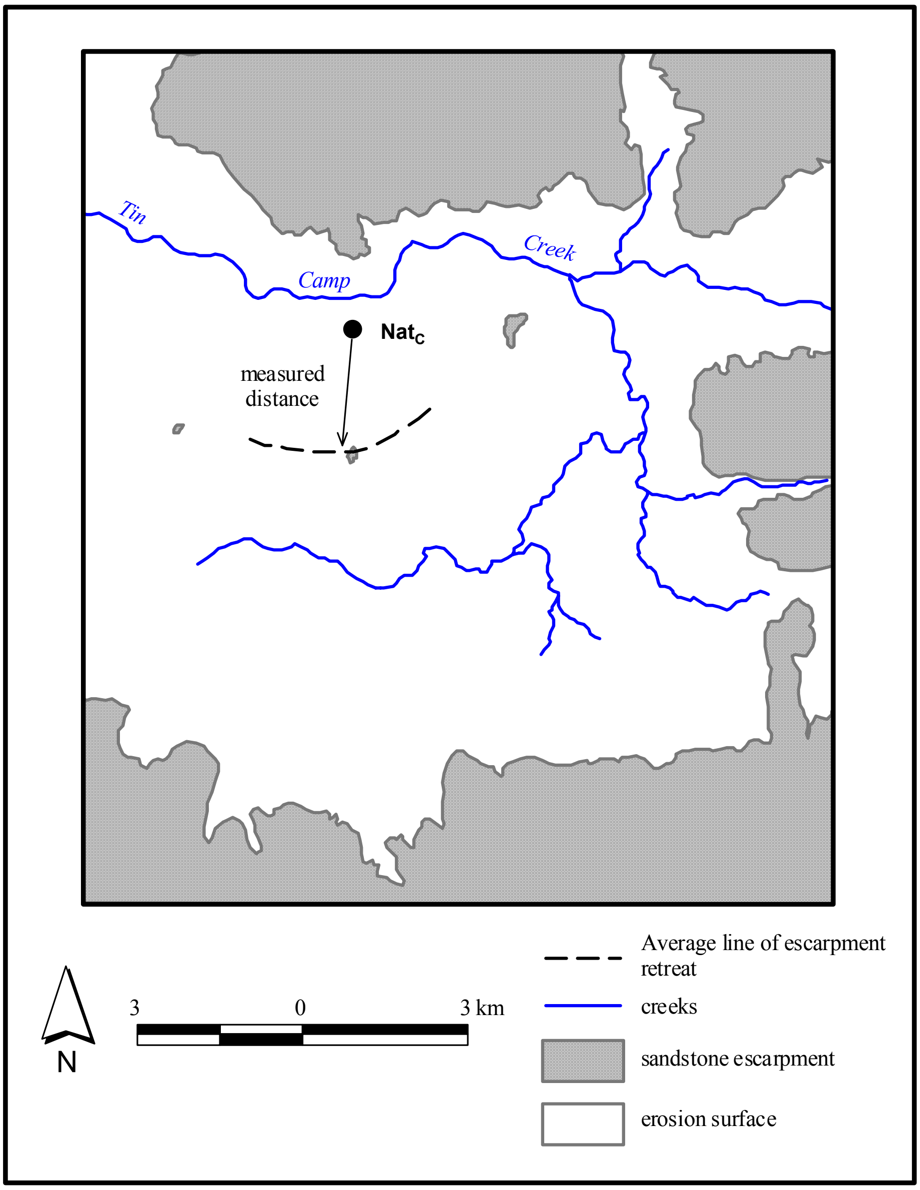

Figure 4.3 Escarpment retreat from Nat_C. Distances were measured from Nat_C to various positions along the average line of escarpment retreat and the average distance was determined.

4.3 Derivation of SIBERIA model parameter values

As discussed in section 1, the WRD_0, WRD_{50}, Nat_C and Nat_S sites are considered to be representative of the surface hydrology and erosion characteristics that would exist on the WRD at Ranger at various stages after rehabilitation (fig 1.2). That is, WRD_0 parameter values represent the landform at zero years immediately after rehabilitation; WRD_{50C} and WRD_{50S} parameter values represent concentrated flow and sheet flow conditions respectively on the landform 50 y after rehabilitation; and the parameter values fitted for the natural sites, Nat_C and Nat_S, represent concentrated flow and sheet flow conditions respectively after rehabilitation on the landform in the long term.

As discussed in section 2, the landform evolution modelling process, using SIBERIA, requires two types of parameters — primary and secondary parameters (fig 2.1). The primary parameters in SIBERIA modelling represent the hydrology and erosion characteristics of the site where monitoring data are collected. The secondary parameters represent the long-term average SIBERIA model parameter values for the landform being modelled and are dependent on the primary parameter values fitted for a site. The primary parameter values were fitted to the DISTFW hydrology model and the sediment transport equation (eqn 2.8) for each study site in section 3. The secondary parameter values for each of the study sites are derived in the following sub-sections.

4.3.1 Secondary parameter values

As shown in figure 2.1, the secondary parameter derivation process is divided into three sections: (1) parameterisation of the area-discharge relationship (eqn 2.10); (2) determination of a long-term average sediment loss rate, Q_s (eqn 2.4); and (3) derivation of the sediment transport rate coefficient, β_1 (eqn 2.12). A final parameter, the scaling coefficient value α, which can be used to predict the relative degree of simulated valley development and incision likely to form on the landform being modelled (Willgoose & Loch 1996) is discussed in section 4.3.1.4.

4.3.1.1 Area-discharge relationship

The standard form of the area-discharge relationship in this modelling is a power function (eqn 2.10). This is the type of relationship also identified for river basins (Rodriguez-Iturbe & Rinaldo 1997). The fitted area-discharge relationships (eqn 2.10) for the 1.6 km^2 catchment on the proposed 'above-grade' option for Ranger, based on the primary DISTFW hydrology model parameter values derived for the WRD_0, Nat_C and Nat_S sites, are described by the following equations (fig 4.4).

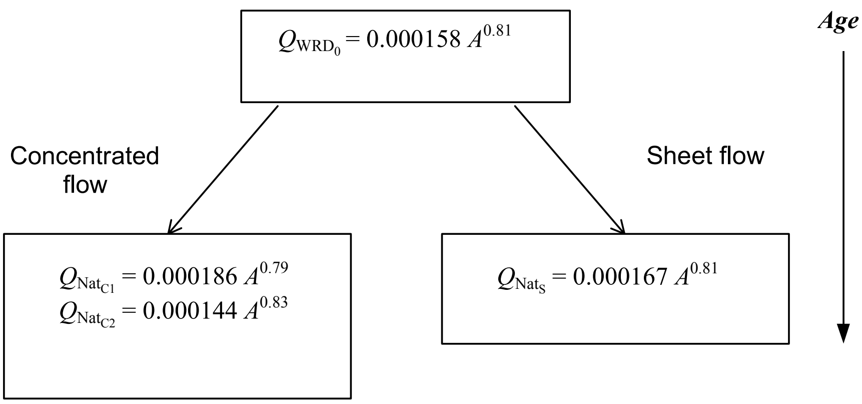

Figure 4.4 A schematic representation showing the area-discharge relationships fitted for the WRD_0, Nat_C and Nat_S sites

A power function area-discharge relationship could not be fitted to the WRD_{50} site data.

Figure 4.5 is a plot of peak discharge against area for the 1.6 km^2 catchment (fig 2.3) for the WRD_0, Nat_{C2} and Nat_S site surface condition. The log-log linear relationship observed in figure 4.5 for the proposed constructed landscape at Ranger is typical of that expected in nature (Rodriguez-Iturbe & Rinaldo 1997).

Figure 4.5 also shows that it is difficult to identify a difference in the m_3 and β_3 values fitted for each site condition. The area-discharge relationship fitted for the surface condition of Nat_C and Nat_S (both natural, undisturbed sites which represent the soil characteristics likely to develop at Ranger in the long term under concentrated flow and sheet flow conditions respectively) is very similar to that fitted for the surface condition of WRD_0 (the least mature site representing the Ranger surface immediately after mining is completed) (figs 4.4 & 4.5).

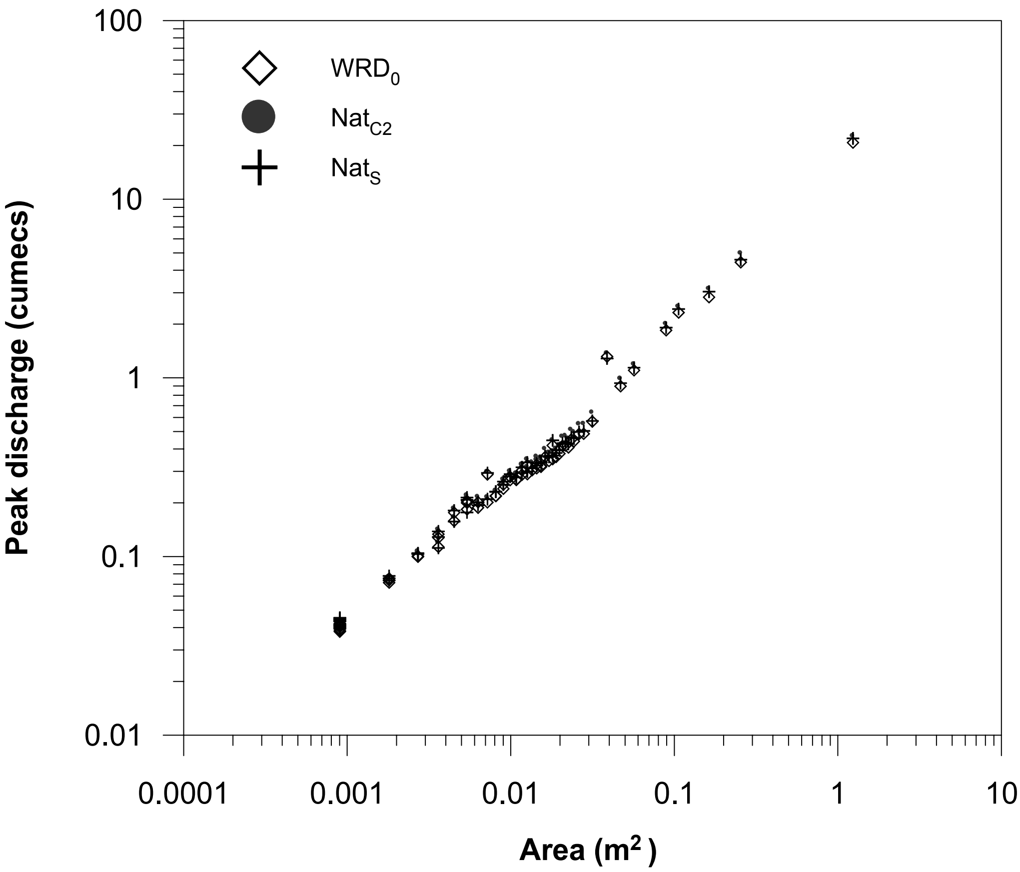

Figure 4.5 Area-discharge relationships for the 1.6 km^2 catchment on the proposed 'above-grade' option at Ranger for the WRD_0, Nat_{C2} and Nat_S site surface condition

It was therefore decided that since the fitted area-discharge relationships (fig 4.4) were almost identical an average value of β_3 and m_3 fitted for the WRD_0, Nat_C and Nat_S site conditions were used for the WRD_{50} site condition (eqn 4.1).

$$Q_{WRD_{50}} = 0.00016\, A^{0.81} \tag{4.1}$$

Minor differences in the coefficient value, β_3, may be attributed to different surface conditions or surface treatments on the WRD (Willgoose & Riley 1998). The coefficient values, β_3, fitted for the various site conditions in this study (table 4.1) suggest that the runoff rates on the 1.6 km^2 catchment for the various sets of conditions are similar.

The acceptable range for m_3 values is 0.5 to 1.0 (Strahler 1964, Willgoose et al 1991a). The m_3 values fitted to the area-discharge relationship (eqn 2.10) for each of the study sites (table 4.1) are within this range. The fitted m_3 values are also similar to those fitted for the proposed rehabilitated landform at Ranger using hydrology model parameters calibrated from various plots on the WRD at Ranger (Willgoose & Riley 1998, Evans et al 1998). The m_3 values fitted in these studies ranged between 0.8 to 0.9.

Table 4.1 The secondary parameter values for each study site

Flow condition	Site	Secondary parameter				
		β_3	m_3	Q_s (m^3 y^{-1})(1)	α	β_1 (2)
Concentrated flow	WRD_0	1.58×10^{-4}	0.81	1.59×10^8	1.51	1.3×10^4
	WRD_{50C}	1.60×10^{-4}	0.81	2.81×10^5	0.47	2.7×10^2
	Nat_{C1}	1.86×10^{-4}	0.79	4.41×10^5	0.47	5.0×10^2
	Nat_{C2}	1.44×10^{-4}	0.83	2.75×10^5	0.57	1.8×10^2
Sheet flow	WRD_0	1.58×10^{-4}	0.81	1.59×10^8	1.51	1.3×10^4
	WRD_{50S}	1.60×10^{-4}	0.81	7.90×10^2	-0.11	3.1×10^0
	Nat_S	1.67×10^{-4}	0.81	8.29×10^2	-0.14	3.1×10^0

(1) Uncorrected for node scale and slope

(2) Corrected for node scale (eqn 2.12)

4.3.1.2 Long-term average sediment loss rate

To determine the long-term sediment loss rate a runoff series for the historical rainfall records at Jabiru was created using the primary DISTFW hydrology model parameter values calibrated for each site (table 3.4). The runoff series from the 1.6 km^2 catchment on the proposed rehabilitated landform at Ranger for each site condition is given in table 4.2.

The runoff series was then used to determine annual sediment losses for the 1.6 km^2 catchment (table 4.2) using the sediment transport equation (eqn 2.8) fitted for each site condition in section 3 (fig 3.13). The average annual sediment loss, Q_s (eqn 2.4), for the WRD_0, WRD_{50}, Nat_C and Nat_S surface conditions are shown in table 4.1. The Q_s value is uncorrected for node scale and slope (see section 2.4.3 'Slope correction') and therefore is not a true prediction of the sediment loss from the catchment.

4.3.1.3 Sediment transport rate coefficient

The sediment transport rate coefficient value (eqn 2.12) is a reflection of the rate of sediment removal likely to occur on the landform being modelled. For example, the comparatively high sediment transport rate coefficient value derived for the WRD_0 site condition (table 4.1) indicates that sediment is removed at a greater rate on the landform with these surface conditions. The comparatively low sediment transport rate coefficient values derived for the WRD_{50S} and Nat_S site condition (table 4.1) indicates that sediment is removed at a slower rate on the landform with these surface conditions.

4.3.1.4 Scaling coefficient

Many studies, such as Flint (1974), Tarboton et al (1989) and Willgoose et al (1991a), have discussed a relationship between area (A) and slope (S) in channels of the form:

$$A^{\alpha}S = \text{constant} \qquad (4.2)$$

Where α is the scaling coefficient value.

Table 4.2 Annual runoff and long-term average sediment loss from the 1.6 km^2 catchment on the proposed rehabilitated landform at Ranger. The sediment losses are uncorrected for node scale and slope.

Year	Rainfall (mm)	WRD_0 Total runoff (m^3 y^{-1} x 10^5)	WRD_0 Sediment loss (m^3 y^{-1} x 10^7)	WRD_{50C} Total runoff (m^3 y^{-1} x 10^5)	WRD_{50C} Sediment loss (m^3 y^{-1} x 10^5)	WRD_{50S} Total runoff (m^3 y^{-1} x 10^5)	WRD_{50S} Sediment loss (m^3 y^{-1} x 10^2)	Nat_{C1} Total runoff (m^3 y^{-1} x 10^6)	Nat_{C1} Sediment loss (m^3 y^{-1} x 10^4)
1972	1163	4.74	12.13	4.34	3.92	4.82	10.88	1.80	40.66
1973	1353	5.49	25.51	5.09	6.29	5.67	13.82	2.11	50.87
1974	1604	3.63	6.82	3.13	2.26	3.41	7.24	2.45	39.83
1975	1642	6.15	28.12	5.73	6.80	6.33	15.04	2.54	57.63
1977	928	3.36	8.33	2.99	2.23	3.21	6.96	1.45	30.84
1978	1467	6.08	11.68	5.61	3.94	6.34	13.78	2.29	51.06
1979	1193	4.05	4.92	3.64	1.99	3.92	7.96	1.86	35.01
1980	1663	6.36	13.74	5.95	4.31	6.73	14.58	2.59	54.38
1984	2082	9.30	72.82	8.73	10.81	9.56	22.62	3.23	8.43
1986	1145	2.51	0.85	2.12	0.55	2.08	3.66	1.75	26.29
1987	1277	3.69	7.47	3.33	2.49	3.68	8.01	1.95	37.34
1988	1135	3.97	10.51	3.68	2.90	4.17	9.13	1.73	34.07
1989	1152	3.85	4.38	3.59	1.86	4.04	8.21	1.74	30.97
Average sediment loss rate, Q_s, (m^3 y^{-1})			1.59 x 10^8		2.81 x 10^5		7.91 x 10^2		4.41 x 10^5

Table 4.2 continued

Year	Rainfall (mm)	Nat_{C2} Total runoff (m^3 y^{-1} x 10^5)	Nat_{C2} Sediment loss (m^3 y^{-1} x 10^4)	Nat_S Total runoff (m^3 y^{-1} x 10^5)	Nat_S Sediment loss (m^3 y^{-1} x 10^2)
1972	1163	9.66	26.44	5.32	8.12
1973	1353	11.4	33.83	6.12	9.69
1974	1604	10.3	21.10	4.35	6.18
1975	1642	12.6	37.24	6.88	10.89
1977	928	8.00	18.89	3.88	5.66
1978	1467	12.8	32.95	6.95	10.37
1979	1193	9.86	20.94	4.75	6.70
1980	1663	13.7	33.73	7.19	10.68
1984	2082	18.4	57.79	10.42	16.28
1986	1145	7.77	13.05	3.08	3.96
1987	1277	9.50	21.66	4.32	6.30
1988	1135	9.04	21.74	4.55	6.75
1989	1152	8.37	18.35	4.35	6.23
Average sediment loss rate, Q_s, (m^3 y^{-1})			2.75×10^5		8.29×10^2

Willgoose et al (1991a) showed that the scaling coefficient value can be determined using an equation of the form:

$$\alpha = \frac{m_3 m_1 - 1}{n_1} \tag{4.3}$$

where m_1 and n_1 are primary parameters fitted to the sediment transport equation (eqn 2.8) and m_3 is a secondary parameter fitted to the area-discharge relationship (eqn 2.10).

The scaling coefficient value, α (eqn 4.3), is not an input parameter for the SIBERIA landform evolution model. However, in this study, the scaling coefficient value is used to establish a prediction of the relative degree of simulated valley development and incision likely to form on the landform being modelled (Willgoose & Loch 1996). Hancock (1997) also used the scaling coefficient value to check the validity of the selected input parameters, m_1 and n_1.

Secondary parameter values, m_3 (table 4.1), and primary parameter values, m_1 and n_1, derived for the WRD_0, WRD_{50}, Nat_C and Nat_S sites in section 3 (fig 3.13), were used to determine the corresponding scaling coefficient values (eqn 4.3). The scaling coefficient values for each study site are given in table 4.1.

Scaling coefficient values between 0.46 and 0.69 were calculated using parameter values, m_1, n_1 and m_3, fitted in previous studies for various plots on the WRD at Ranger (Willgoose & Riley 1998, Evans et al 1998). Tarboton et al (1989), using digital maps of the St Joe River network, Idaho, found the value of the scaling coefficient to be about 0.47. The scaling coefficient values calculated for WRD_{50C} and the Nat_C sites fall within the range of values previously determined in the above studies. The large scaling coefficient value calculated for WRD_0 (1.51), and the low scaling coefficient values calculated for WRD_{50S} (-0.11) and Nat_S (-0.14) however, do not fall within this range and this is probably because of the relatively high and low m_1 parameter values fitted to the sediment transport equation respectively (fig 3.13).

The scaling coefficient, α (eqn 4.3), influences the degree of incision, valley depths and the number of valleys on a landform (Willgoose & Loch 1996). A more incised landform with deeper and more valleys will occur with a greater scaling coefficient value. Data presented in Evans et al (1998) showed a similar trend. In this study, the comparatively large scaling coefficient value fitted for WRD_0 site conditions (table 4.1) would indicate a greater ability to develop valleys and ridges on the landform with these surface conditions in the long term. The comparatively low scaling coefficient values fitted for WRD_{50S} and Nat_S site conditions (table 4.1) would indicate that less erosion and fewer valleys will form on the landform with these surface conditions in the long term.

4.4 Temporal effect on SIBERIA model parameter values

4.4.1 Primary parameter values

In section 3 primary parameter values were fitted to the DISTFW hydrology model (c_r, e_m, Sphi & phi) (table 3.4) and the sediment transport equation (eqn 2.8) (m_1 and n_1) (fig 3.13) for each study site.

Parameters c_r and e_m are the two parameters that determine the kinematic wave component of the DISTFW hydrology model. It was difficult to identify a temporal change in kinematic wave parameter values because (1) the e_m parameter values fitted in this study represent the flow geometry that exists at each site (table 3.4) (Willgoose & Kuczera 1995), and (2) except for WRD_{50S}, the fitted c_r values for each study site are of the same order of magnitude (table 3.4). In other words, the conveyance properties of the surface do not appear to change significantly with time.

It is also difficult to assess whether there is a temporal trend in infiltration parameter values, phi and Sphi, fitted for each of the sites. Studies by Jorgensen and Gardner (1987) and Ritter (1990) in Pennsylvania showed that the infiltration capacity of newly reclaimed minesoils are an order of magnitude less than undisturbed, natural soils. In this study, the long-term infiltration parameter value, phi, fitted for the sites on the waste rock dumps (WRD_0, WRD_{50C} and WRD_{50S}) are greater than that derived for the natural, undisturbed sites (Nat_C and Nat_S) (table 3.4). And the sorptivity value, Sphi, fitted for WRD_0 is similar to that fitted for Nat_C and Nat_S (table 3.4). This result does not correspond to the findings in Jorgensen and Gardner (1987) and Ritter (1990).

Therefore, in this case, the factors that influence the infiltration parameter value, such as surface particle size (Agassi & Levy 1991) and the unconsolidated nature of the WRD sites, could exceed any temporal effect which may exist between the sites. Regular bushfires in the region may also have reduced infiltration rates on the natural sites, Nat_C and Nat_S (Evans et al 1999).

A temporal trend in n_1 parameter values could not be identified because of the difficulties in fitting parameter values to the sediment transport equation (eqn 2.8). However, figure 4.6 shows the rapid change in the m_1 parameter value within the first 50 years after rehabilitation under both concentrated flow and sheet flow conditions, at which time the m_1 values return to near that of an old, natural landform.

4.4.2 Secondary parameter values

There is no apparent temporal trend in the β_3 and m_3 parameter values, indicated by the similarity in values fitted for each site condition (table 4.1). The fact that there is no apparent temporal effect on the β_3 and m_3 parameter values is attributed to the fact that there is no clear temporal trend in the DISTFW parameter values, the primary parameters used to fit β_3 and m_3 to the area-discharge relationship (fig 2.1).

Of the primary parameter values used to determine the long-term average sediment loss value, Q_s (eqn 2.4), only the m_1 value is influenced by the age and erosional stability of a site (fig 4.6). As such, Q_s reflects the temporal trend in the m_1 value (fig 4.6). The values for long-term average sediment loss, Q_s, in figure 4.6 are measured in $m^3\ y^{-1}$ and are uncorrected for node scale and slope. Figure 4.6 shows that, similar to m_1, Q_s values decrease rapidly within the first 50 years after rehabilitation for both concentrated flow and sheet flow conditions, at which time the Q_s value returns to values near that of the natural landform.

The sediment transport rate coefficient value, β_1, is a reflection of the rate of sediment removal likely to occur on the landform being modelled. The temporal trend in the β_1 value (fig 4.6) indicates that the sediment removal rate on the landform at Ranger is likely to be relatively high in the early years after rehabilitation, under both concentrated flow and sheet flow conditions, and will decrease rapidly within the first 50 y. At 50 y the sediment removal rate, β_1, at Ranger returns to values near that of the natural landform (fig 4.6), indicating a temporal trend reflecting those of the primary parameter m_1 and the secondary parameter Q_s. Temporal changes in the m_1 value have strongly influenced the values of the corresponding secondary parameters Q_s and β_1.

As mentioned above, the α value can be used to predict the relative degree of simulated valley development and incision likely to form on the landform being modelled (Willgoose & Loch 1996). The temporal trend in the α value (fig 4.6) indicates that the degree of valley development and incision on the landform at Ranger is likely to be relatively high in the early years after rehabilitation, under both concentrated flow and sheet flow conditions, and will decrease rapidly within the first 50 y. For the landform under sheet flow conditions the α value is very low at 50 y which suggests that very little further valley development is expected to occur on the landform after the initial 50 y period.

4.4.3 Summary of temporal trends in parameters

A temporal trend in hydrology parameter values (c_r, e_m, phi, Sphi, β_2 and m_2) fitted for each site condition, and therefore the hydrological characteristics of the landform, cannot be determined. Other studies have shown that hydrological characteristics of a reclaimed mine surface is likely to change with time, particularly the infiltration capacity of the surface which increases with time (Gardner et al 1987, Jorgensen & Gardner 1987). The hydrology parameter values determined in this study suggest that the volume of runoff from the rehabilitated landform at Ranger will not change significantly with time. However, this is unlikely to be the case and therefore the results of this study, with respect to hydrological characteristics, are inconclusive. It may be that different surface conditions influence infiltration rates on the landform through time. In the early years, compaction and surface seals may reduce infiltration. In the long term, even though increased vegetation and bioturbation may increase infiltration, the cumulative effects of fire may reduce infiltration and increase runoff (Evans et al 1999).

It has been demonstrated that parameters which reflect the erosion rate likely to occur on the landform (m_1, Q_s, β_1 and α) will change in time (fig 4.6). The parameter m_1 is significant. This parameter reflects sediment detachment/transport capacity and the reduction with time indicates more discharge is required to maintain constant sediment loss rates. The temporal trend in the erosion rate parameters, particularly m_1, indicates that the amount of sediment transported from the rehabilitated landform at Ranger will decrease with time, particularly in the first 50 y after rehabilitation. The surface condition at WRD_{50} indicates that initially, sediment availability will decrease rapidly principally due to surface armouring on the landform. The surface conditions at Nat_C and Nat_S indicate that in the long term, an increase in vegetation on the landform will also contribute to the sediment transport limiting conditions.

Graf (1977) found that following a human-impacted disturbance, the geomorphic processes on the landform developed rapidly at first, followed by a much slower asymptotic approach to an apparent equilibrium state. The results in Graf (1977) are similar to the predicted long-term temporal trends in erosion rate and landform stability at Ranger. This study has been able to quantify changes in erosion rate in terms of parameter values. This ‘short-term’ change in input parameter values should be incorporated within landform evolution modelling to better predict the stability of the rehabilitated landform at Ranger for a 1000 y simulation period.

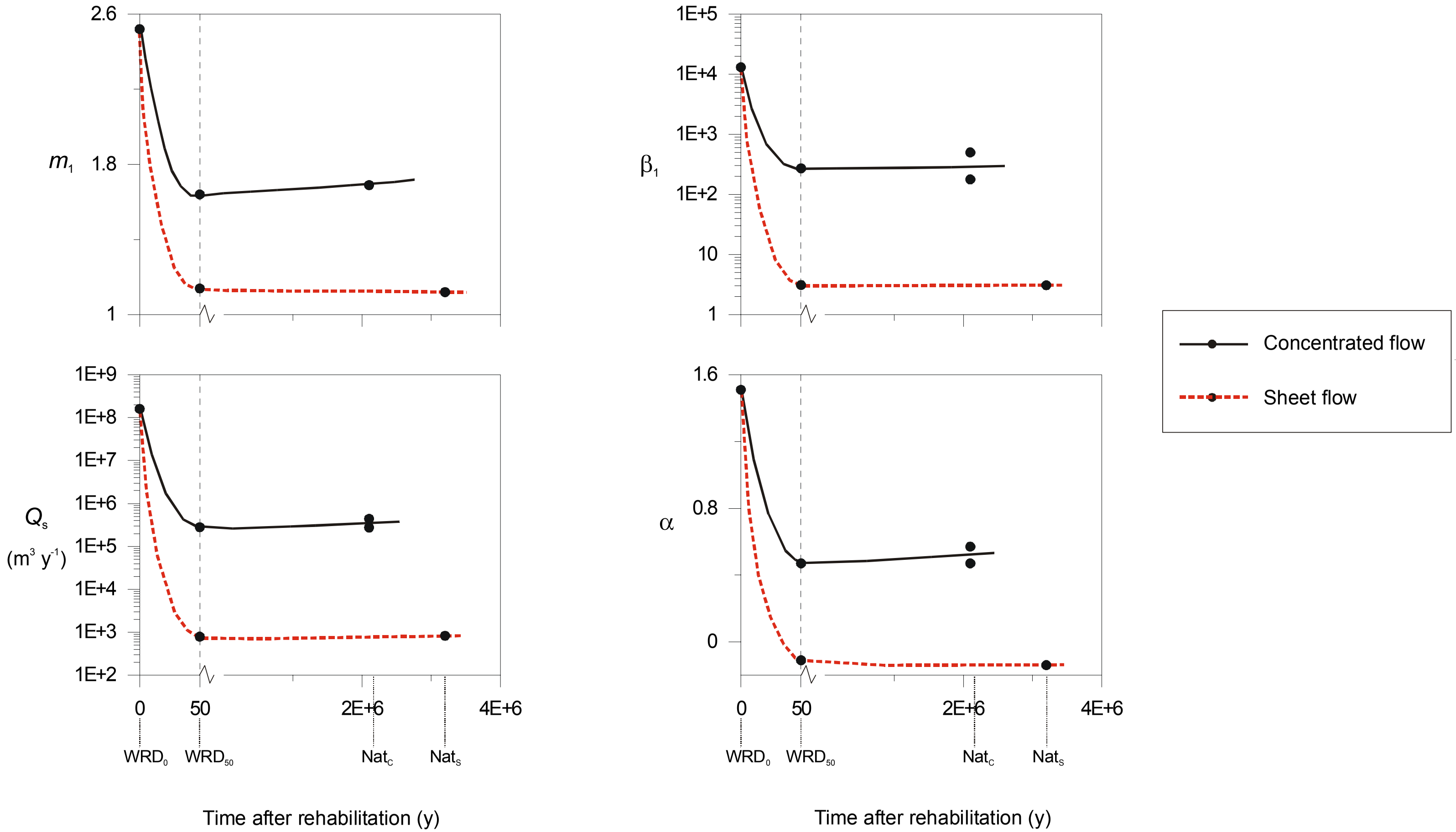

Figure 4.6 Parameter values m_1, Q_s, β_1 and α at various times after rehabilitation at Ranger. Approximate lines of best fit for the concentrated flow (bold) and sheet flow (dashed) conditions are also shown.

4.5 Incorporation of temporal changes of input parameters into SIBERIA modelling

The surface condition of WRD_0 represents the landform at zero years after rehabilitation. As soil and ecosystem development occurs at Ranger the fitted parameter values for WRD_0 will change towards those fitted for the surface condition of (1) WRD_{50S} under sheet flow conditions, or (2) WRD_{50C} under concentrated flow conditions (fig 1.6). To incorporate this 'short-term' temporal change in input parameters into SIBERIA modelling, it is assumed that this change is linear for both concentrated flow and sheet flow conditions during the first 50 y of the 1000 y simulation period.

Of the derived parameter values used as input into the SIBERIA model (fig 1.6) only m_1 and β_1 will change in time on the rehabilitated landform at Ranger. Therefore, input parameters m_1 and β_1 were changed at 10 y intervals during the initial 50 y simulation period, starting with fitted parameter values for the WRD_0 site condition. A schematic diagram of this process is shown in figure 4.7 for the m_1 value under concentrated flow conditions.

After 50 y of simulation the input parameter values are assumed to be those fitted for the WRD_{50} sites, and these remain constant throughout the remainder of the 1000 y simulation period.

In the SIBERIA model, input parameters m_1 and β_1 were changed at 10 y intervals during the initial 50 y simulation period, starting with fitted parameter values for the batter site condition. A schematic diagram of this process is shown in figure 4.7 for the m_1 value under concentrated flow conditions.

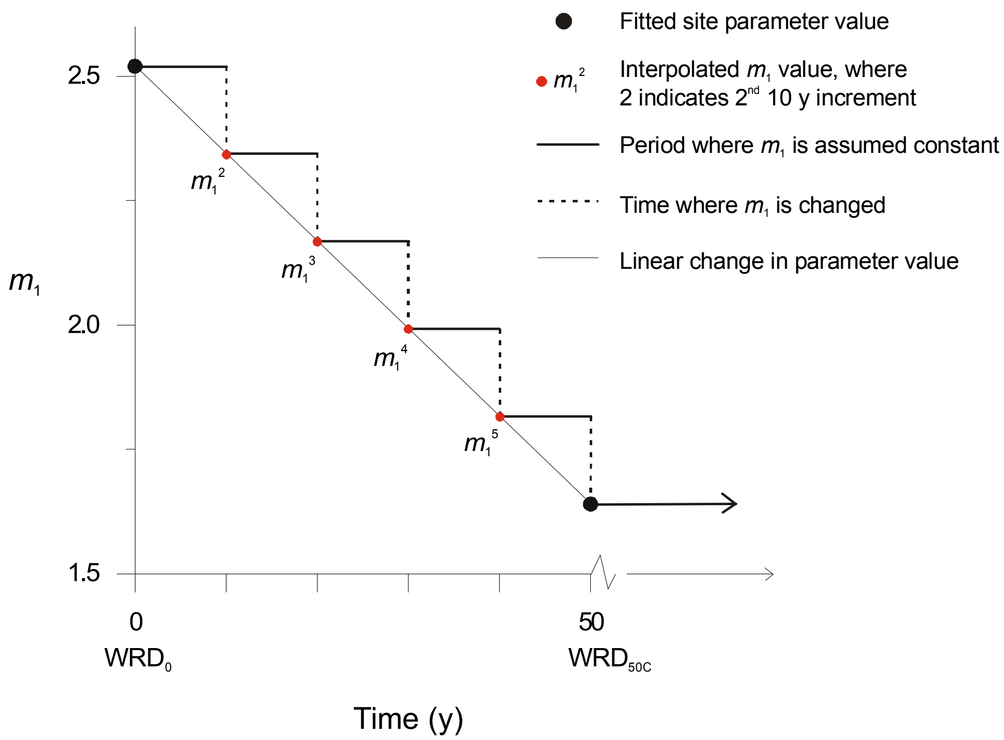

Figure 4.7 Schematic diagram of the process used to incorporate the change in m_1 value under concentrated flow conditions into SIBERIA modelling for the first 50 y of simulation

4.5.1 SIBERIA analysis

The SIBERIA landform evolution model is used to describe how a landform will look, on average, at a given time. SIBERIA (version 7.05) was run on a Sun Ultra-1 Sparc workstation, simulating a time period of the 'design life' (1000 y) of the proposed above-grade rehabilitation option at Ranger. The 'short-term' temporal changes in input parameter values were incorporated into SIBERIA for both concentrated flow and sheet flow conditions.

Figure 1.1 (section 1) shows the proposed rehabilitated landform at Ranger at zero years, based on a grid spacing of 30 m. The landform was modelled for an initial simulation period of 50 y. Figure 4.8 shows the erosion and deposition that occurs within the central depression area (fig 1.1) on the landform, where the majority of the valley development occurs, after 50 y under concentrated flow and sheet flow conditions.

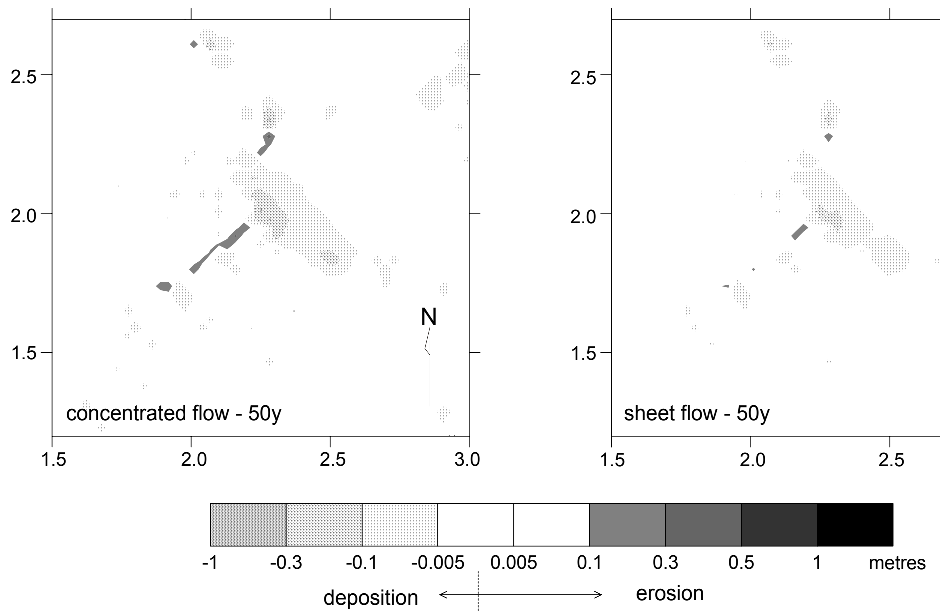

Figure 4.8 Erosion and deposition occurring within the central depression area at 50 y on the landform using parameter values that change with time under (1) concentrated flow conditions, and (2) sheet flow conditions. Dimensions are in kilometres. The X and Y axis corresponds to that on figure 1.1.

The two predicted landforms at 50 y, under concentrated flow and sheet flow conditions, were then modelled for the remainder of the 1000 y simulation period using parameter values fitted for the WRD_{50C} and WRD_{50S} surface condition respectively. The landforms predicted at 1000 y under concentrated flow and sheet flow conditions are shown in figure 4.9. The erosion and deposition that occurs within the central depression area on each landform at 1000 y is shown in figure 4.10.

4.5.2 Discussion

Table 4.3 shows the maximum depths of simulated erosion and deposition that occur on the landform at Ranger, using parameter values that change with time under concentrated flow and sheet flow conditions, at 50 y and 1000 y.

The maximum depth of simulated erosion and deposition within the main valley is the same for the two flow conditions at 50 y (table 4.3). However, figure 4.8 shows that simulated valley development at 50 y on the landform with concentrated flow conditions is greater than that on the landform with sheet flow conditions.

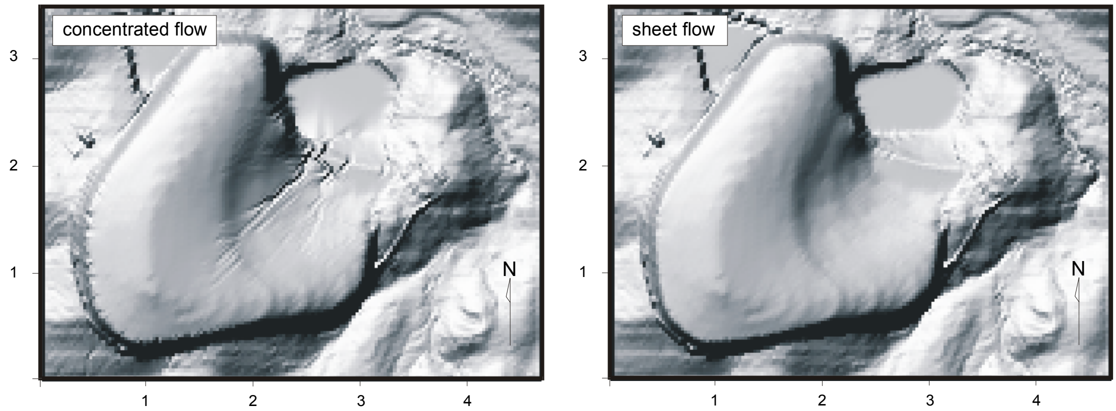

Figure 4.9 SIBERIA simulations for the proposed rehabilitated landform at Ranger at 1000 y using parameter values that change with time under (1) concentrated flow conditions, and (2) sheet flow conditions. Dimensions are in kilometres.

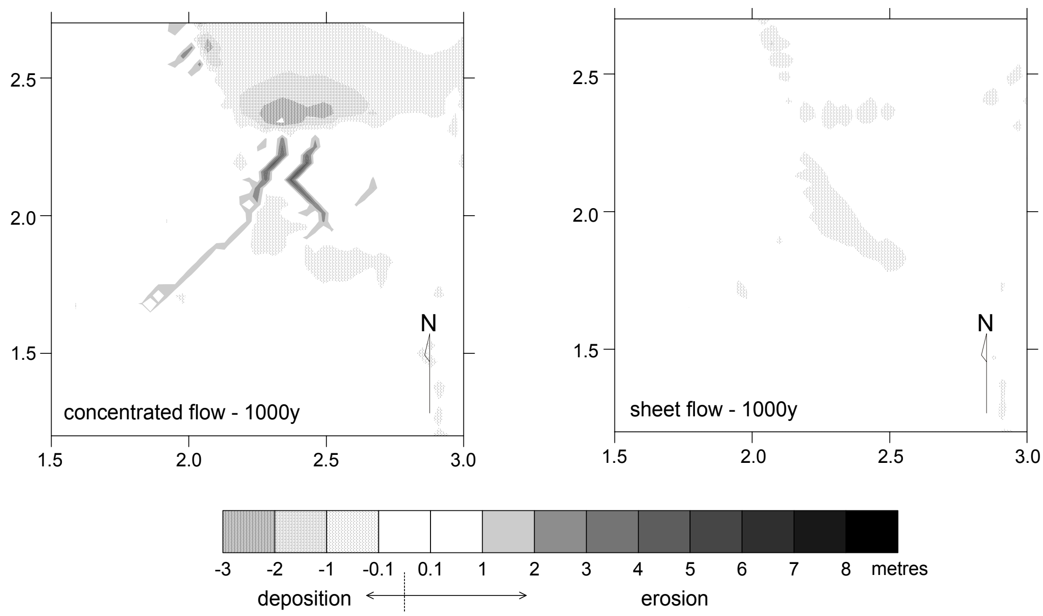

Figure 4.10 Erosion and deposition occurring within the central depression area at 1000 y on the landform using parameter values that change with time under (1) concentrated flow conditions, and (2) sheet flow conditions. Dimensions are in kilometres. The X and Y axis corresponds to that on figure 1.1.

Table 4.3 Maximum depths of erosion and deposition on the proposed rehabilitated landform at Ranger at 50 y and 1000 y of simulation

Flow condition	Sediment movement	Max depth at 50 y (m)	Max depth at 1000 y (m)
Concentrated flow	Erosion	1.48	5.31
	Deposition	0.95	3.14
Sheet flow	Erosion	1.48	1.48
	Deposition	0.95	1.42

The location of the main valley is similar for the two landforms at 50 y (fig 4.8). As discussed above, for the first 10 y of simulation the initial surface conditions were identical for both landforms (fig 4.7), after which the input parameter values moved from those fitted for the WRD_0 site condition *towards* those fitted for the surface condition of (1) WRD_{50C} under concentrated flow conditions, and (2) WRD_{50S} under sheet flow conditions. The location of the main valley appears to have been determined in the first few years of simulation by the parameter values fitted for the initial WRD_0 surface condition. This has also been demonstrated in previous natural (Morisawa 1964) and experimental (Hancock & Willgoose 2001) studies.

The maximum depth of erosion in the main valley on the landform with concentrated flow conditions at 50 y is 28% of the 1000 y maximum depth (table 4.3). This indicates that after the initial 50 y simulation period where input parameter values move from those fitted for the WRD_0 site condition to those fitted for the WRD_{50C} site condition, the rate of incision and valley development on the landform decreased. This result reflects the temporal trends in erosion parameters (m_1, Q_s, β_1 and α) shown in fig 4.6.

The maximum depth of erosion in the main valley on the landform with sheet flow conditions at 50 y is 100% of the 1000 y maximum depth (table 4.3). The maximum depth of deposition on this landform at 50 y is 70% of the 1000 y maximum depth (table 4.3). This indicates that after the initial 50 y simulation period where input parameter values move from those fitted for the WRD_0 site condition to those fitted for the WRD_{50S} site condition, very little incision and valley development occurs on the landform. This is also shown in figures 4.7 and 4.9. This result reflects the rapid drop in the erosion parameter values under sheet flow conditions within the first 50 y after rehabilitation (fig 4.6). At 50 y, parameter values β_1 and α, which represent the sediment removal and level of incision likely to occur on the landform respectively, are significantly lower than those fitted for the concentrated flow condition (fig 4.6).

4.6 Conclusions

The age of the WRD_0, WRD_{50}, Nat_C and Nat_S sites are approximately 0 y, 50 y, 2.1 Ma and 3.2 Ma respectively. The SIBERIA model input parameter values for each study site were determined, and the actual rate of temporal change in parameter values was studied.

There is no apparent temporal trend in model parameters that reflect the hydrological characteristics of the landform at Ranger. There is, however, a very clear temporal effect on model parameters that reflect the erosion rate likely to occur on the landform probably due to surface armouring and soil and ecosystem development on the rehabilitated landform at Ranger. The change is rapid and occurs within the first 50 y after mining is completed, after which the parameter values return to near that of the natural landform.

The erosion rate and valley development on the simulated landforms with input parameters that change with time decline relatively quickly in the short term, particularly on the landform with sheet flow conditions where sediment movement stabilises almost completely after 50 y of simulation.

The incorporation of temporal changes in input parameter values, due to soil and ecosystem development and surface armouring, into the SIBERIA model has provided a best estimate of what the rehabilitated landform at Ranger will look like after 1000 y, under both concentrated flow and sheet flow conditions. This is a significant advance in landform evolution modelling.

5 Quantitative assessment of incorporating temporal trends in SIBERIA modelling

5.1 Introduction

Landform evolution modelling using SIBERIA has been used to predict the stability of the ‘above-grade’ option of rehabilitation at Ranger in studies by Willgoose and Riley (1998) and Evans et al (1998). In these previous studies landform evolution modelling has been based on input parameter values derived from data collected from areas of the WRD at Ranger and these were assumed to remain constant throughout the period that was simulated.

In this study temporal changes in input parameter values – due to soil and ecosystem development and surface armouring, were incorporated into landform evolution modelling of the rehabilitated landform at Ranger (section 4). This is a significant advance on previous erosion modelling studies at Ranger. However, an estimation of the reliability of incorporating temporal changes in SIBERIA modelling is required.

The aim of this section is to conduct a sensitivity analysis on the simulation results in section 4, where temporal effects were incorporated into SIBERIA modelling. This analysis will also provide an understanding of the effect different sets of input parameter values have on overall long-term landform evolution simulations by SIBERIA.

5.1.1 Sensitivity analysis

Figure 5.1 is a schematic representation of the SIBERIA modelling conducted in this section, the results of which will provide the basis for the sensitivity analysis on the simulation results in section 4.

As discussed in section 1, parameter values fitted to WRD_0 represent the landform at zero years immediately after rehabilitation. SIBERIA modelling was used to predict the valley development on the landform at 1000 y using parameter values fitted for the zero year surface condition. In this case, similar to previous studies at Ranger (Willgoose & Riley 1998, Evans et al 1998), it was assumed that there was no soil and ecosystem development on the surface of the landform and therefore the parameter values would remain constant for the simulation period (1000 y). This is a ‘*worst-case*’ scenario for the rehabilitated landform at Ranger (fig 5.1).

In section 4 it was considered that, in the long term, the surface condition of the landform at Ranger could evolve from the zero year condition to a surface condition similar to that of (1) the Nat_C sites under concentrated flow conditions, or (2) the Nat_S site under sheet flow conditions. In this section, SIBERIA modelling was used to predict the valley development on the landform at 1000 y using parameter values fitted for these two long-term conditions (Nat_C and Nat_S) as zero year parameters. In other words, it is assumed that immediately after mining the surface condition at Ranger is similar to that of the natural, undisturbed sites. The parameter values remain constant for the period that is simulated (1000 y). These are the ‘*best-case*’ scenarios for the rehabilitated landform at Ranger under the two flow conditions (fig 5.1).

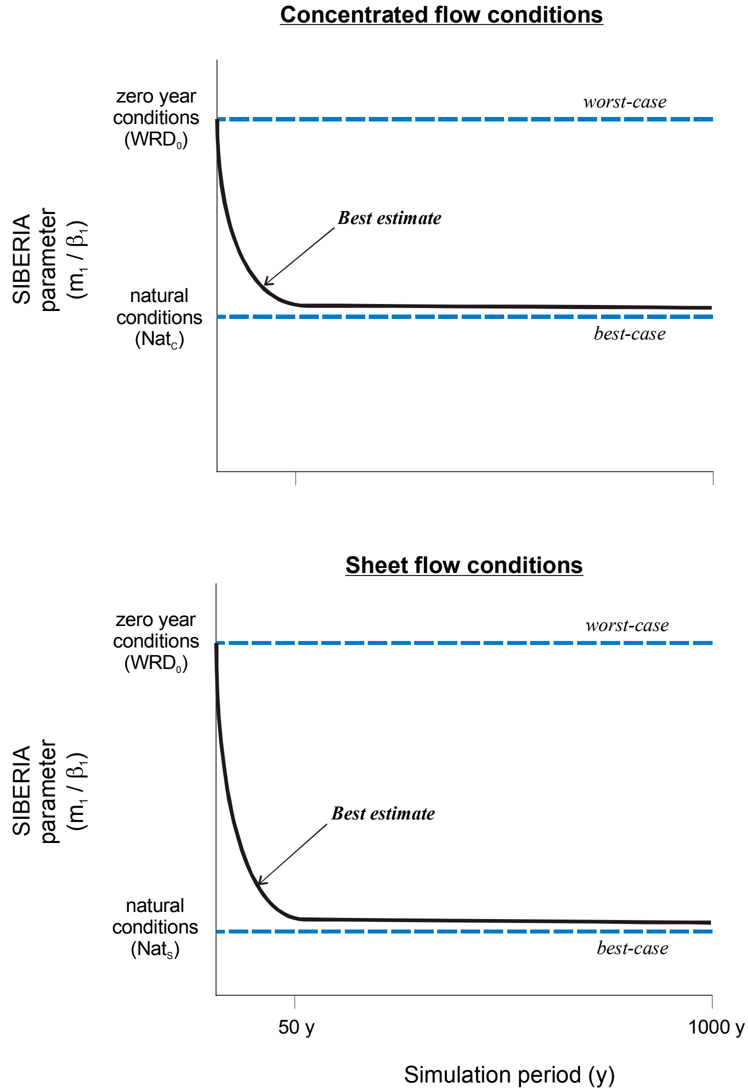

Figure 5.1 A schematic representation of the SIBERIA modelling conducted in this section. Parameter values fitted for the zero year (worst-case) and the long-term (best-case) conditions are used to model the rehabilitated landform at Ranger for 1000 y. These are shown as dashed lines on the graph.

The above worst-case and best-case scenarios for the rehabilitated landform at Ranger at 1000 y provide a range of valley development that may occur on the landform under concentrated flow or sheet flow conditions. This can be considered to be an error range for the '*best estimate*' simulations conducted in section 4, where temporal changes in input parameter values were incorporated into SIBERIA modelling.

5.2 SIBERIA analysis

SIBERIA (version 7.05) was run on a Sun Ultra-1 Sparc workstation, simulating a time period of the 'design life' (1000 y) of the proposed above-grade rehabilitation option at Ranger. Figure 1.1 (section 1) shows the proposed rehabilitated landform for Ranger at zero years, based on a grid spacing of 30 m.

Figure 5.2 shows the simulated landform at 1000 y using input parameter values derived for (1) the zero year condition (WRD_0); the long-term condition under concentrated flow conditions (Nat_{C1} and Nat_{C2}); and the long-term condition under sheet flow conditions (Nat_S). As shown in figure 5.1, the input parameter values for each of these surface conditions were input as zero year parameter values and assumed to remain constant throughout the simulation period (1000 y).

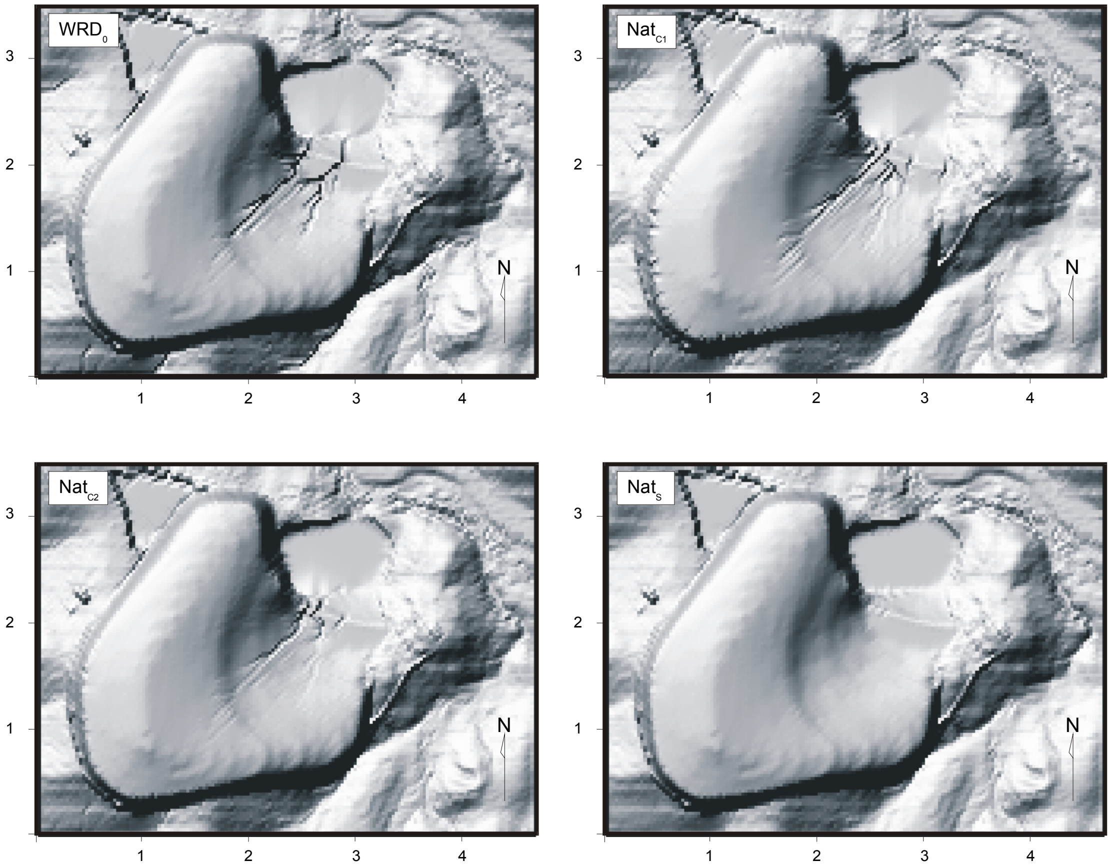

Figure 5.2 SIBERIA simulations for the proposed rehabilitated landform at Ranger at 1000 y for the surface conditions at WRD_0; Nat_{C1} and Nat_{C2}; and Nat_S. SIBERIA input parameters used are given in table 4.1. Dimensions are in kilometres.

5.2.1 Nat_C site conditions (concentrated flow)

The general simulated rate of valley development on the landform for the Nat_{C1} site surface condition was greater than that on the landform for the Nat_{C2} site surface condition throughout the simulation period (fig 5.2). On both landforms most of the simulated valley development has occurred in the central depression area above Pit 3 (fig 5.2). Figure 5.3 shows the erosion and deposition that occurs within this central depression area after 1000 y using the input parameter values derived for Nat_{C1} and Nat_{C2}. Valley depth and valley length is greater on the landform with Nat_{C1} site conditions than that with Nat_{C2} site conditions (fig 5.3).

Figure 5.3 also indicates the difference in spatial location of the main valley between the two landforms after 1000 y. Valley A is the main channel on the landform with Nat_{C2} site conditions, valley B is the main channel on the landform with Nat_{C1} site conditions (fig 5.3).

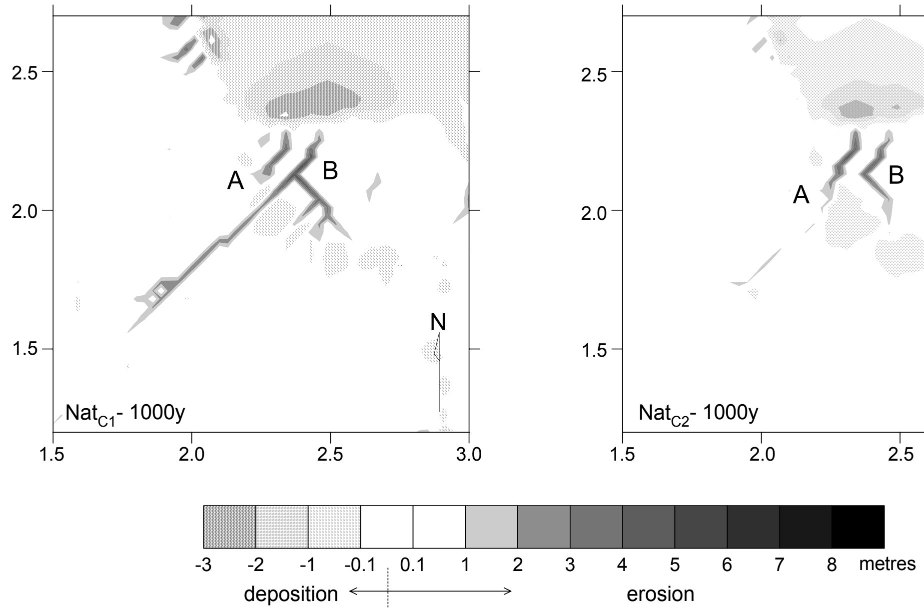

Figure 5.3 Erosion and deposition occurring within the central depression area at 1000 y on the landforms with Nat_{C1} and Nat_{C2} site conditions. Dimensions are in kilometres. The X and Y axis corresponds to that on figure 5.2.

Figure 5.4 shows the simulated valley development within the central depression area on the landforms with Nat_{C1} and Nat_{C2} site conditions at 500 y and 2000 y respectively. At 500 y valley B is the main valley on the landform with Nat_{C1} site conditions (fig 5.4), as it is at 1000 y (fig 5.3), which suggests that valley B is the main valley on this landform throughout the whole 1000 y simulation period. At 2000 y valley A is still the main valley on the landform with Nat_{C2} site conditions (fig 5.4), as it was at 1000 y (fig 5.3). It would appear that valley B is unlikely to develop as the main valley on this landform in the longer term.

Figures 5.3 and 5.4 indicate that it is unlikely that the location of the simulated valleys, particularly the main valley, on the landforms with Nat_C site conditions will change in the long term due to processes of infilling and branching. Other studies, such as Morisawa (1964) and Hancock and Willgoose (2001), have demonstrated similar results. Therefore, not only is there a difference in the rate of sediment removal between the landforms with Nat_C site conditions, but also a difference in spatial location of the valley development.

Given that the observed surface condition at the two Nat_C sites are very similar, such a difference in simulated valley development at 1000 y on the landforms with Nat_C site conditions is unexpected. This difference in simulated valley development on the two landforms can only be attributed to a significant difference in at least one of the SIBERIA input parameter values fitted for the two Nat_C site conditions. Each input parameter is related to the primary parameter values derived directly from monitored rainfall event data (fig 2.1) — the parameters fitted to the DISTFW hydrology model (c_r, e_m, Sphi & phi) and the sediment transport equation (eqn 2.8), m_1 and n_1. As m_1 and n_1 are the same for both Nat_C sites (fig 3.13), it would be reasonable to assume that the parameter values fitted to the DISTFW hydrology model for the Nat_C sites have resulted in a difference in simulated valley development for the Nat_{C1} and Nat_{C2} site conditions. This is discussed below.

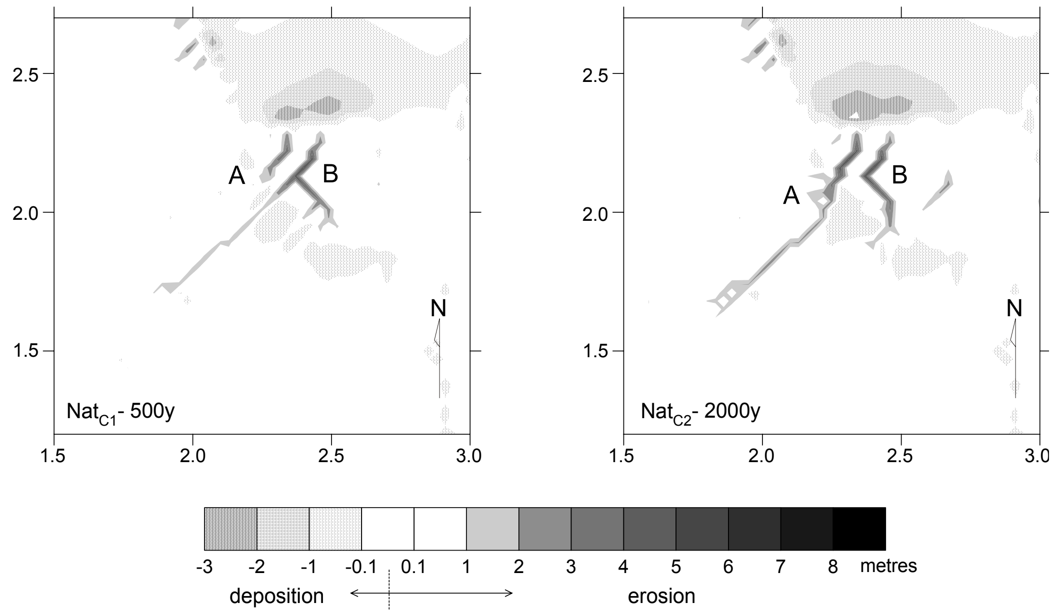

Figure 5.4 Erosion and deposition occurring within the central depression area on the landforms with Nat_{C1} and Nat_{C2} site conditions at 500 y and 2000 y respectively. Dimensions are in kilometres. The X and Y axes correspond to those on figure 5.2.

5.2.1.1 Nat_C DISTFW hydrology model parameter values

DISTFW hydrology model parameter values were fitted to monitored rainfall events at Nat_{C1} and Nat_{C2} using NLFIT (section 3.1). Two sets of parameter values were fitted to the DISTFW hydrology model using NLFIT–kinematic wave parameters (c_r and e_m) and infiltration parameters (Sphi & phi).

Kinematic wave parameter values were also measured from a combination of flow geometry and surface flow resistance for the two sites (table 3.5). As discussed in section 3, these 'geometric' kinematic wave parameter values measured for the two sites were similar to those fitted using NLFIT.

However, the 'geometric' kinematic wave parameter values fitted for Nat_{C1} and Nat_{C2} were almost identical (table 3.5) and therefore are considered to be a better indication of the surface condition and catchment form of the two Nat_C sites than indicated by those fitted using NLFIT. Therefore, the 'geometric' kinematic wave parameter values calculated for Nat_{C1} and Nat_{C2} (table 3.5), combined with the corresponding 'NLFIT' infiltration parameter values, were used to derive the subsequent SIBERIA input parameters for the Nat_C site conditions (table 5.1). These input parameter values were then used to model the proposed rehabilitated landform at Ranger (fig 5.5).

Table 5.1 The SIBERIA input parameter values derived using 'geometric' and 'NLFIT' kinematic wave parameter values

Site	Kinematic wave parameter value used	SIBERIA input parameter				
		m_1	n_1	β_3	m_3	β_1 [(1)]
Nat_{C1}	NLFIT	1.69	0.69	1.86×10^{-4}	0.79	5.0×10^2
	Geometric	1.70*	0.69	1.52×10^{-4}	0.82	3.4×10^2
Nat_{C2}	NLFIT	1.69	0.69	1.44×10^{-4}	0.83	1.8×10^2
	Geometric	1.70*	0.69	1.40×10^{-4}	0.83	1.8×10^2

1 Corrected for node scale (eqn 2.12); * Hydrology model parameter values for Nat_C were used to predict missing runoff data to combine with observed data in order to calibrate a significant sediment transport equation (eqn 2.8) (see section 3.3.2.2). The change in kinematic wave parameter values has meant a slight change to the fitted sediment transport equation for Nat_C sites.

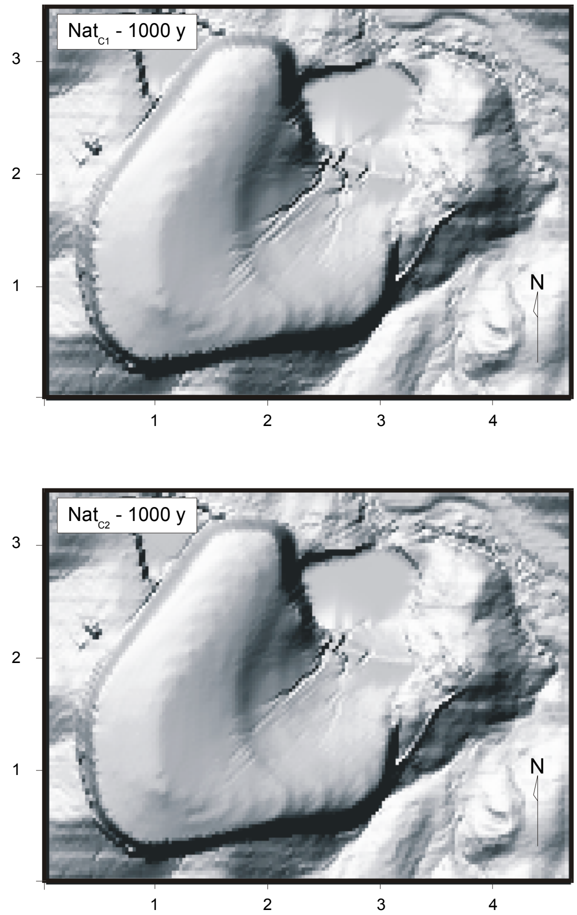

Figure 5.5 The simulated landform at 1000 y for the Nat_{C1} and Nat_{C2} site conditions. SIBERIA input parameters (table 5.1) were derived using 'geometric' kinematic wave parameter values. Dimensions are in kilometres.

5.2.1.2 Nat_C site conditions — remodelled

Table 5.1 shows that, using kinematic wave parameter values measured from flow geometry and surface flow resistance compared with those derived using NLFIT, for the Nat_{C1} site condition:

- there was a change in parameter values β_3 and m_3 fitted to the area-discharge relationship (eqn 2.10) and, as a result
- there was a statistically significant change in the β_1 value,

and for the Nat_{C2} site condition:

- there was no significant change to any of the SIBERIA model input parameter values.

Figure 5.5 shows that, in terms of the spatial location of the main valleys, simulated valley development on the two landforms for the Nat_{C1} and Nat_{C2} site conditions is now similar. The similar spatial location of the main valley on the two landforms better reflect the observed similarity between the two site surfaces at Nat_C.

However, valley development is still greater on the landform with Nat_{C1} site conditions than that on the landform with Nat_{C2} site conditions (fig 5.5). This result reflects the higher sediment transport rate coefficient, β_1, fitted for the Nat_{C1} site conditions than that for the Nat_{C2} site conditions (table 5.1).

As discussed above in section 5.2.1, primary parameter values fitted to the DISTFW hydrology model for the Nat_C sites directly influence the value of β_1 and subsequent simulated valley development on the landform. Given that the above landform simulations (fig 5.5) for the Nat_{C1} and Nat_{C2} site surface conditions were conducted using similar primary kinematic wave parameter values, the difference in simulated valley depth between the landforms can be attributed to the difference in primary infiltration values fitted to Nat_{C1} and Nat_{C2}. The long-term infiltration value, phi, fitted to Nat_{C2} is an order of magnitude greater than that fitted to Nat_{C1} (table 3.4). As a result, a lower sediment transport rate value, β_1 (table 5.1), was fitted for the landform with Nat_{C2} site surface conditions compared with that for Nat_{C1} site surface conditions.

Given the observed similarities between surface characteristics at the two Nat_C sites, it is uncertain whether or not this difference in phi values fitted for the two Nat_C sites (table 3.4) is an accurate reflection of the surface conditions that exist at Nat_{C1} and Nat_{C2}.

In summary:

- For the Nat_{C2} site conditions, using 'geometric' kinematic wave parameter values to derive SIBERIA input parameter values has no effect on subsequent landform simulations compared with using 'NLFIT' kinematic wave parameter values (figs 5.2 and 5.5). This result suggests that the kinematic wave parameter values fitted to the DISTFW hydrology model using NLFIT are reliable.
- The simulated landform for the Nat_{C1} site condition at 1000 y, using 'geometric' kinematic wave parameter values to derive SIBERIA input parameter values (fig 5.5), is significantly different to that for the Nat_{C1} site condition using 'NLFIT' kinematic wave parameter values (fig 5.2). This difference between the two simulated landforms for the Nat_{C1} site condition reflects the difficulty in fitting primary parameters to the DISTFW hydrology model (section 3.2.2.1) and suggests that (1) the kinematic wave parameter values fitted to the DISTFW hydrology model using NLFIT are unreliable, and therefore (2) there may also be some doubt on the reliability of the fitted infiltration parameter values.

This section has demonstrated the importance of accurately fitting hydrology parameters for long-term landform evolution modelling. Primary parameter values fitted for Nat_{C2} are a more reliable set of parameter values to describe the erosion and hydrology characteristics of the Nat_C surface. For this reason, SIBERIA simulations for the Nat_{C1} site surface condition (fig 5.2) will not be considered for the sensitivity analysis in this study.

5.3 Discussion

Figures 5.6 and 5.7 show the simulated valley development on the landform using the parameter values that change with time (section 4) under concentrated flow and sheet flow conditions respectively. These are the 'best estimates' of what the landform at Ranger will look like at 1000 y after rehabilitation under the two flow conditions.

These 'best estimates' of the landform are compared with the best- and worst-case scenarios for valley development on the rehabilitated landform at 1000 y (figs 5.6 & 5.7). As discussed in section 5.1.1, if the rehabilitated landform at Ranger is modelled using parameter values fitted for the zero year condition (WRD_0) and it is assumed that no soil and ecosystem development occurs during the simulation period, this is the worst-case scenario for the landform (figs 5.6 & 5.7).

The best-case scenario for the rehabilitated landform is considered to be if the surface condition of the landform is similar to that on natural, undisturbed sites (>2 million years old) for the whole simulation period. Figure 5.6 shows the best-case for valley development under concentrated flow conditions, using input parameter values fitted for the Nat_C site condition. Figure 5.7 shows the best-case for valley development under sheet flow conditions, using input parameter values fitted for the Nat_S site condition.

On each landform the majority of the sediment movement has occurred within the central depression area above Pit 3 (figs 5.6 & 5.7). Figure 5.8 shows the erosion and deposition that occurs within this central depression area on each landform at 1000 y, highlighting the exact location and depths of incision and deposition on the landform to allow an easy means of comparison between simulations for each of the sets of site input parameter values.

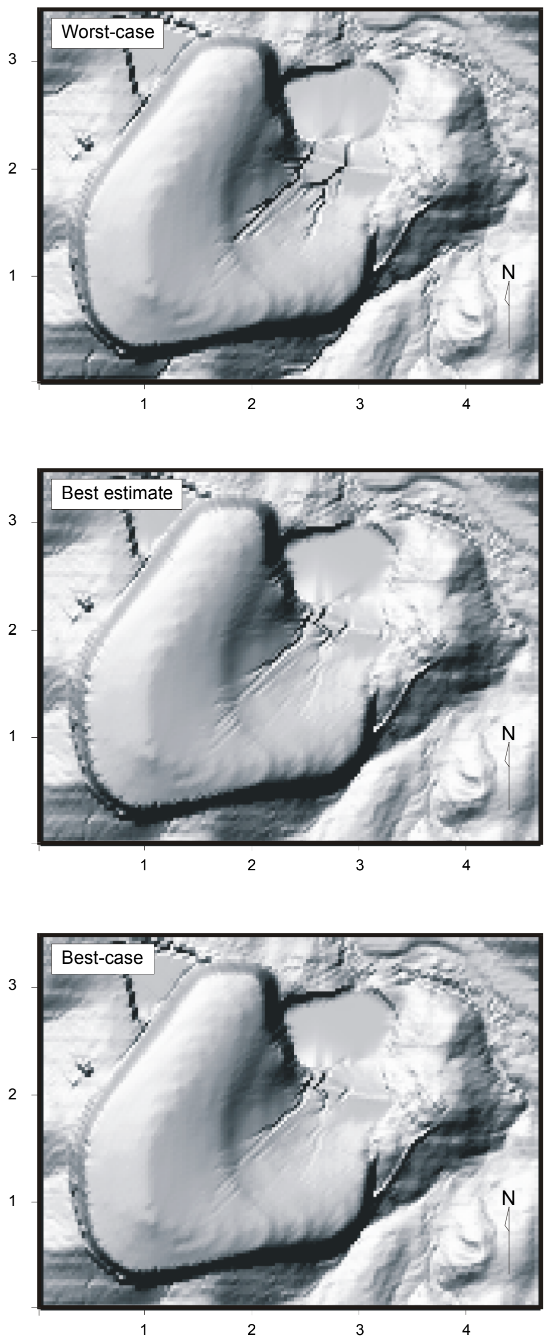

Figure 5.6 3-D representation of the valley development on the proposed rehabilitated landform at Ranger at 1000 y under concentrated flow conditions using parameter values that (1) were fitted for the zero year surface condition (worst-case); (2) were fitted for the long-term surface condition (best-case); and (3) change with time (best estimate). Dimensions are in kilometres.

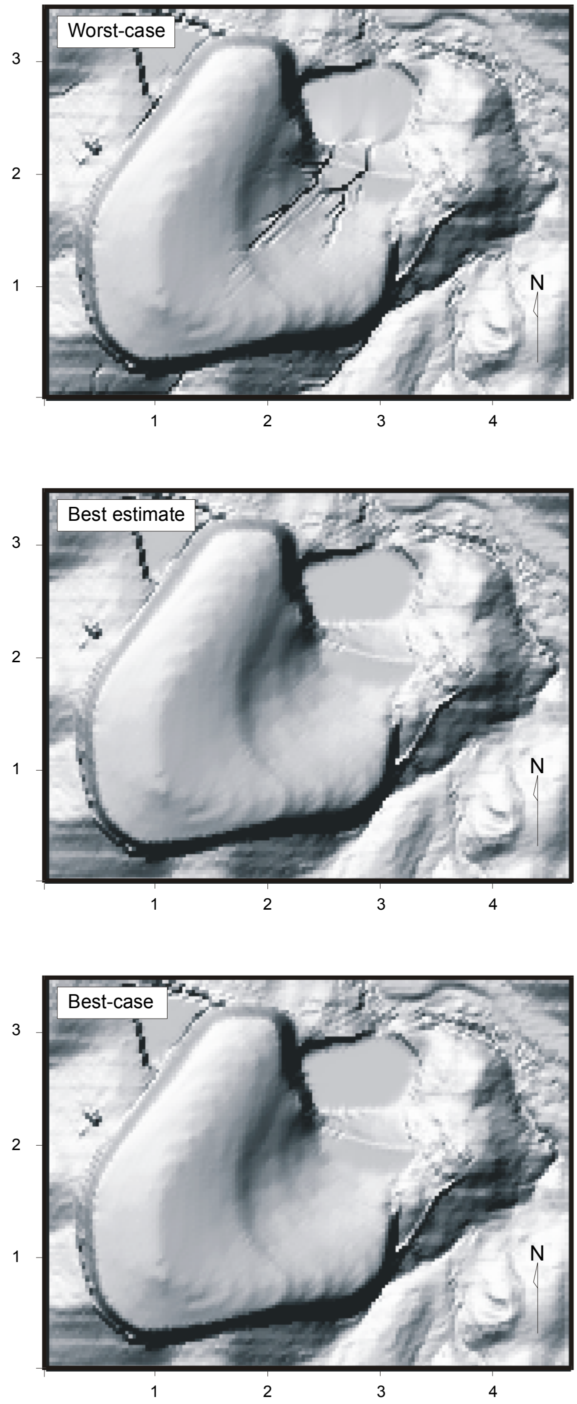

Figure 5.7 3-D representation of the valley development on the proposed rehabilitated landform at Ranger at 1000 y under sheet flow conditions using parameter values that (1) were fitted for the zero year surface condition (worst-case); (2) were fitted for the long-term surface condition (best-case); and (3) change with time (best estimate). Dimensions are in kilometres.

5.3.1 Concentrated flow conditions

Figures 5.6 and 5.8 indicate that the degree of valley development, valley depth and valley length is greatest on the landform using the parameters for the zero year surface conditions (worst-case).

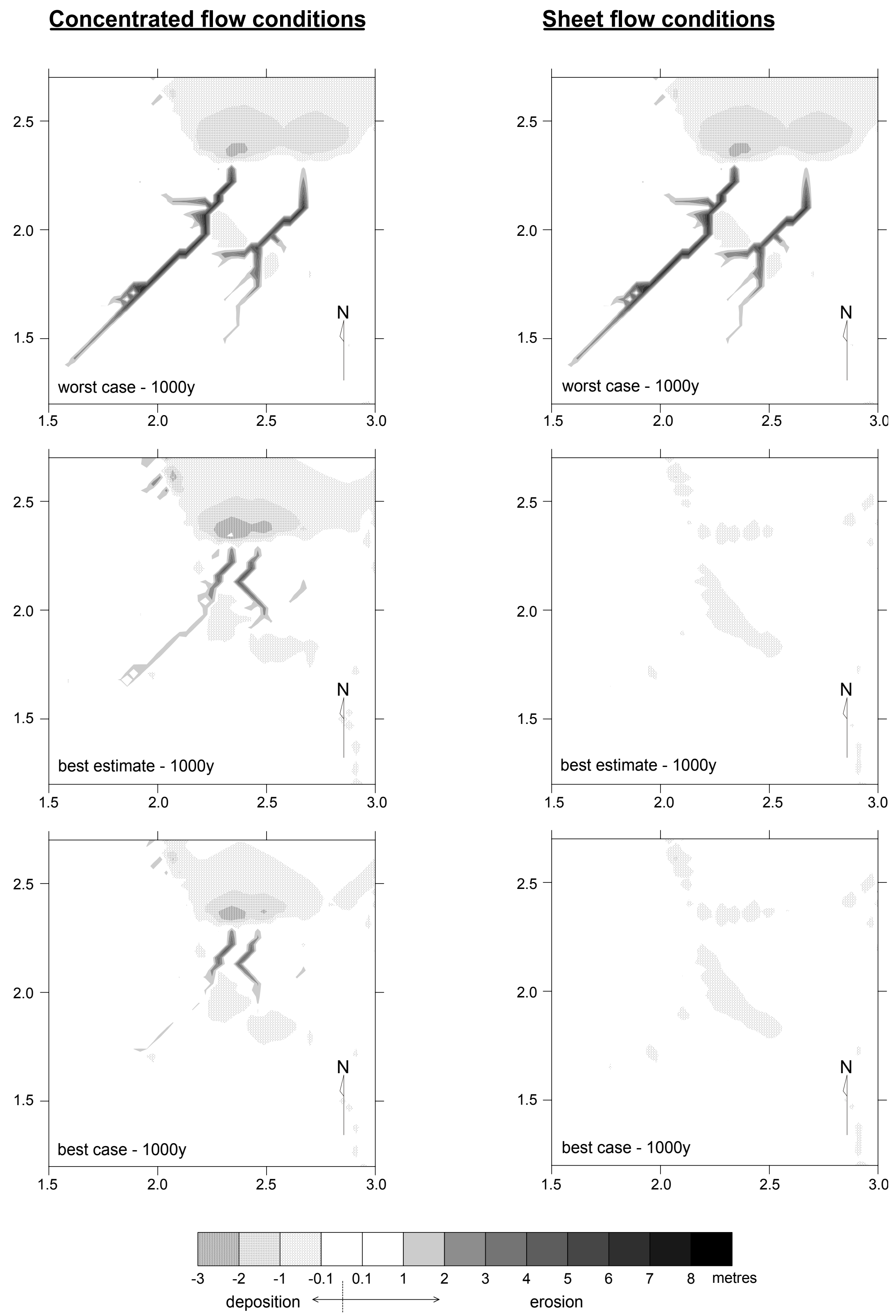

Figure 5.8 Erosion and deposition in the central depression area on the rehabilitated landform at 1000 y using parameter values that (1) were fitted for the zero year surface condition (worst-case); (2) were fitted for the long-term surface condition (best-case); and (3) change with time (best estimate). Dimensions are in kilometres.

Using parameter values fitted for the zero year surface condition to model the rehabilitated landform, and assuming no soil and ecosystem development for the simulation period, will over-predict the long-term stability of the landform at Ranger. Therefore, the worst-case scenario for the landform at 1000 y is a conservative prediction of landform stability at Ranger. The spatial location of the second valley on the landform using worst-case parameter values is also different to that on the landform using parameter values that change with time (figs 5.6 & 5.8).

The rate of valley development and the spatial location of the main valleys on the two simulated landforms at 1000 y, using best-case parameter values and parameter values that change with time (best estimate), are similar (figs 5.6 & 5.8). This result shows that using input parameter values fitted for the long-term surface condition (Nat_{C2}), with surface properties similar to those likely to exist on the landform at Ranger in the long term, may only slightly under-predict the rate of valley development on the landform in 1000 y (figs 5.6 & 5.8). It also indicates that using the best-case parameter values to model the landform may reasonably predict where the actual location of the main valley development will occur.

5.3.2 Sheet flow conditions

As discussed in section 1, if, as time passes after rehabilitation, runoff is directed away from the batter slope and the surface only receives direct rainfall, the landform should retain a planar surface with sheet flow conditions. If these sheet flow conditions are maintained on the landform in the long term, using parameter values fitted for the initial zero year condition (worst-case) to model the rehabilitated landform will over-predict valley development at Ranger at 1000 y compared with the best estimate simulation (figs 5.7 & 5.8).

Similar to that for concentrated flow conditions, the rate of valley development and the spatial location of the areas of deposition on the two simulated landforms at 1000 y, using best-case parameter values and parameter values that change with time (best estimate), are similar (figs 5.7 & 5.8). This result shows that using input parameter values fitted for the long-term surface condition (Nat_S), with surface properties similar to those likely to exist on the landform at Ranger in the very long term, will provide a reasonable prediction of valley development on the landform in 1000 y (figs 5.7 & 5.8).

5.3.3 Cross-sectional analysis

Figure 5.9 is a cross-section taken up the main valley that develops above Pit 3 on each of the simulated landforms discussed in this section. The cross-section through the predicted landforms at 1000 y using parameter values that change with time (best estimate), under both flow conditions, are also shown.

The depth of erosion in the main valley on the landform with natural, long-term surface conditions (best-case) closely resembles that on the landforms using parameter values that change with time (best estimate), particularly when the landform is modelled under sheet flow conditions (fig 5.9). Using the long-term parameter values as zero year parameters to model the rehabilitated landform under concentrated flow conditions will only slightly under-predict erosion and deposition in the long term (fig 5.9).

Figure 5.9 shows that using the initial WRD_0 parameter values as zero year parameters in SIBERIA modelling will over-predict erosion in the main valley during landform simulations in the long term, particularly when the landform is modelled under sheet flow conditions. This result reflects the simulation results shown in figures 5.6 and 5.7.

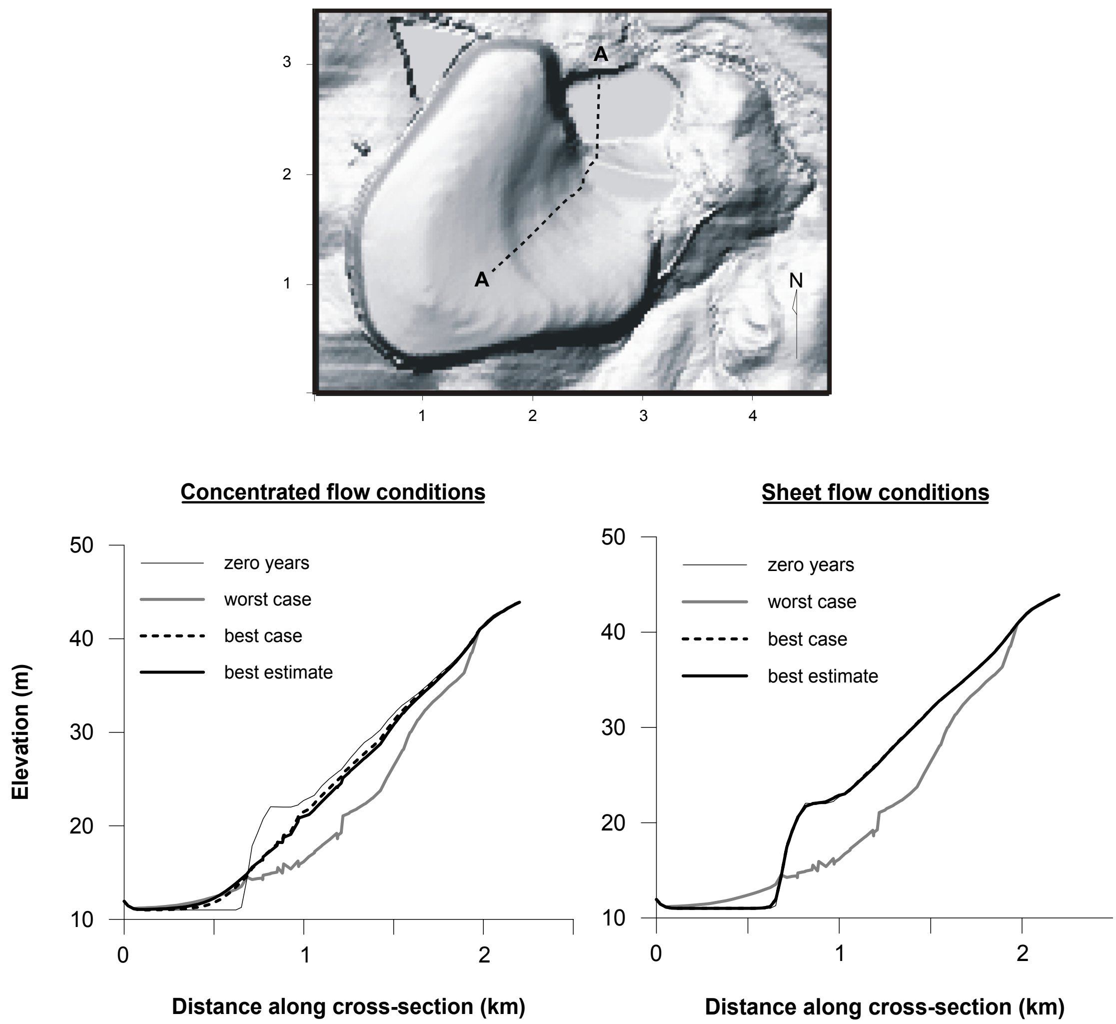

Figure 5.9 Section A-A through the simulated landform at 1000 y (top) under concentrated flow (left) and sheet flow (right) conditions. The section through the simulated landforms at 1000 y using input parameter values that change with time are shown as a continuous bold line.

Table 5.2 shows the maximum depths of simulated erosion and deposition that occur within the main valley on the landform at 1000 y using the best- and worst-case parameter values and those that change with time (best estimate), under concentrated flow and sheet flow conditions. As mentioned above, using the best- and worst-case parameter values to model the landform at Ranger provides a range of valley development that may occur on the landform under concentrated flow or sheet flow conditions. For example, the best estimate of the maximum depth of erosion that may occur after 1000 y within the main valley on the landform under concentrated flow conditions can be written as follows:

$$\text{Max depth of erosion} = 5.31^{+2.25}_{-0.45}\ \text{m}$$

The best estimate of the maximum depth of erosion likely to occur on the landform, under sheet flow conditions, is 1.48 m, significantly less than the best estimate of the maximum depth of erosion on the landform under concentrated flow conditions, and only 20% of that predicted on the landform using worst-case parameter values (table 5.2).

Table 5.2 Maximum depths of erosion and deposition on the proposed rehabilitated landform at Ranger at 1000 y

Flow condition		Maximum erosion depth at 1000 y (m)	Maximum deposition depth at 1000 y (m)
Concentrated flow	Worst-case	7.56	2.31
	Best estimate	5.31	3.14
	Best-case	4.86	2.83
Sheet flow	Worst-case	7.56	2.31
	Best estimate	1.48	1.42
	Best-case	1.49	1.50

Maximum deposition on the landform using worst-case parameter values is relatively low compared with that on the landforms using best-case parameter values and parameter values that change with time under concentrated flow conditions (table 5.2). Depths of deposition of this magnitude have occurred at the outlet of the two main valleys above Pit 3 (fig 5.8). On the simulated landforms, sediment is eroded on the steep batter slopes above Pit 3 and deposited at the outlet of the valley against the batter slope. On the landform with zero year conditions, the level of this deposition is higher than the lowest point of the valley at the outlet (fig 5.9). Therefore, since there is greater incision on the landform with zero year parameter values (table 5.2), valley outlets are at a lower level on the steep batter slopes. This results in lower depths of deposition compared with that predicted on the landforms using best-case parameter values and parameter values that change with time (table 5.2 & fig 5.9). A similar result was observed in Evans et al (1998).

In summary, the results of the simulations have shown that incorporating temporal effects in parameter values into the SIBERIA model under both concentrated flow and sheet flow conditions may be considered reasonable, as valley development on these landforms is within the range of valley development determined by the best- and worst-case surface conditions. The sensitivity analysis has also provided two results of some importance:

1 Using zero year parameter values (worst-case) to model the rehabilitated landform at Ranger, assuming, similar to previous studies (Willgooose & Riley 1998, Evans et al 1998), that no soil and ecosystem development occurs during the simulation period, overall valley development will be over-predicted.

2 Using natural, long-term surface conditions (best-case) to model the rehabilitated landform at Ranger will only slightly under-predict overall valley development compared with that on the landforms using parameter values that change with time. In section 4 it was shown that input parameter values reach an apparent equilibrium state at 50 y (fig 4.6). Therefore, using SIBERIA, a reasonable prediction of the rate of valley development and the spatial location of the valleys on the landform could be made using parameter values fitted to a site with surface conditions similar to those likely to occur 50 y after rehabilitation.

5.4 Conclusions

In this section a sensitivity analysis was conducted on the landform simulation results where temporal effects were incorporated into SIBERIA modelling (section 4). A best- and worst-case surface condition for the proposed rehabilitated landform at Ranger was used to model a range of valley development that may occur on the landform in 1000 y.

The simulated landforms using parameter values that change with time under both concentrated flow and sheet flow conditions may be considered reliable, as valley development on these landforms is within the range of valley development determined by the best- and worst-case surface conditions.

Simulated valley development at 1000 y on the rehabilitated landform at Ranger using zero year parameter values (worst-case) is considered to be a conservative prediction of the stability of the landform. However, if sheet flow conditions are maintained on the landform in the long term, using parameter values fitted for the zero year condition to model the rehabilitated landform will grossly over-predict valley development at Ranger at 1000 y.

The simulated landforms at 1000 y with natural, long-term surface conditions (best-case) closely resemble the simulated landforms using parameter values that change with time, particularly when the landform is modelled under sheet flow conditions. Given that input parameter values reach a stable equilibrium at 50 y, a reasonable prediction of the rate of valley development and the spatial location of the valleys could be made using SIBERIA to model the landform with surface conditions of a short-term analogue site.

6 Overview

6.1 Study summary

An important part of rehabilitation planning for Ranger Mine is the design of a stable landform at the completion of mining, which minimises erosion and environmental impact offsite. A prediction of the surface stability of the final landform, using erosion and landform evolution modelling techniques, is an integral part of the design process.

During the initial stages of rehabilitation at Ranger, at the completion of mining, the waste rock dump (WRD) would be constructed as a planar surface with sheet flow conditions. In time the batter slopes on the WRD could have two evolutionary paths: (1) the surface will remain planar under sheet flow conditions, and (2) the surface will become incised under concentrated flow conditions.

If, as time passes after rehabilitation, runoff is directed away from the batter slope and the surface only receives direct rainfall, the site should retain a planar surface with sheet flow conditions. If however, overland flow from the upper WRD surface breaches the bund at the top of the batter slope and flows over the surface then channelised flow will occur and a gully may develop.

Therefore, it is considered necessary to predict the surface stability of the final landform under both concentrated flow and sheet flow conditions. In this study, temporal changes in the surface condition — due to soil and ecosystem development and surface armouring — which may occur, were also considered in the landform evolution modelling process.

Rainfall, runoff and sediment loss data were collected from sites that represent the surface hydrology and erosion characteristics that would exist on the WRD at Ranger at various stages after rehabilitation under both concentrated flow and sheet flow conditions.

The monitoring data collected at each of the sites were used to derive primary parameter values for the DISTFW hydrology model and the sediment transport equation. These primary parameter values were used to derive input parameter values for the landform evolution model SIBERIA. The SIBERIA input parameter values represent the erosion and hydrology characteristics of the study site surface condition, and are used to simulate valley development on the rehabilitated landform at Ranger.

The specific conclusions in the following section arising from this study correlate with the sub-objectives stated in section 1.

6.2 Conclusions

1 ***Available runoff and sediment loss data collected at two natural sites at Tin Camp Creek were found to be insufficient to establish a significant relationship between sediment loss and runoff for an event. A method of predicting missing runoff and sediment data was developed and combined with observed data in order to calibrate a significant sediment loss-runoff relationship.***

The observed suspended sediment concentration data for all monitored events at these natural sites (Nat_C) were used to obtain an equation to predict suspended sediment concentration where data were missing. A temporal component was incorporated into the sediment concentration-discharge relationship in order to more accurately predict the suspended sediment concentration where data were missing. This 'time' parameter removed the observed hysteresis effect in individual hydrographs.

Hydrology model parameter values fitted for Nat_{C1} using DISTFW-NLFIT were used to predict the runoff on part of a hydrograph for a rainfall event monitored at Nat_{C1}.

All rainfall event data at Nat_C, including the events consisting of predicted runoff and sediment loss data, were used to obtain a significant sediment loss-runoff relationship.

2 ***Surface hydrology and soil loss prediction relationships were determined for each study site.***

Rainfall-runoff data collected at the study sites were used to fit parameter values to the DISTFW hydrology model using NLFIT. Two sets of parameter values were fitted to the DISTFW hydrology model–kinematic wave parameters (c_r and e_m) and infiltration parameters (Sphi & phi).

Parameters n_1 and m_1 were fitted to the sediment transport equation using complete data sets of sediment loss, rainfall and runoff from discrete rainfall events collected at each study site. A temporal trend in n_1 parameter values could not be identified because of the difficulties in fitting parameter values to the sediment transport equation. However, there is a clear temporal effect on the m_1 parameter value between the study sites. A rapid change in the m_1 parameter value within the first 50 years after rehabilitation was observed under both concentrated flow and sheet flow conditions, after which, the m_1 value changes little over the remainder of the simulated period.

Parameters fitted to both the DISTFW hydrology model and the sediment transport equation are considered *primary* parameters. The primary parameter values for each site condition were used to derive input parameter values for the SIBERIA model.

3 ***It was argued that parameter values fitted for each site represented a different point on the time line. The age of each study site was determined and the SIBERIA input parameter values for each site were compared to assess the rate of temporal changes in parameter values.***

The age of the WRD_0, WRD_{50}, Nat_C and Nat_S sites are approximately 0 y, 50 y, 2.1 Ma and 3.2 Ma respectively.

There is no apparent temporal trend in SIBERIA input parameters β_3, m_3 and n_1 indicated by the similarity in values fitted for each of the site conditions. There is, however, a very clear temporal effect due to soil and ecosystem development on SIBERIA input parameters m_1 and β_1, under both concentrated flow and sheet flow conditions. The change is rapid and occurs within the first 50 years after mining is completed, at which time the parameter values near that of an old, natural landform. This study has quantified temporal changes of erosion processes in terms of these input parameter values.

It is important to incorporate the 'short-term' change in input parameter values within landform evolution modelling to better predict the stability of the rehabilitated landform at Ranger for a 1000 y simulation period.

4 ***SIBERIA landform evolution simulations of the proposed rehabilitated landform at Ranger were conducted incorporating the rate of temporal change in input parameter values due to ecosystem development.***

The incorporation of temporal changes in input parameter values, due to soil and ecosystem development and surface armouring, into the SIBERIA model has provided a 'best estimate' of what the rehabilitated landform at Ranger will look like after 1000 y, under both concentrated flow and sheet flow conditions. This is a significant advance in landform evolution modelling.

The erosion rate and valley development on the simulated landforms with input parameters that change with time decline relatively quickly in the short term, particularly on the landform with sheet flow conditions where sediment movement stabilises almost completely after 50 y of simulation.

5 ***A sensitivity analysis showed that the incorporation of temporal changes in SIBERIA modelling is reliable.***

A best- and worst-case surface condition for the proposed rehabilitated landform at Ranger was used to model a range of valley development that may occur on the landform in 1000 y.

The simulated landforms using parameter values that change with time under both concentrated flow and sheet flow conditions may be considered reliable, as valley development on these landforms is within the range of valley development determined by the best- and worst-case surface conditions.

6.3 Further work

This study has showed that there is a change in model input parameter values as a result of temporal effects within 50 y after rehabilitation. By 50 y the input parameters approach that of an old, natural landform and remain constant for the remainder of the simulation period (1000 y).

Previous studies, such as Gardner et al (1987), Jorgensen and Gardner (1987) and Ritter (1990), have indicated that there may be a rapid change in hydrology characteristics on reclaimed mine soils in the early years (< 10 y) after rehabilitation. Loch and Orange (1997) found considerable improvement in soil physical properties on topsoils used in mine rehabilitation within 4 years. It would be important to determine if the temporal effect on hydrology characteristics and soil properties that occur in the very early years after rehabilitation (Ritter 1990, Loch & Orange 1997) have implications for SIBERIA landform evolution modelling at Ranger in the long term. To achieve this it would be necessary to include a study site in the analysis with soil properties similar to those likely to develop at Ranger in the very short term.

In this study, it was assumed that the change in SIBERIA input parameter values during the first 50 y after rehabilitation was linear. To include a very short-term analogue site (< 50 y old) for the WRD will:

- more accurately define the rate of change in SIBERIA input parameter values in the short term, and/or
- establish the length of time required for the input parameter values fitted to the WRD surface at Ranger to reach equilibrium.

References

Agassi M & Levy GJ 1991. Stone-cover and rain intensity: Effects on infiltration, erosion and water splash. *Australian Journal of Soil Research* 29, 565–575.

Arkinstal M, Willgoose GR, Loch RJ & Pocknee C 1994. *Calibration of DISTFW parameters for the QDPI rainfall simulator Oaky Creek,* Research report no 093.04.1994, Department of Civil, Surveying and Environmental Engineering, The University of Newcastle, New South Wales.

Bell LSJ & Willgoose GR 1997. Determination of hydrology and erosion model parameters: Natural site adjacent to Pit #1 at ERA Ranger Mine, Northern Territory, Australia. Internal report 270, Supervising Scientist, Canberra. Unpublished paper.

Birkeland PW 1984. *Soils and geomorphology*. Oxford University Press, New York.

Bureau of Meteorology 1999. *Hydrometeorological analyses relevant to Jabiluka*. Supervising Scientist Report 140, Supervising Scientist, Canberra.

Chow VT 1959. *Open channel hydraulics*. McGraw-Hill, New York.

Cowan WL 1956. Estimating hydraulic roughness coefficients. *Agricultural Engineering* 37, 473–475.

Crick IH, Muir MD, Needham RS & Roarty MJ 1980. The geology and mineralisation of the South Alligator River Valley uranium field. In *Uranium in the Pine Creek Geosyncline*. eds Ferguson J & Goleby AB, Proceedings of the International Uranium Symposium Sydney 4–8 June 1979, International Atomic Energy Agency, Vienna, 273–285.

DHA&E (Department of Home Affairs & Environment) 1982. *Code of Practice on the Management of Radioactive Wastes from the Mining and Milling of Radioactive Ores: Guidelines*. Australian Government Publishing Service, Canberra.

DHC 1986. *Survey of abandoned mines, Gimbat Pastoral Lease*. Northern Territory Department of Housing and Construction, Commonwealth of Australia.

Dingman SL 1984. *Fluvial hydrology*. WH Freeman, New York.

Edwards K 1987. *Runoff and soil loss studies in NSW*. Technical Handbook 10, Soil Conservation Service of NSW and Macquarie University, Sydney.

Edwards WM & Owens LB 1991. Large storm effects on total soil erosion. *Journal of Soil and Water Conservation* 46, 75–78.

Evans KG 2000. Methods for assessing mine site rehabilitation design for erosion impact. *Australian Journal of Soil Research* 38, 231–247.

Evans KG & Willgoose GR 1994. An experimental study on the effect of vegetation on erosion of the Ranger Uranium Mine waste rock dump: A proposal. Internal report 164, Supervising Scientist for the Alligator Rivers Region, Canberra. Unpublished paper.

Evans KG & Willgoose GR 2000. Post-mining landform evolution modelling. II. Effects of vegetation and surface ripping. *Earth Surface Processes and Landform* 25 (8), 803–823.

Evans KG, Loch RJ, Aspinall TO & Bell LC 1997. Laboratory rainfall simulator studies of selected open-cut coal mine overburden spoils from Central Queensland. *Australian Journal of Soil Research* 35, 15–29.

Evans KG, Saynor MJ & Willgoose GR 1999. Changes in hydrology, sediment loss and microtopography of a vegetated mine waste rock dump impacted by fire. *Land Degradation & Development* 10, 507–522.

Evans KG, Willgoose GR, Saynor MJ & House T 1998. *Effect of vegetation and surface amelioration on simulated landform evolution of the post-mining landscape at ERA Ranger Mine, Northern Territory*. Supervising Scientist Report 134, Supervising Scientist, Canberra.

Evans KG, Willgoose GR, Saynor MJ & Riley SJ 2000. Post-mining landform evolution modelling. I. Derivation of sediment transport model and rainfall-runoff model parameters. *Earth Surface Processes and Landforms* 25, 743–763.

Field WG & Williams BJ 1987. A generalised kinematic catchment model. *Water Resources Research* 23 (8), 1693−1696.

Finnegan LG 1993. Hydrolic characteristics of deep ripping under simulated rainfall at Ranger uranium mine. Internal report 134 (thesis), Supervising Scientist for the Alligator Rivers Region, Canberra. Unpublished paper.

Flint JJ 1974. Stream gradient as a function of order, magnitude and discharge. *Water Resources Research* 10 (5), 969−973.

Foster GR 1982. Modelling the erosion process. In *Hydrologic modelling of small watersheds*. eds CT Haan, HP Johnson & DL Brakensiek, Monograph 5, American Society of Agricultural Engineers, Michigan, 297–380.

Galloway RW 1976. *Lands of the Alligator Rivers Area: Part IV. Geomorphology*. Land Research Series 38, CSIRO, Melbourne, 52–70.

Gardner TW, Gryta JJ, Lemieux CR, Jorgensen DW, Touysinhthiphonexay K & Kimball CN 1987. Geomorphology and hydrology of surface-mined watersheds, bituminous coal fields, central Pennsylvania. In *Central Pennsylvania geology revisited*, 50th Annual field conference of Pennsylvania geologists, Harrisburg 3–5 October 1985, ed DP Gold, Department of Geosciences, Pennsylvania State University, 263–273.

Graf WL 1977. The rate law in fluvial geomorphology. *American Journal of Science*. 277: 178–191.

Guy BT, Dickenson WT & Rudra RP 1987. The role of rainfall and runoff in the sediment transport capacity of interrill flow. *Transactions of the American Society of Agricultural Engineers* 30, 1378–86.

Hancock GR 1997. Experimental testing of the SIBERIA landscape evolution model. PhD thesis (unpublished), The University of Newcastle, Newcastle, NSW.

Hancock GR & Willgoose GR 2001. The interaction between hydrology and geomorphology in a landscape simulator experiment. *Hydrological Processes* 15, 115–133.

Hancock GR, Evans KG, Willgoose GR, Moliere DR, Saynor MJ & Loch RJ 2000. Medium-term erosion simulation of an abandoned mine site using the SIBERIA landscape evolution model. *Australian Journal of Soil Research* 38, 249−263.

Hancock GR, Willgoose GR & Evans KG 2002. Testing of the SIBERIA landscape evolution model using the Tin Camp Creek, Northern Territory, Australia, field catchment. *Earth Surface Processes and Landforms* 27, 125–143.

Hays J 1971. Land surfaces and laterites in the north of the Northern Territory. In *Landform studies from Australia and New Guinea*, eds JN Jennings & JA Mabbutt, Australian National University Press, Canberra, 182–210.

Henderson FM 1966. *Open channel flow*. Prentice Hall, Englewood Cliffs, NJ.

Howard AD 1994. A detachment-limited model of drainage basin evolution. *Water Resources Research* 30, 2261−2285.

Jorgensen DW & Gardner TW 1987. Infiltration capacity of disturbed soils: temporal change and lithologic control. *Water Resources Research* 23 (6), 1161−1172.

Kirkby MJ 1971. Hillslope process-response models based on the continuity equation. In *Slopes form and process*, Institute of British Geographers Special Publication 3, London, 15−30.

Kinnell PIA & Cummings D 1993. Soil/slope gradient interactions in erosion by rain-impacted flow. *Transactions of the American Society of Agricultural Engineers* 36 (2), 381–387.

Knisel WG 1980. CREAMS. *A field scale model for chemicals, runoff and erosion from agricultural management systems*. Conservation Research Report 26, US Department of Agriculture, Science and Education Administration, Washington.

Kuczera G 1989. An application of Bayesian nonlinear regression to hydrologic modelling. *Advances in Engineering Software* 11 (3), 149−155.

Kuczera G 1994. NLFIT: A bayesian nonlinear regression program suite Version 1.00g. Department of Civil, Surveying and Environmental Engineering, The University of Newcastle, NSW.

Leopold LB, Wolman MG & Miller JP 1964. *Fluvial processes in geomorphology*. Freeman, London.

Loch RJ & Orange DN 1997. Changes in some properties of topsoil at Tarong Coal–Meandu Mine coalmine with time since rehabilitation. *Australian Journal of Soil Research* 35, 777−784.

Morisawa ME 1964. Development of drainage systems on an upraised lake floor. *American Journal of Science* 262, 340–354.

Nanson GC, East TJ, Roberts RG, Clark RL & Murray AS 1990. Quaternary evolution and landform stability of Magela Creek catchment, near the Ranger Uranium Mine, northern Australia. Open file record 63, Supervising Scientist for the Alligator Rivers Region, Canberra. Unpublished paper.

Needham RS 1988. *Geology of the Alligator Rivers Region uranium field, Northern Territory*. Bureau of Mineral Resources Bulletin 224, Australian Government Publishing Service, Canberra.

Needham RS 1982. Nabarlek Region, Northern Territory. *Bureau of Mineral Resources, Geology and Geophysics, Australia, 1:100 000 Geological Map Commentary*, Australian Government Publishing Service, Canberra.

Rickenmann D 1997. Sediment transport in Swiss Torrents. *Earth Surface Processes and Landforms* 22, 937−951.

Riley SJ 1992. Small scale studies of the erodibility of Ranger Waste Rock Dump. Internal report 64, Supervising Scientist for the Alligator Rivers Region, Canberra. Unpublished paper.

Riley SJ 1994. Hydrological monitoring of Tin Camp Creek mica and quartz catchments, 1993–94 Wet season. Internal report 151, Supervising Scientist for the Alligator Rivers Region, Canberra. Unpublished paper.

Ritter JB 1990. Surface hydrology of drainage basins disturbed by surface mining and reclamation, Central Pennsylvania. PhD thesis, The Pennsylvania State University.

Rodriguez-Iturbe I & Rinaldo A 1997. *Fractal river basins: Chance and self-organisation.* Cambridge University Press, Cambridge.

Strahler AN 1964. Quantitative geomorphology of drainage basins and channel networks. In *Handbook of applied hydrology*, McGraw-Hill, New York, 4.40–4.74.

Tarboton DG, Bras RL & Rodriguez-Iturbe I 1989. Scaling and elevation in river networks. *Water Resources Research* 25 (9), 2037−2052.

Unger CJ & Milnes AR 1992. Rehabilitation at Ranger uranium mines. In *Conservation and development issues in north Australia*, eds I Moffat & A Webb, North Australia Research Unit ANU, Darwin, 221−231.

Uren C 1992. An investigation of surface geology in the Alligator Rivers Region for possible analogues of uranium mine rehabilitation structures. Internal report 56, Supervising Scientist for the Alligator Rivers Region, Canberra. Unpublished paper.

Watson DA & Laflen JM 1986. Soil strength, slope, and rainfall intensity effects on interrill erosion. *Transactions of the American Society of Agricultural Engineers*. 29, 98–102.

Willgoose GR 1992. *User manual for SIBERIA (Version 7.05)*. Research Report 076.04.1992, Department of Civil, Surveying and Environmental Engineering, The University of Newcastle, NSW.

Willgoose GR 1994. A physical explanation for an observed area-slope-elevation relationship for catchments with declining relief. *Water Resources Research* 30 (2), 151−159.

Willgoose G 1995. A preliminary assessment of the effect of vegetation on the long-term erosional stability of the proposed above-grade rehabilitation strategy at Ranger Uranium Mine. Open file record 119, Supervising Scientist for the Alligator Rivers Region, Canberra. Unpublished paper.

Willgoose GR, Bras RL & Rodriguez-Iturbe I 1989. Modelling of the erosional impacts of land use change: A new approach using a physically based catchment evolution model. In *Hydrology and Water Resources Symposium 1989*, Christchurch NZ, National Conference publication no 89/19, The Institute of Engineers Australia, Melbourne, 325−329.

Willgoose GR, Bras RL & Rodriguez-Iturbe I 1991a. Results from a new model of river basin evolution. *Earth Surface Processes and Landforms* 16, 237−254.

Willgoose GR, Bras RL & Rodriguez-Iturbe I 1991b. A coupled channel network growth and hillslope evolution model 1. Theory. *Water Resources Research* 7, 1671−1684.

Willgoose GR, Bras RL & Rodriguez-Iturbe I 1991c. A coupled channel network growth and hillslope evolution model 2. Nondimensionalization and applications. *Water Resources Research* 7, 1685−1696.

Willgoose GR, Bras RL & Rodriguez-Iturbe I 1992. The relationship between catchment and hillslope properties: Implications of a catchment evolution model. *Geomorphology* 5, 21–37.

Willgoose GR & Kuczera G 1995. Estimation of subgrid scale kinematic wave parameters for hillslopes. *Hydrological Processes* 9, 469–482.

Willgoose GR, Kuczera GA & Williams BJ 1995. *DISTFW-NLFIT: Rainfall-runoff and erosion model calibration and model uncertainty assessment suite user manual*. Research Report 108.03.1995, Department of Civil, Surveying and Environmental Engineering, The University of Newcastle, New South Wales, Australia.

Willgoose GR & Loch RJ 1996. An assessment of the Nabarlek rehabilitation, Tin Camp Creek and other mine sites in the Alligator Rivers Region as test sites for examining long term erosion processes and the validation of the SIBERIA model. Internal report 229, Supervising Scientist, Canberra. Unpublished paper.

Willgoose G & Riley SJ 1998. *Application of a catchment evolution model to the production of long-term erosion on the spoil heap at the Ranger uranium mine: Initial analysis*. Supervising Scientist Report 132, Supervising Scientist, Canberra.

Williams GP 1989. Sediment concentration versus water discharge during single hydrologic events in rivers. *Journal of Hydrology* 111, 89–106.

Wockner GW & Freebairn DM 1991. Water balance and erosion study on the eastern Darling Downs — An update, *Australian Journal of Soil and Water Conservation* 4, 41–47.

Appendix A.1 — DISTFW-NLFIT input file (.fw)

```
Data file is for a natural rainfall plot (subcatchment version)
Hydrological Monitoring of TIN CAMP CREEK Quartz Catchment
1993-94 Wet Season
CATCHMENT
# No of elements, No of reservoirs, no of u/S elements
     3            0            2
# No of U/S element draining into D/S elements
#
# zero time (hrs), timestep (minutes), time of duration of storm (hrs)
#
0.  0.1  6.
#
#  OUTPUT PARAMETERS
#
# no of pts for output discharge,psteps
1 1
# subareas at which discharge requested
3
#  maximum discharge on output graph
0.002
#
INCIDENCES
  0   0   1
  0   0   2
```

Flow path matrix for the sub-catchments

```
PARAMETERS
# Kind of element
  0
#  No Area Length   U/S      D/S     SWSupply Gamma Sorpt   Phi   GWsupply
#               Elevation Elevation
#
  1   1187.9  58.5   3.20    11.8     1.0     1.0   1.0     1.0      1.0
  2    273.6  32.7  0.10    11.8     1.0     1.0   1.0     1.0      1.0
  3   1484.9  42.0  11.8    17.5     1.0     1.0   1.0     1.0      1.0
```

Sub-catchment physical properties

```
#  Hillslope and Channel conveyances
#
#    1st set are hillslope conveyances
#    2nd set are  channel  conveyances
#
#  Element No, No of conveyances
#  CR, EM, CONVEY
#
CONVEYANCES
1 2
0.141       1.      0.
0.141       1.      1000.
```

c_r parameter values for each sub-catchment

```
2 2
0.261       1.      0.
0.261       1.      1000.
3 2
0.097       1.      0.
0.097       1.      1000.
#
#  Parameter Multpliers
#  Ch-CR  Ch-EM  SWSupply SWGamma Sorptivity   Phi  GWSupply  timing(sec)
MULTIPLIERS
  7.8   1.33    0.03      0.375  0.00001     6.5     1000.    0.0
1
0.0 0.0
#
# No of pluvios
#
RAINFALL #1
   1
CUMPLUVIO quar25.rf
```

Rainfall input file

```
1.00 1.00 1.00
#
#  No of known initial flows at stations
#
INITIALQ
title line 1
title line 2
title line 3
   1
# stations at which flows known and initial flow (cumecs)
  3 0.0
#  No of stations with known inflows
INFLOWQ NONE
#  Hydrograph to calibrate with (no of values)
CALIB #1 quar25.ro
END
```

Runoff input file

Appendix A.2 — DISTFW-NLFIT rainfall input file (.rf)

TCC site
Nat_{C2} catchment
25 Dec 1993 1751 h Rainfall
54

No. of data points

Time (dec. hours) and cumulative rainfall (mm)

0.000000	0
0.008328	0.4
0.016680	0.6
0.025008	1.2
0.033336	2.2
0.041664	3
0.050016	3.6
0.058344	4
0.066672	4.2
0.075000	4.2
0.083328	4.4
0.091680	4.6
0.100008	4.6
0.108336	4.6
0.116664	4.6
0.125016	4.6
0.133344	4.8
0.183336	4.8
0.191664	5
0.566667	5
0.575002	5.2
0.583335	5.4
0.591667	5.6
0.600000	6.2
0.608335	6.4
0.616668	6.8
0.625001	7.4
0.633334	7.8
0.641667	8.6
0.650002	9.2
0.658335	9.4
0.666667	9.6
0.691668	9.6
0.700001	9.8
0.708334	10
0.716667	10
0.725002	10.2
0.733335	10.4
0.766668	10.4
0.775001	10.6
0.783334	10.6
0.791667	10.8
0.800002	11
0.808335	11.4
0.816667	11.4
0.825000	11.6
0.850001	11.6
0.858334	11.8
0.866667	12
0.875002	12.2
0.883335	12.4
0.891667	12.4
0.900000	12.6
2.000000	12.6

Appendix A.3 — DISTFW-NLFIT runoff input file (.ro)

TCC site
Nat$_{C2}$ catchment
25 Dec 1993 1751 h Discharge
127

No. of data points

0.000000	0
0.066667	0
0.074995	0.000609
0.083323	0.000811
0.091675	0.001278
0.100003	0.002219
0.108331	0.002395
0.116659	0.002219
0.125011	0.002083
0.133339	0.001787
0.141667	0.001662
0.149995	0.001662
0.158323	0.001392
0.166675	0.00114
0.175003	0.000933
0.183331	0.000811
0.191659	0.000609
0.200011	0.000609
0.208339	0.00043
0.216667	0.00043
0.224995	0.00034
0.233323	0.00034
0.241675	0.000259
0.250003	0.0002
0.258331	0.0002
0.266659	0.000135
0.308323	0.000135
0.316675	9E05
0.325003	5.3E05
0.333331	9E05
0.341659	5.3E05
0.350011	9E05
0.358339	5.3E05
0.366667	1.7E05
0.374995	5.3E05
0.383323	1.7E05
0.391675	5.3E05
0.400003	1.7E05
0.449995	1.7E05
0.458323	1E06
0.500011	1E06
0.508339	0

Time (dec. hours) and runoff (cumecs)

Appendix B.1 — WRD_{50C} monitoring data

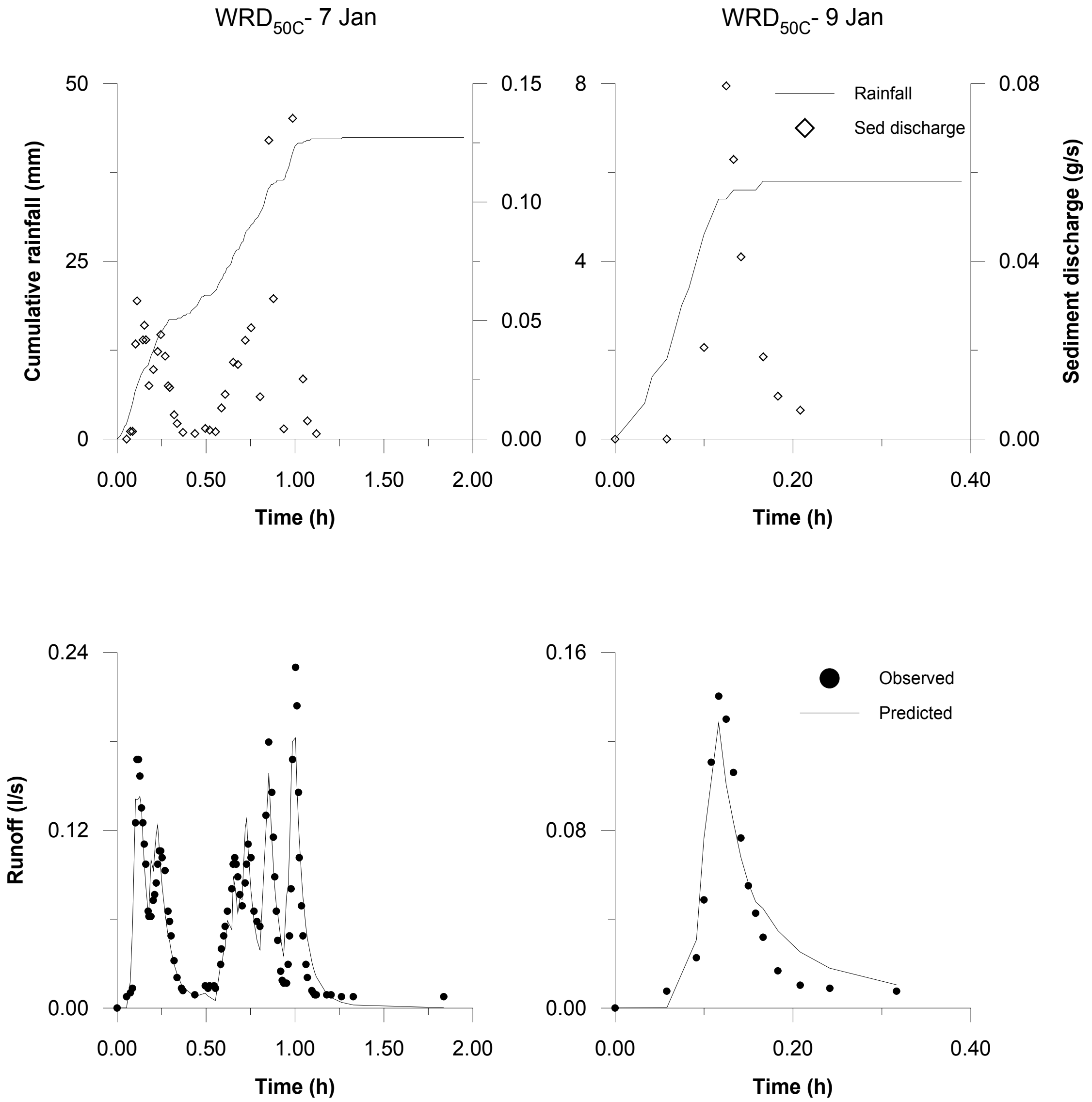

7 January

Parameter	Mean	St Deviation
c_r	0.25	0.34
e_m	1.27	0.29
Sphi	4.28	0.60
Phi	33.89	1.65

9 January

Parameter	Mean	St Deviation
c_r	32049	
e_m	3.94	6.14
Sphi	5.05	22.2
Phi	0.001	81.8

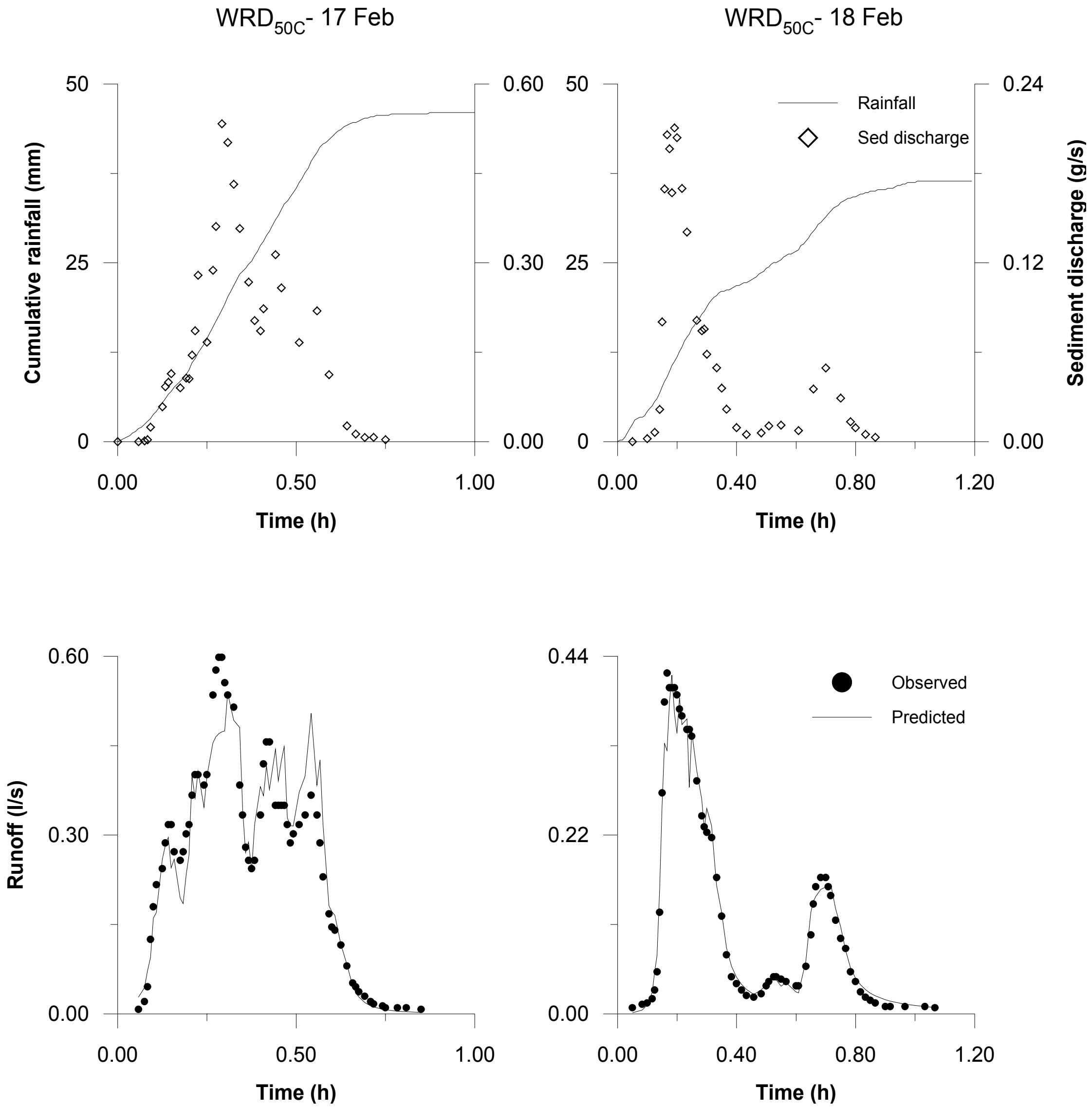

17 February

Parameter	Mean	St Deviation
c_r	4.34	11.8
e_m	1.65	0.62
Sphi	0.001	2217
Phi	25.12	246.9

18 February

Parameter	Mean	St Deviation
c_r	80902	
e_m	4.44	0.57
Sphi	1.27	0.74
Phi	22.06	1.35

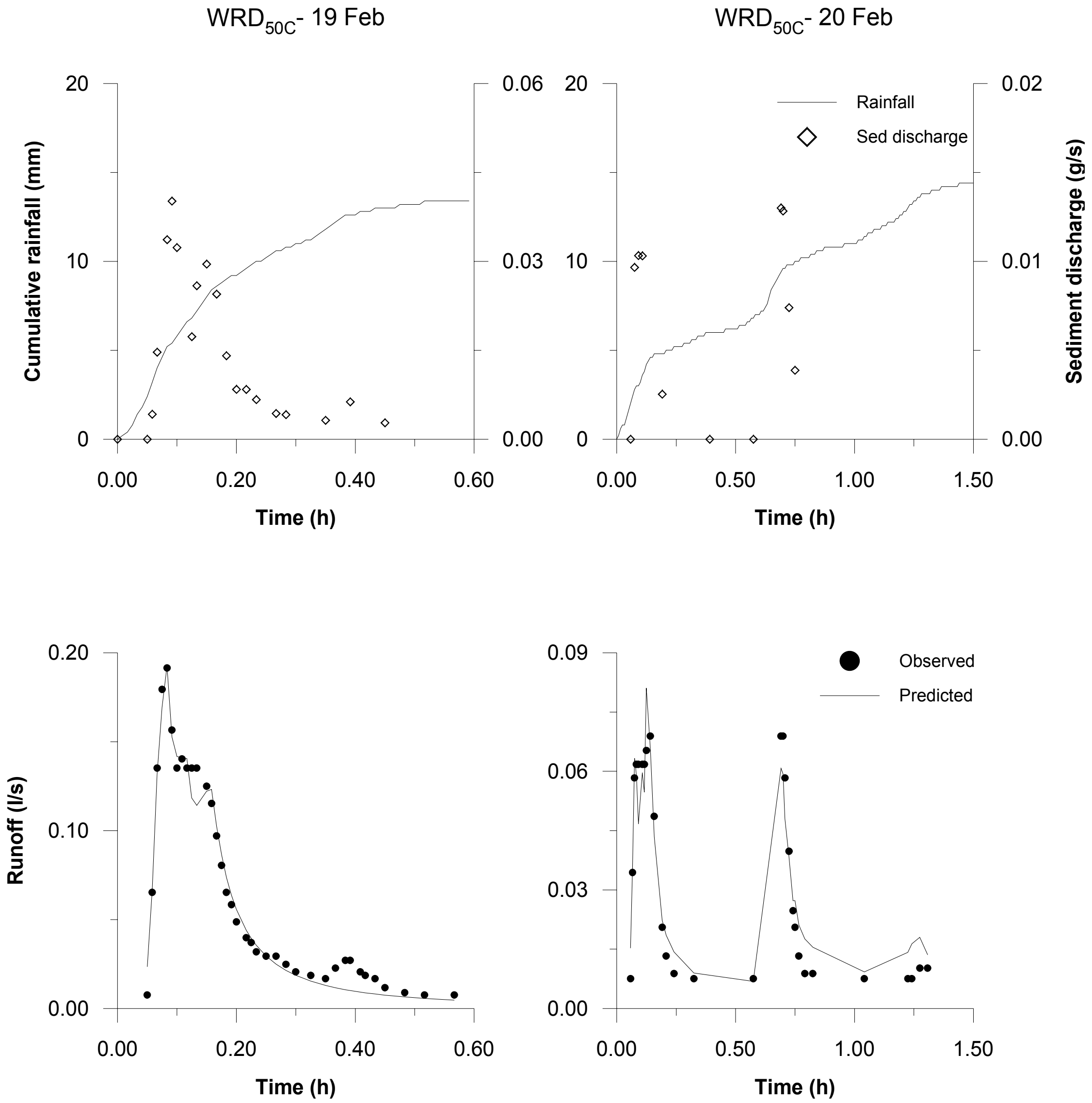

19 February

Parameter	Mean	St Deviation
c_r	29.73	35.8
e_m	2.42	0.31
Sphi	0.04	2.89
Phi	27.29	9.89

20 February

Parameter	Mean	St Deviation
c_r	674	1666
e_m	2.76	0.48
Sphi	2.38	0.49
Phi	11.55	1.28

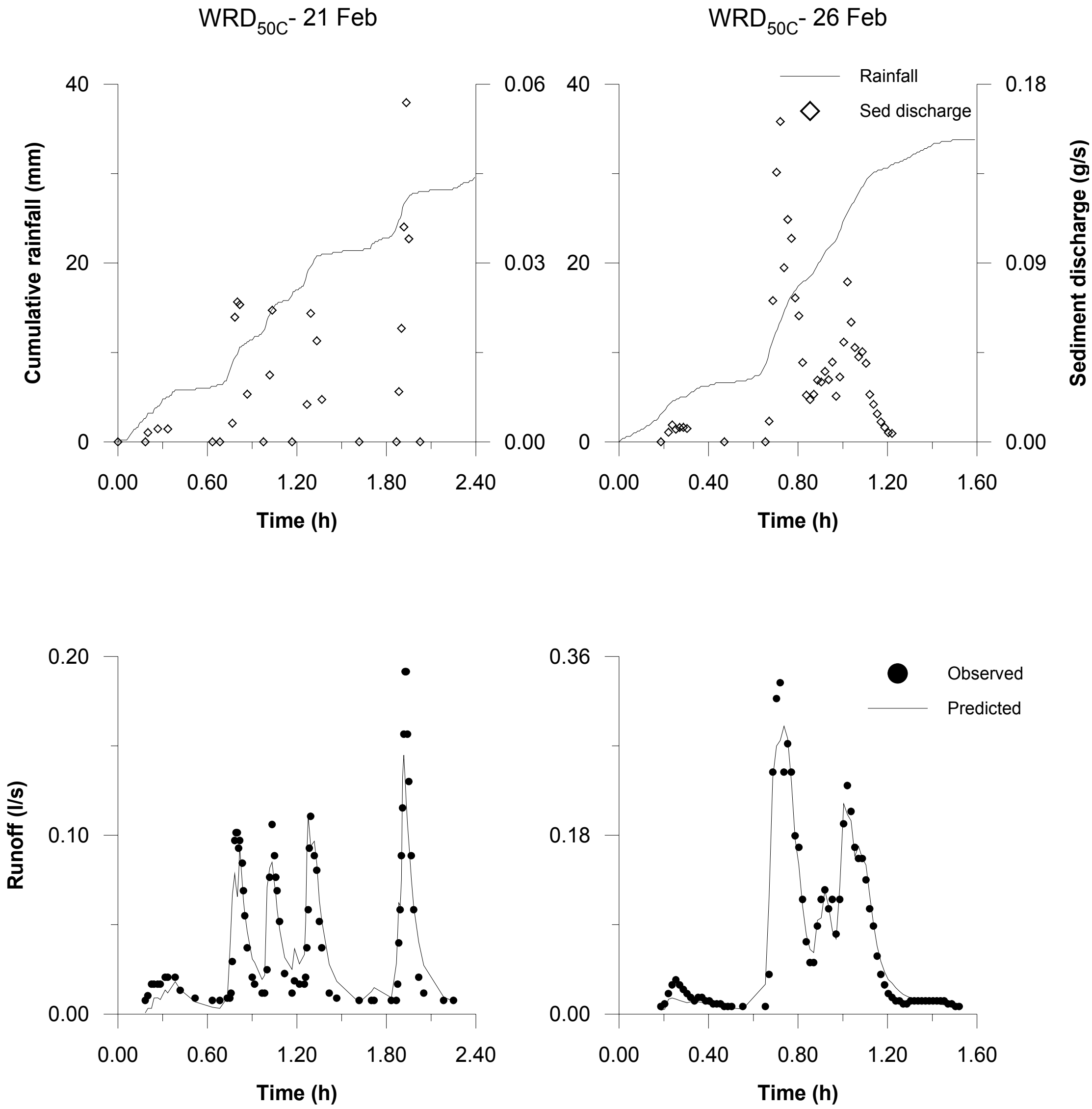

21 February

Parameter	Mean	St Deviation
c_r	1.78	5.27
e_m	1.77	0.67
Sphi	2.66	1.23
Phi	14.78	2.15

26 February

Parameter	Mean	St Deviation
c_r	19.51	41.9
e_m	2.33	0.56
Sphi	0.001	346.3
Phi	20.39	113.7

WRD$_{50C}$- 5 Mar

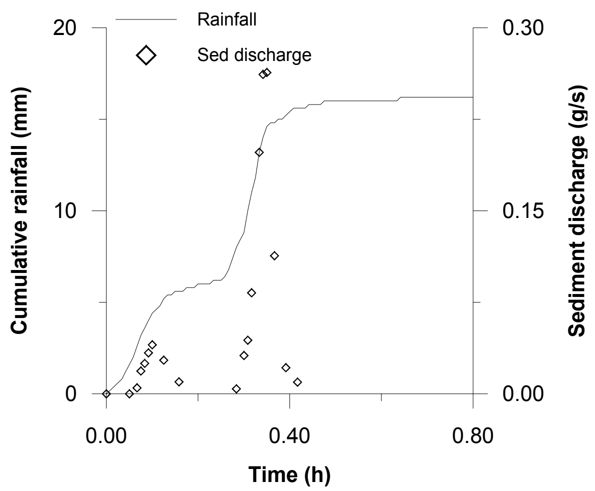

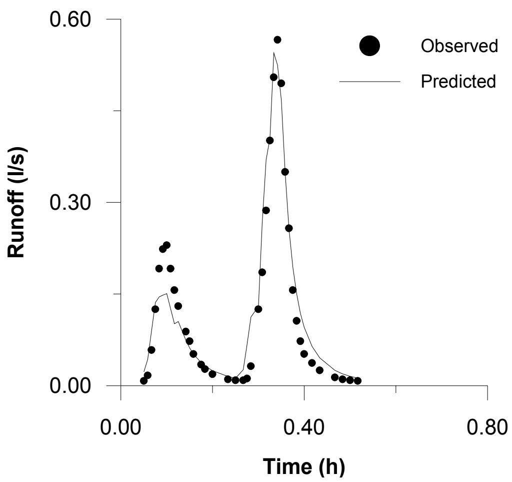

5 March

Parameter	Mean	St Deviation
c_r	0.91	1.20
e_m	1.50	0.33
Sphi	0.001	1747
Phi	24.30	188.3

Appendix B.2 — WRD_{50S} monitoring data

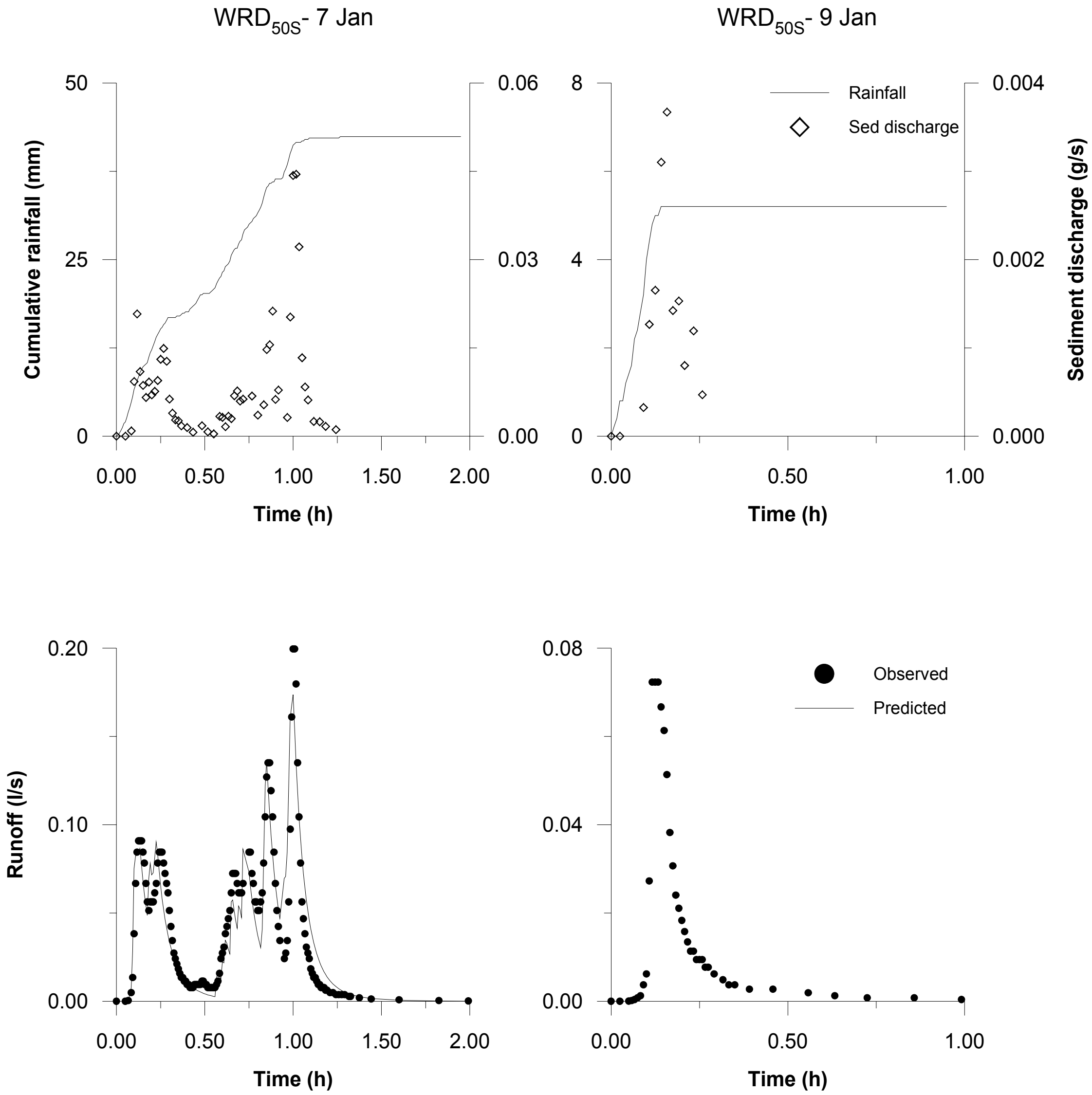

7 January

Parameter	Mean	St Deviation
c_r	0.15	0.10
e_m	1.20	0.15
Sphi	4.97	0.42
Phi	41.56	1.24

9 January

Did not fit

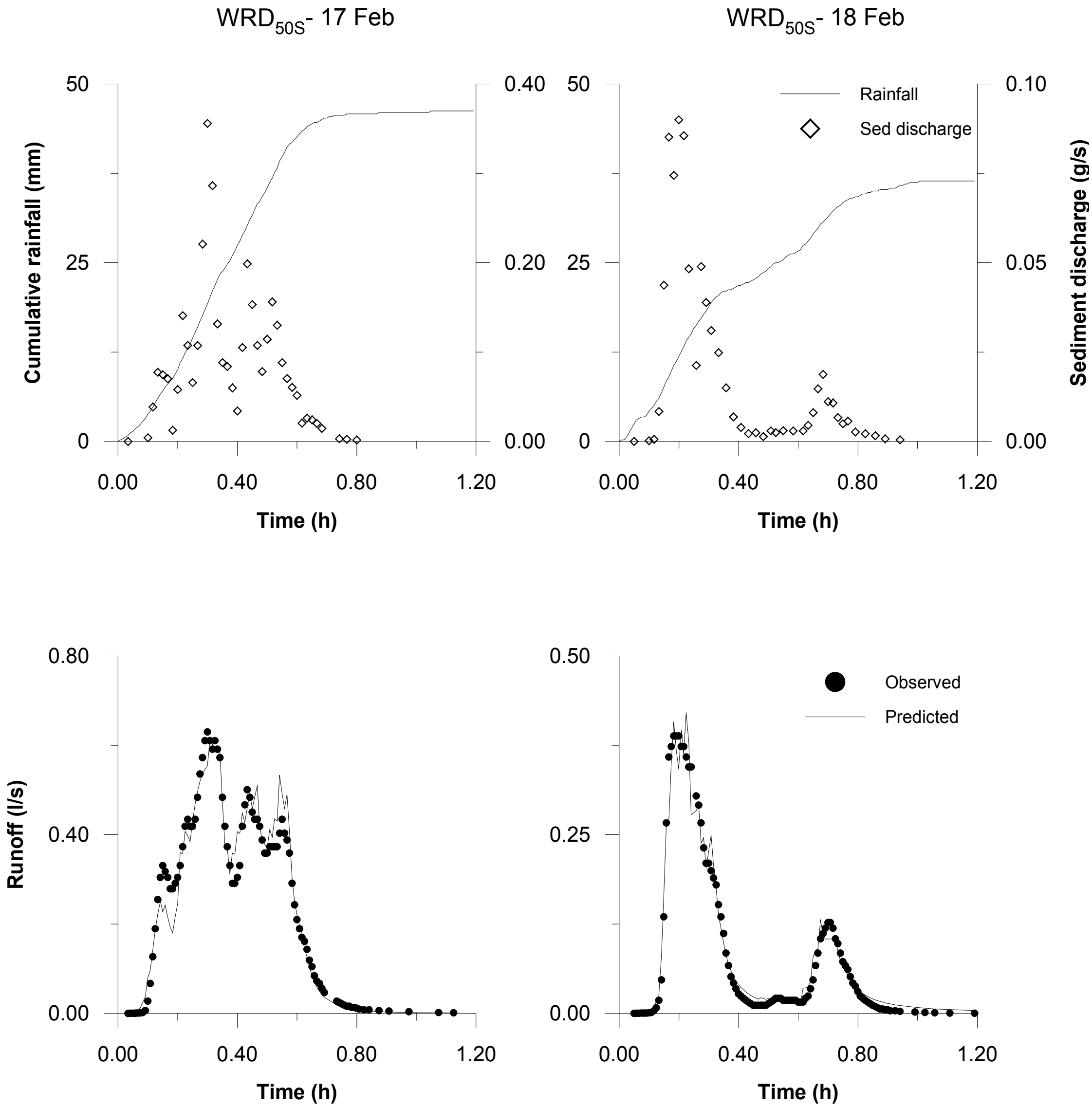

17 February

Parameter	Mean	St Deviation
c_r	0.74	0.56
e_m	1.43	0.19
Sphi	0.001	10.0
Phi	35.77	3.84

18 February

Parameter	Mean	St Deviation
c_r	283.4	398.2
e_m	2.89	0.37
Sphi	2.89	0.44
Phi	32.52	0.99

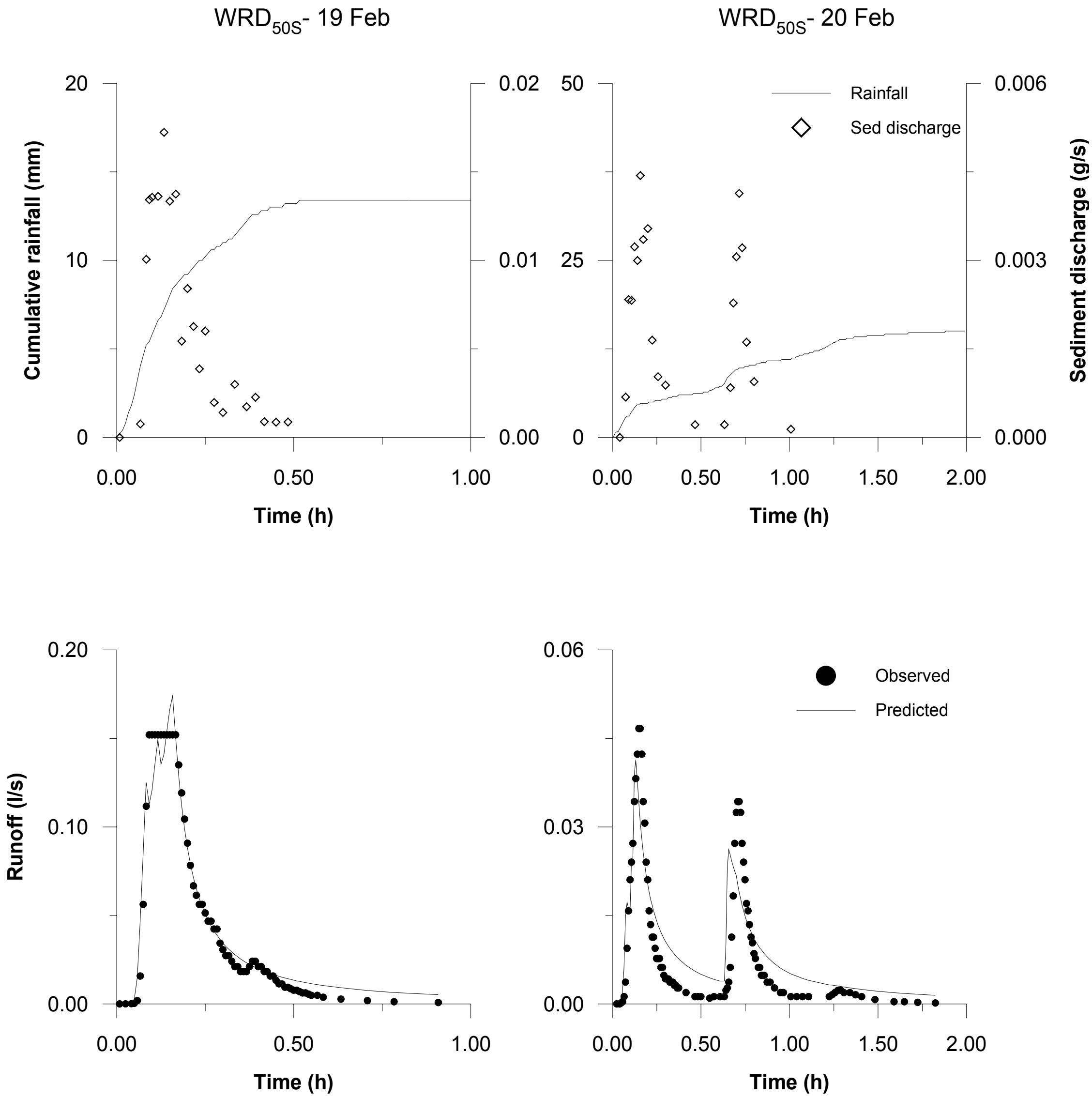

19 February

Parameter	Mean	St Deviation
c_r	953.6	4021
e_m	3.75	1.37
Sphi	0.001	5166
Phi	24.02	522.5

20 February

Parameter	Mean	St Deviation
c_r	247611	
e_m	4.59	1.27
Sphi	0.52	0.81
Phi	21.72	1.83

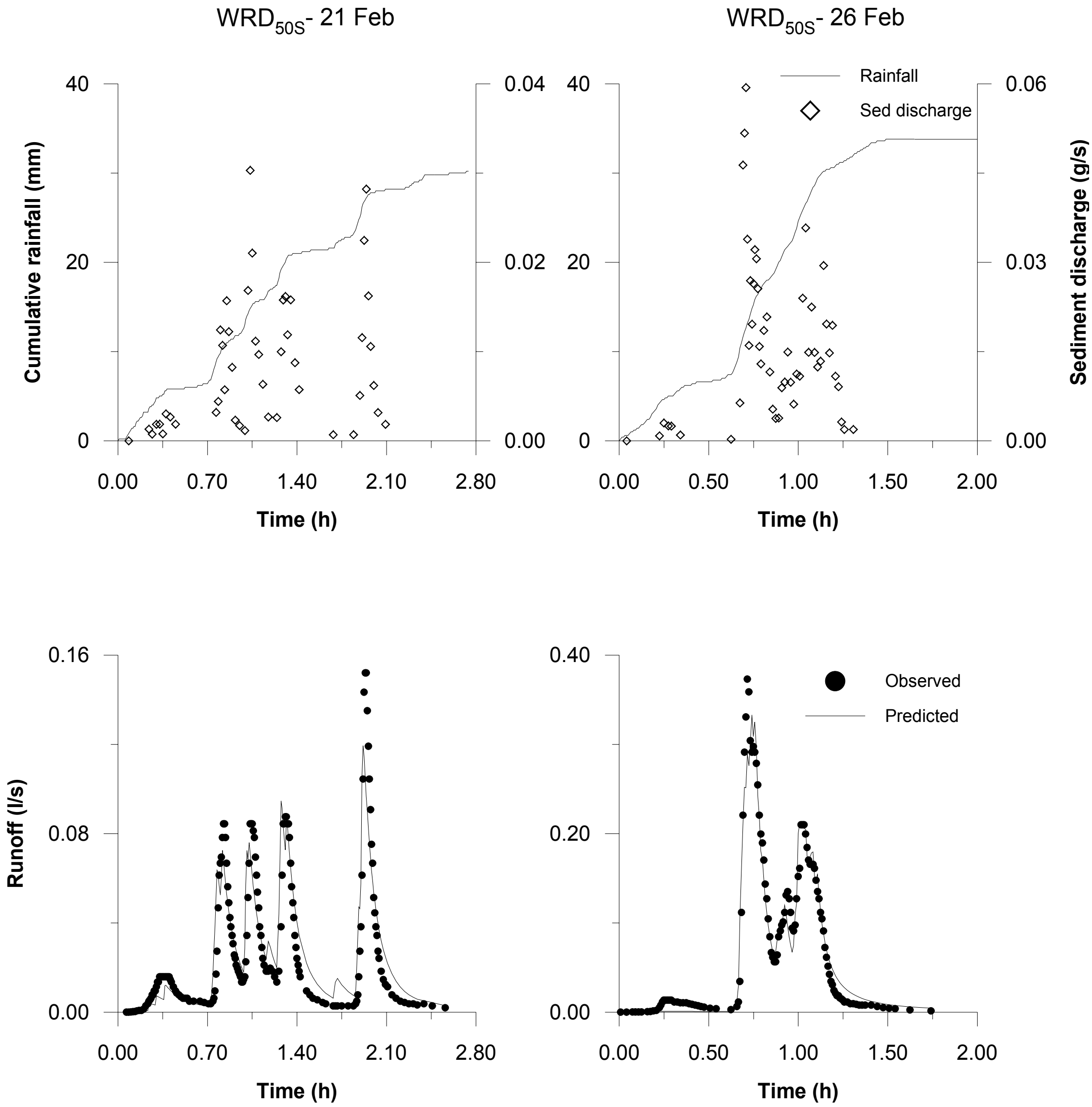

21 February

Parameter	Mean	St Deviation
c_r	0.27	0.35
e_m	1.44	0.31
Sphi	2.83	0.75
Phi	18.79	1.28

26 February

Parameter	Mean	St Deviation
c_r	30.84	30.4
e_m	2.61	0.28
Sphi	0.03	1.42
Phi	26.98	3.06

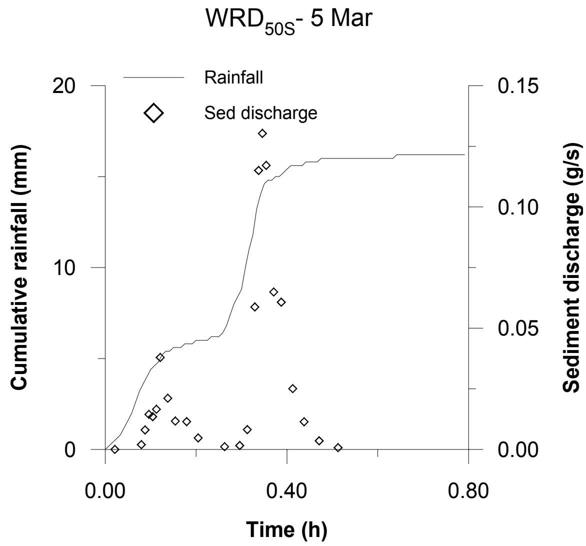

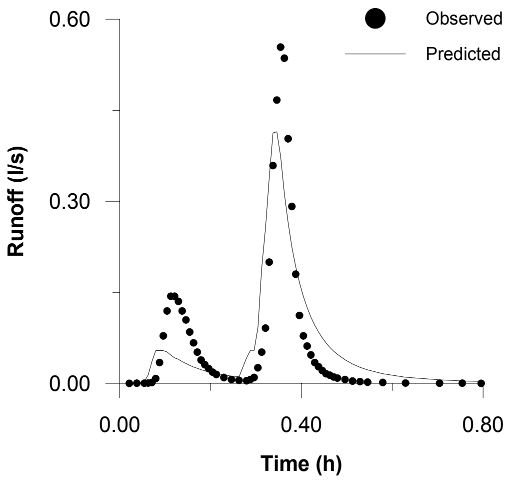

5 March

Parameter	Mean	St Deviation
c_r	0.28	0.55
e_m	1.35	0.53
Sphi	0.001	1505
Phi	42.44	445.2

Appendix B.3 — Nat$_{C1}$ monitoring data

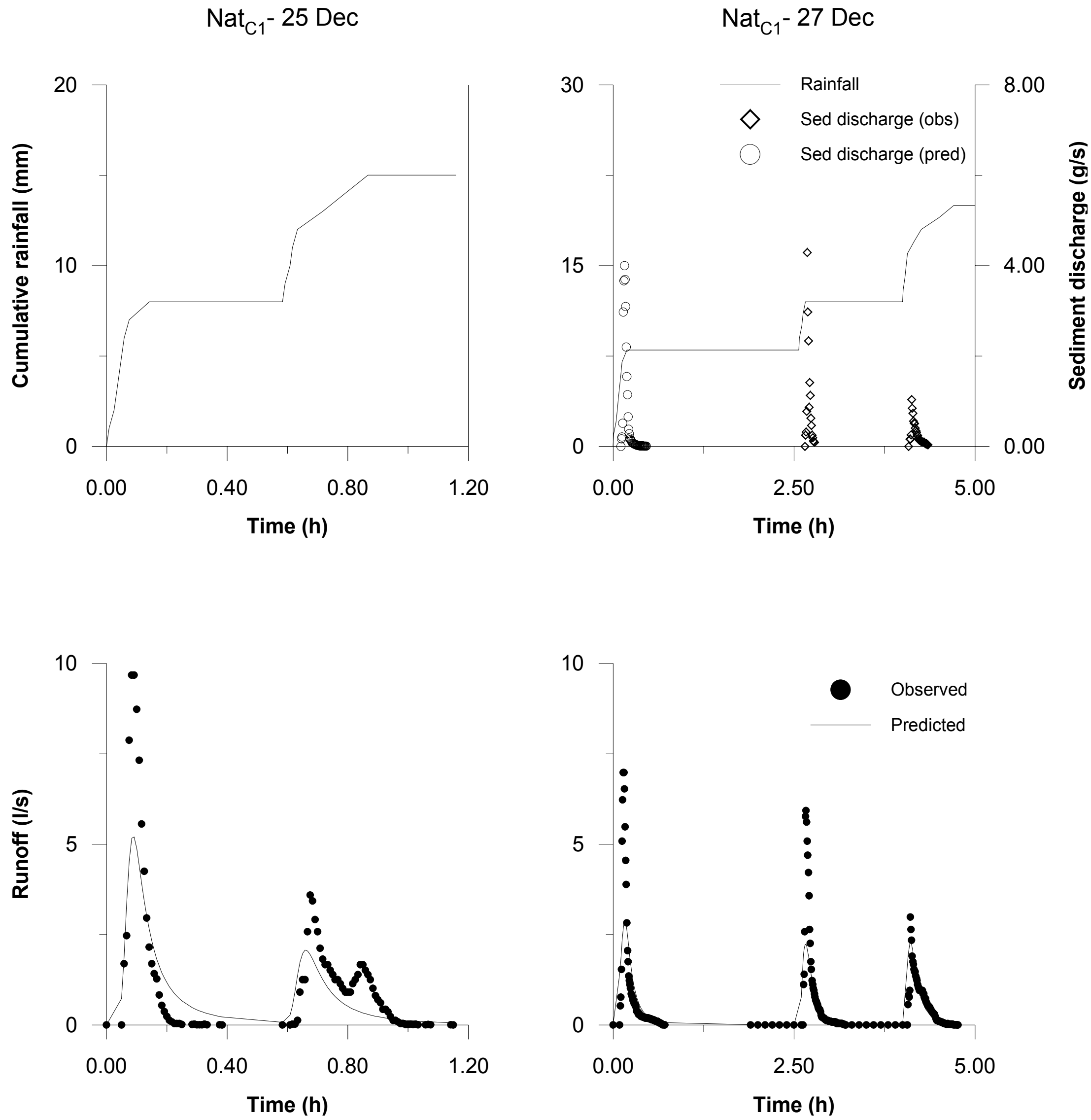

25 December

Parameter	Mean	St Deviation
c_r	8.34	3.71
e_m	1.47	0.11
Sphi	2.08	0.40
Phi	72.52	4.01

27 December

Parameter	Mean	St Deviation
c_r	2.35	0.84
e_m	1.28	0.08
Sphi	0.11	8.60
Phi	50.98	16.04

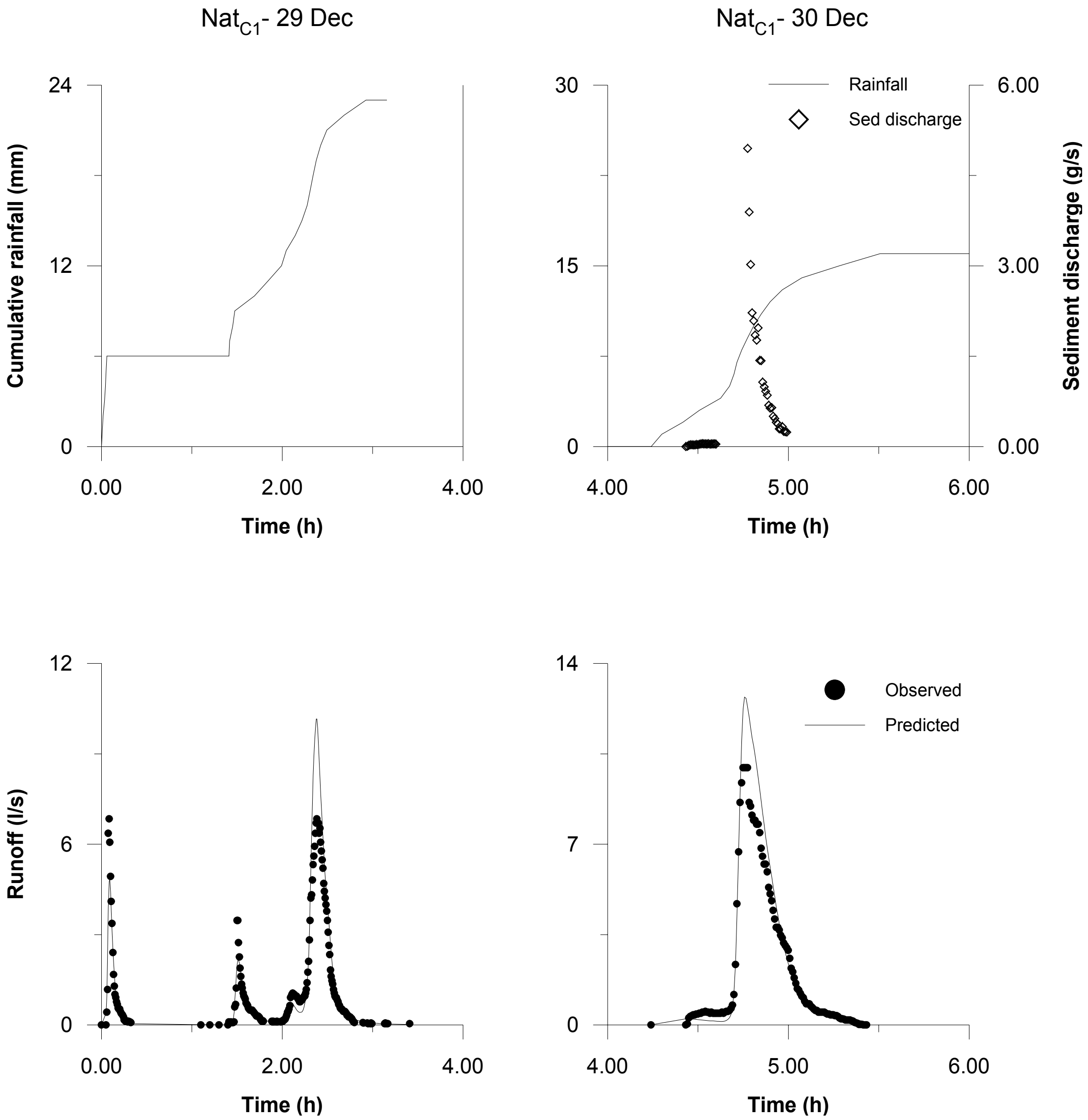

29 December

Parameter	Mean	St Deviation
c_r	3.0 (10.9)	5.0 (6.8)
e_m	1.1 (1.5)	0.3 (0.2)
Sphi	10.5 (4.1)	69.2 (0.2)
Phi	19.8 (4.2)	455 (0.4)

30 December

Parameter	Mean	St Deviation
c_r	10.56	2.59
e_m	1.62	0.07
Sphi	0.001	3.82
phi	13.36	1.19

Paranthesis indicates a separate fit for the second event. Storms could not be fitted in sequence on 29 December.

Appendix B.4 — Nat$_{C2}$ monitoring data

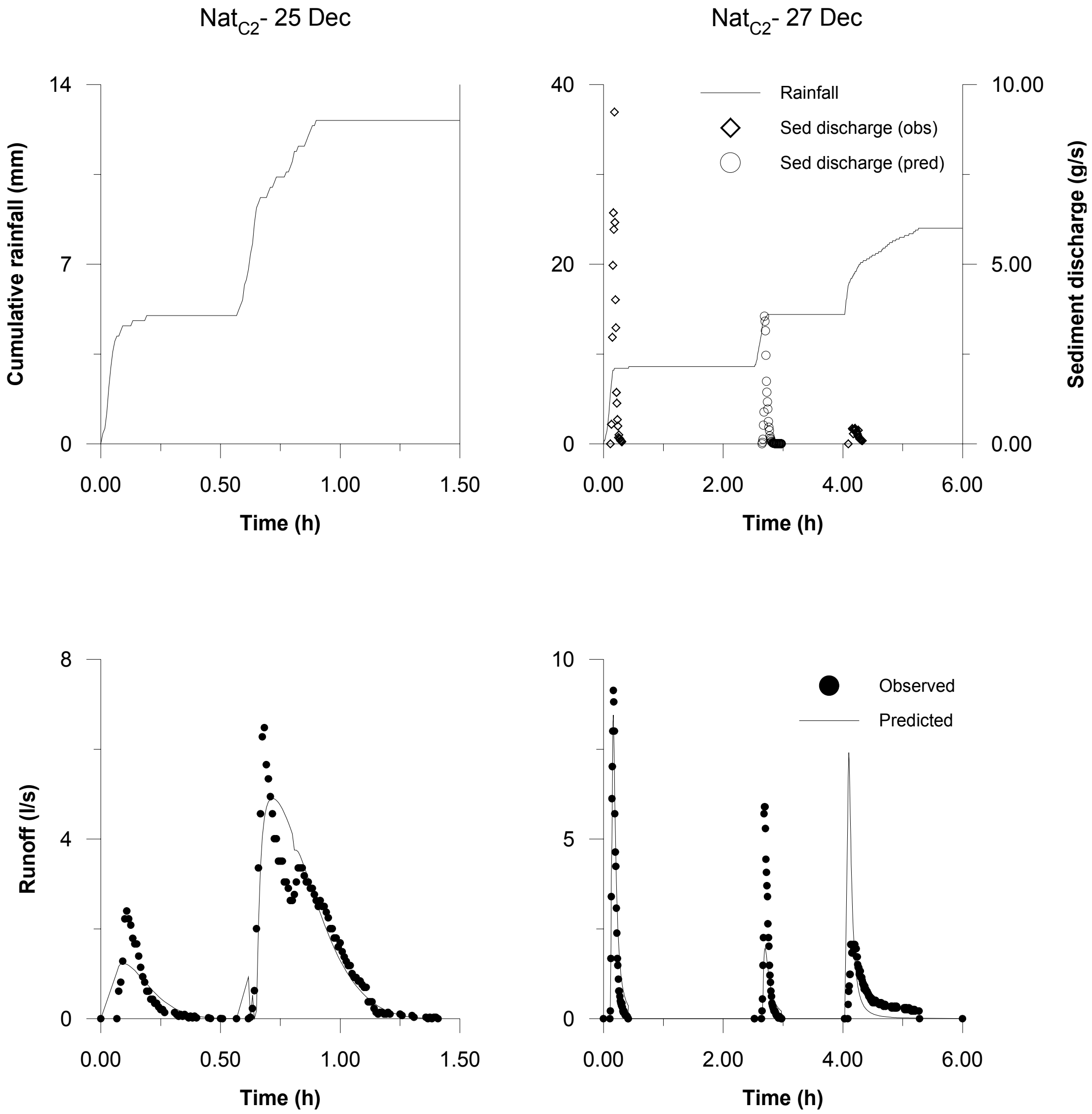

25 December

Parameter	Mean	St Deviation
c_r	0.73	0.12
e_m	0.79	0.05
Sphi	15.27	0.55
Phi	11.86	1.69

27 December

Parameter	Mean	St Deviation
c_r	31.15	24.6
e_m	1.63	0.22
Sphi	13.27	1.43
Phi	18.60	2.36

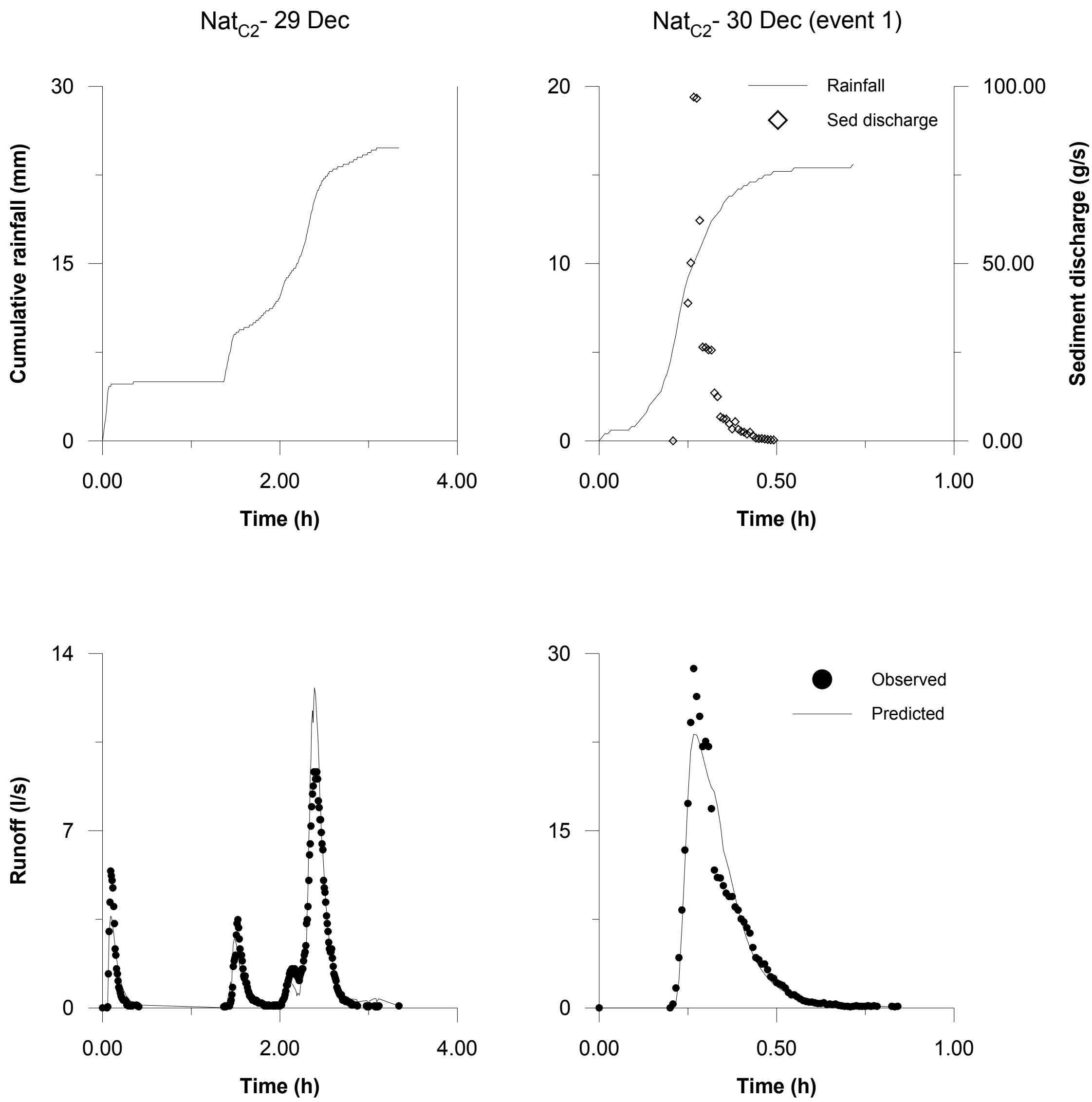

29 December

Parameter	Mean	St Deviation
c_r	7.35	1.14
e_m	1.24	0.04
Sphi	17.62	0.32
Phi	3.44	0.26

30 December

Parameter	Mean	St Deviation
c_r	7.44	1.12
e_m	1.31	0.06
Sphi	17.81	0.78
phi	4.73	0.50

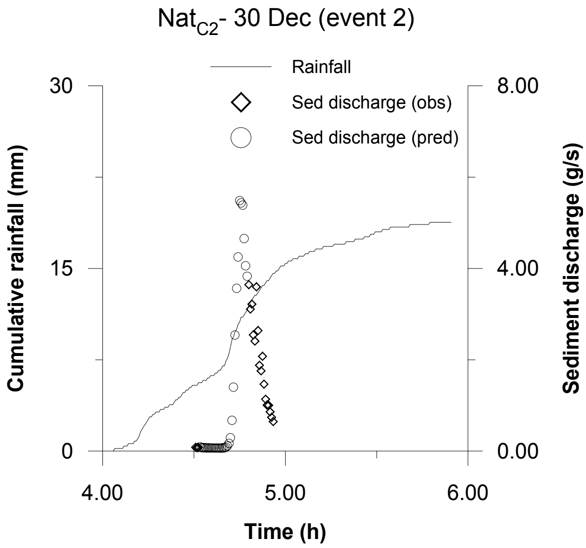

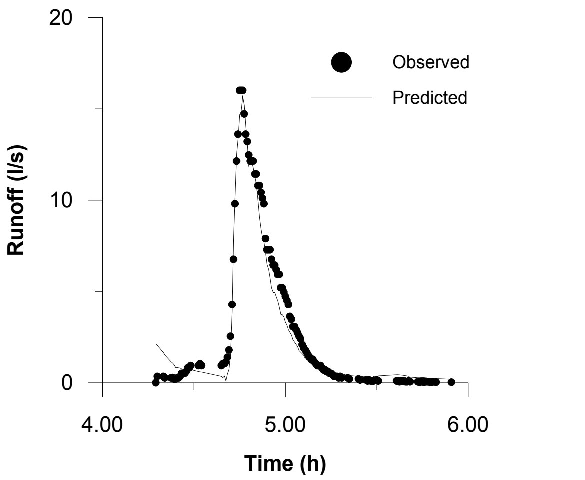

30 December

Parameter	Mean	St Deviation
c_r	7.44	1.12
e_m	1.31	0.06
Sphi	17.81	0.78
Phi	4.73	0.50

Appendix C.1 — Fitted and observed hydrographs — WRD_{50C}

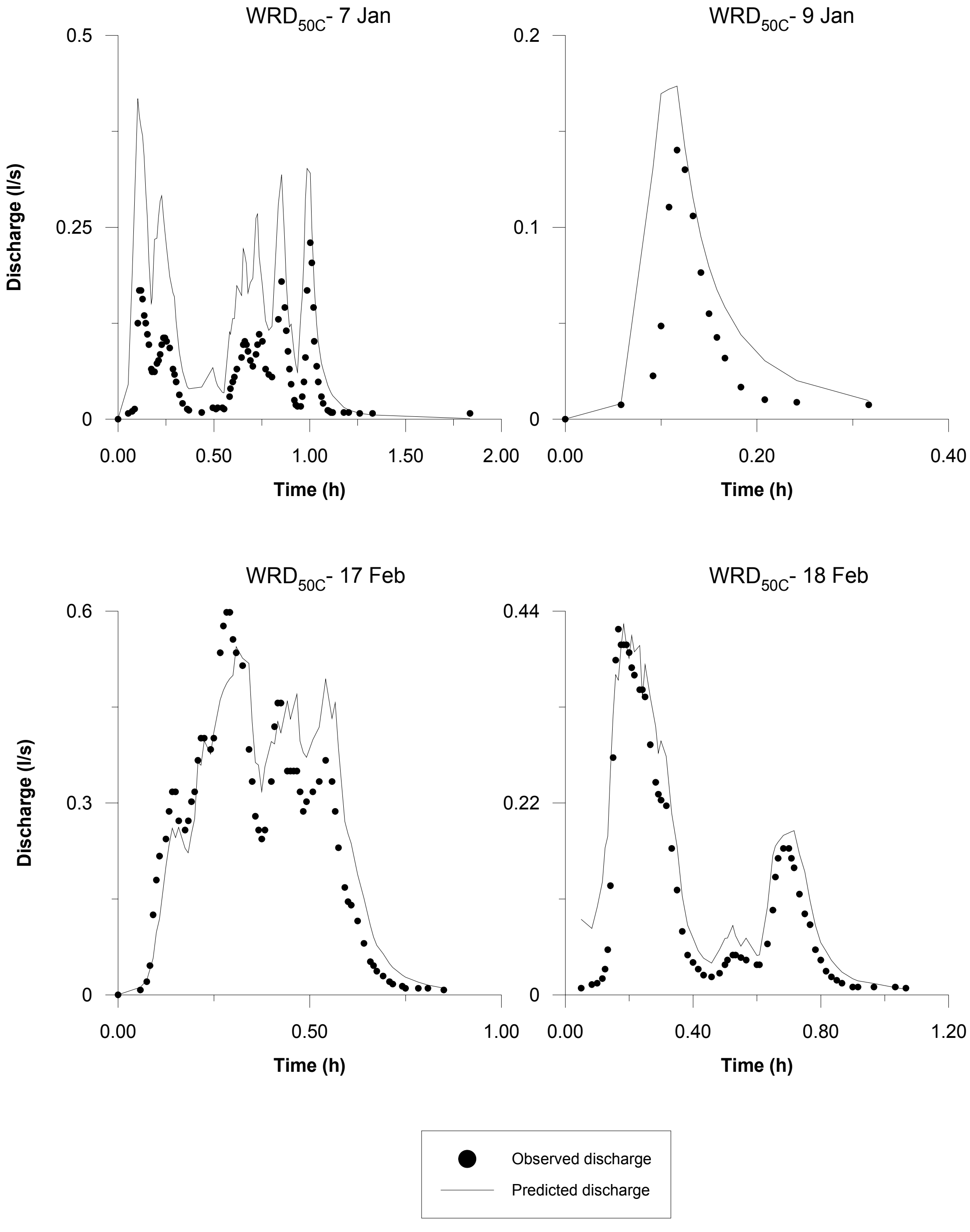

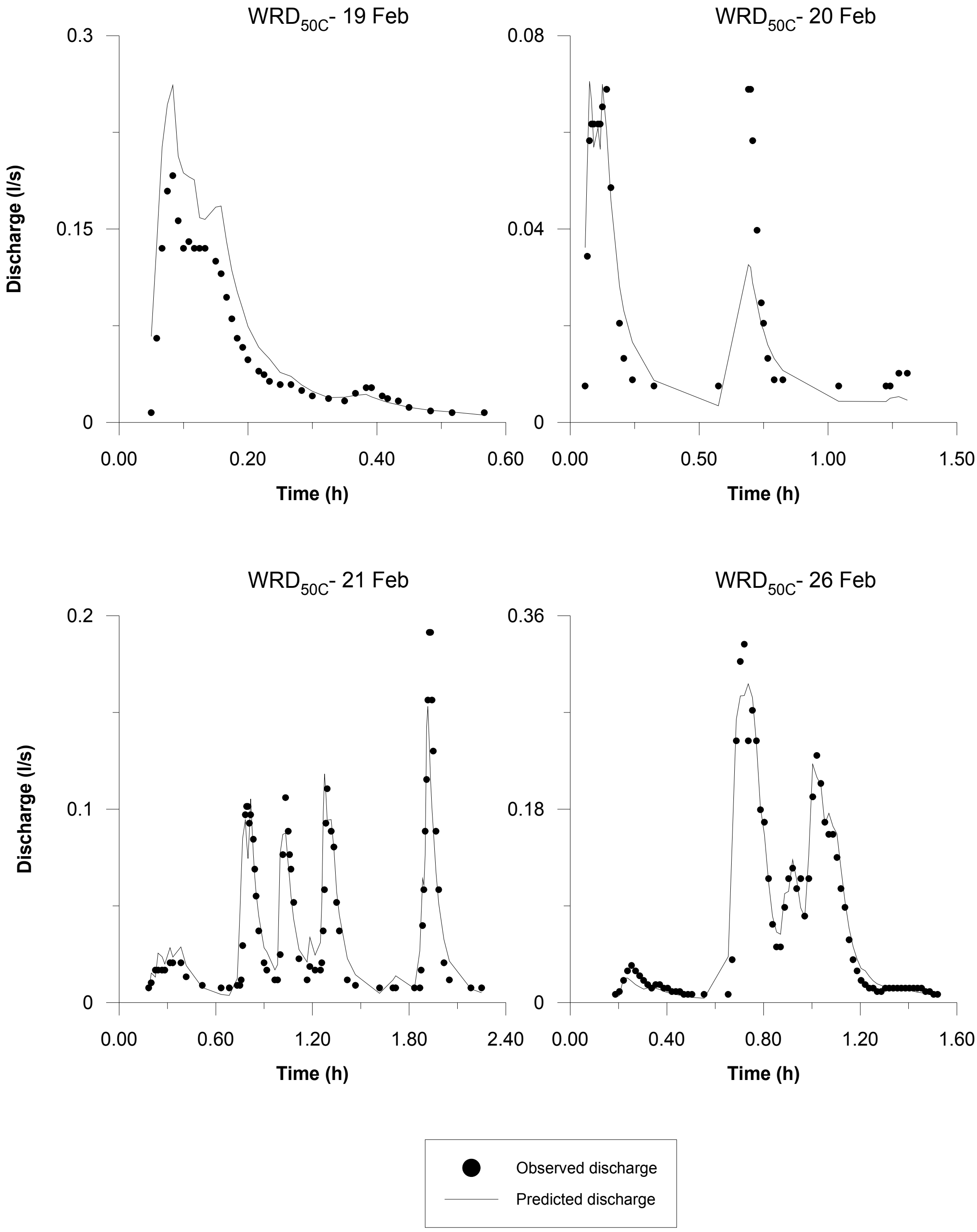
WRD50C- 19 Feb
WRD50C- 20 Feb
WRD50C- 21 Feb
WRD50C- 26 Feb
Discharge (l/s)
Time (h)
0.3
0.15
0
0.08
0.04
0.2
0.1
0.36
0.18
0.00
0.20
0.40
0.60
0.50
1.00
1.50
1.20
1.80
2.40
0.80
1.60
Observed discharge
Predicted discharge

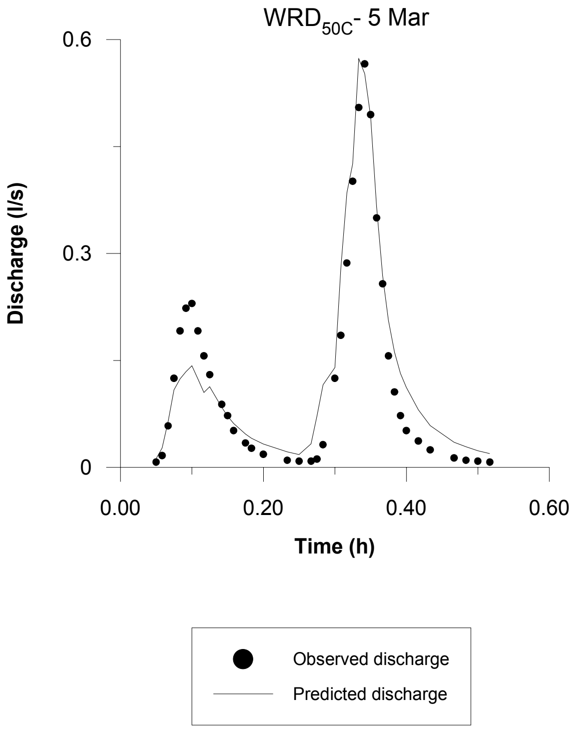
WRD$_{50C}$- 5 Mar
0.6
0.3
0
Discharge (l/s)
0.00
0.20
0.40
0.60
Time (h)
Observed discharge
Predicted discharge

Appendix C.2 — Fitted and observed hydrographs — WRD_{50S}

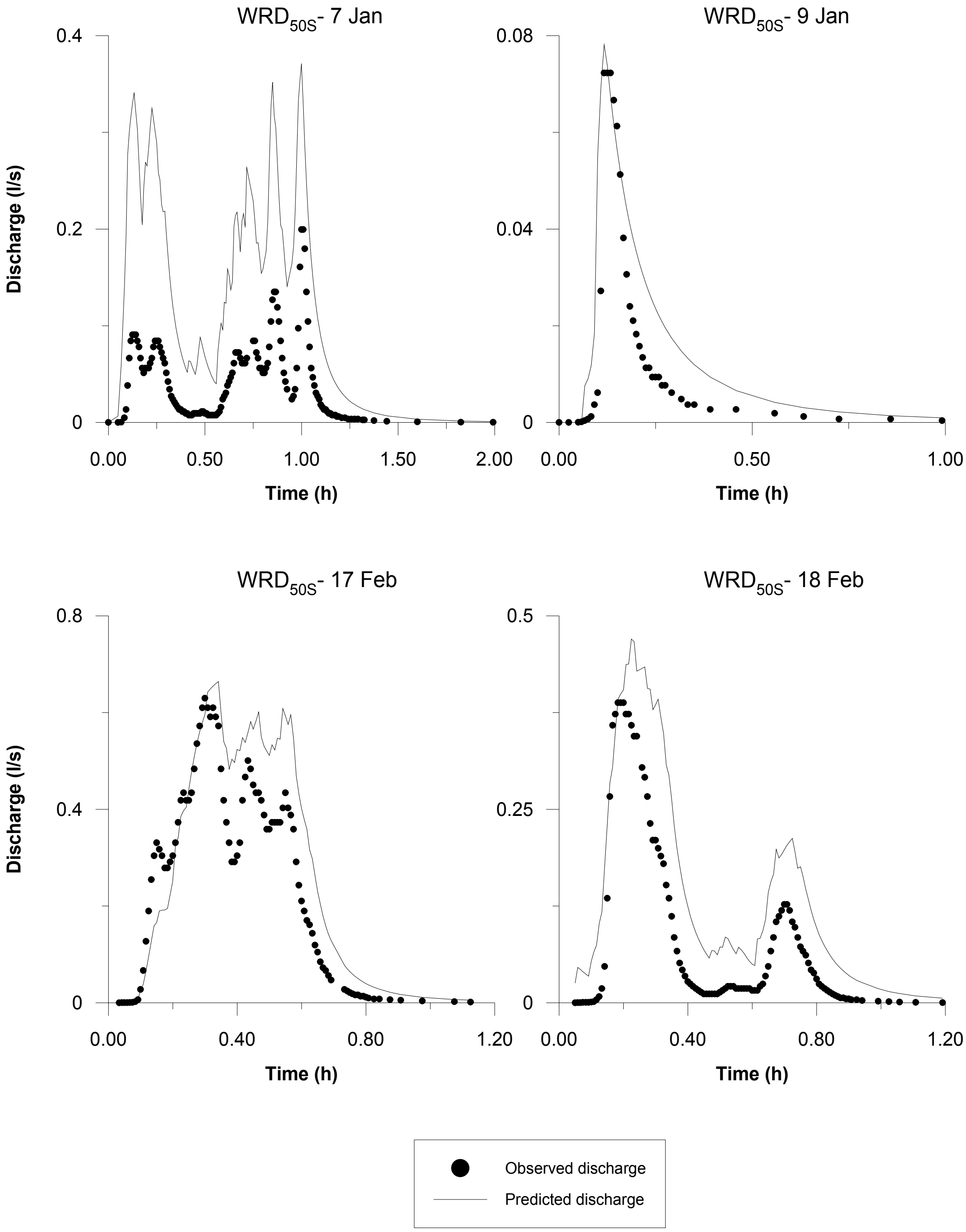

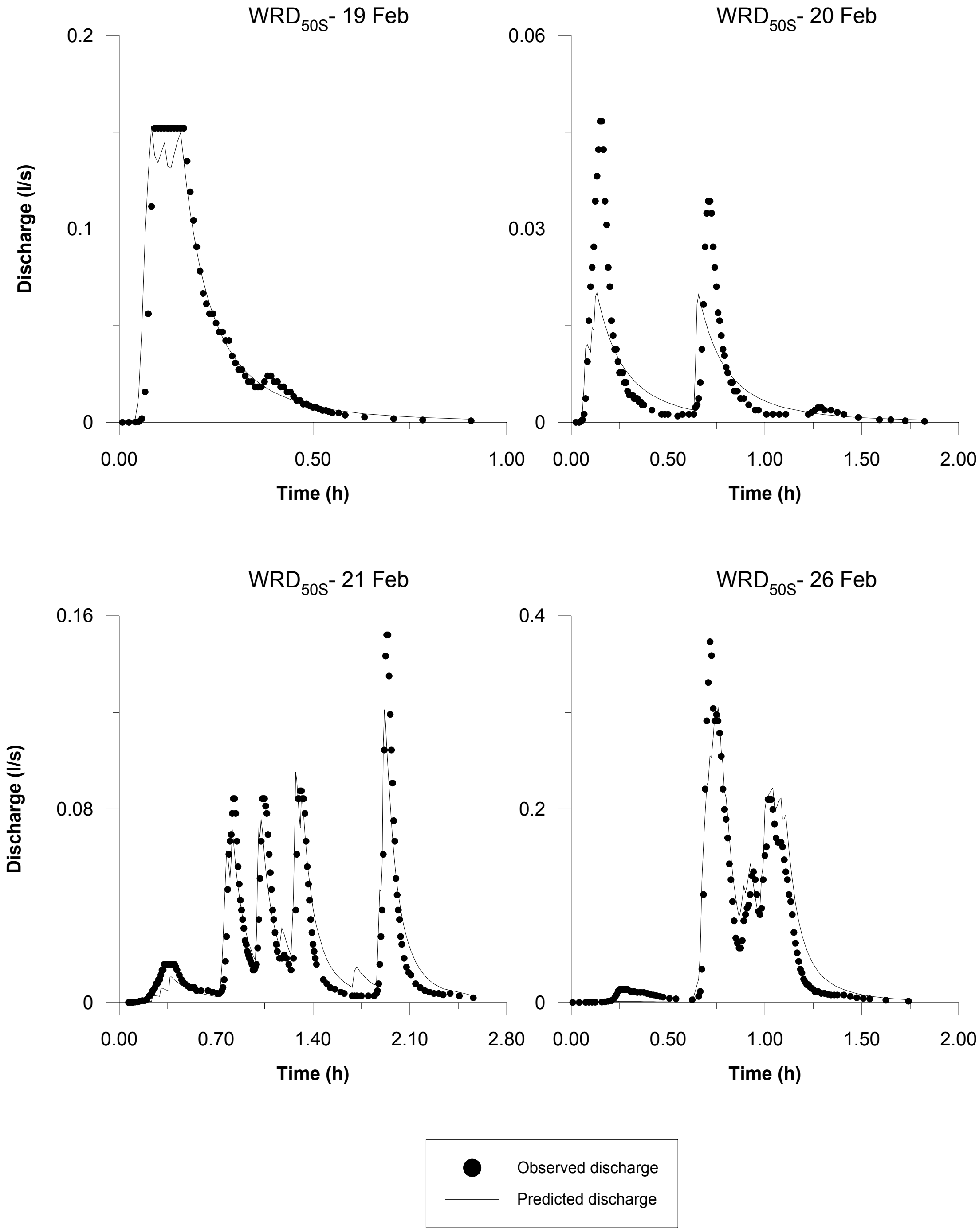

WRD50S- 19 Feb
WRD50S- 20 Feb
WRD50S- 21 Feb
WRD50S- 26 Feb
Discharge (l/s)
Time (h)
0.2
0.1
0
0.06
0.03
0.16
0.08
0.4
0.2
0.00
0.50
1.00
1.50
2.00
0.70
1.40
2.10
2.80
Observed discharge
Predicted discharge

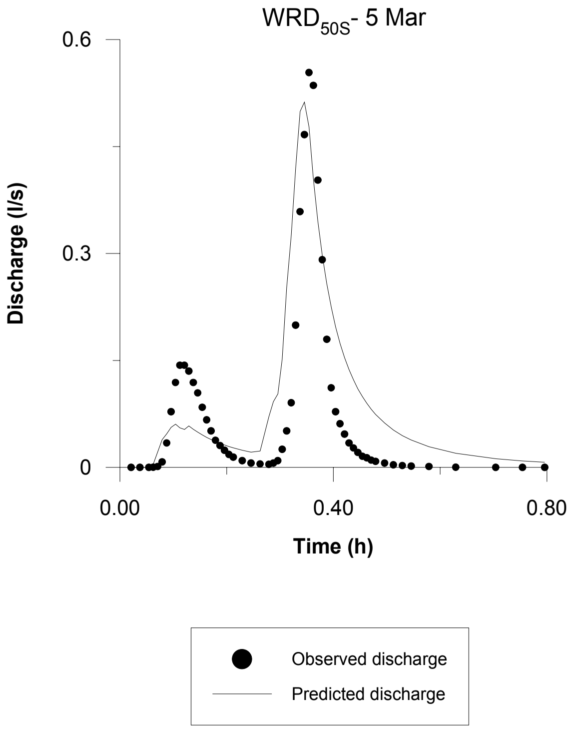
WRD50S- 5 Mar
0.6
0.3
0
Discharge (l/s)
0.00
0.40
0.80
Time (h)
Observed discharge
Predicted discharge

Appendix C.3 — Fitted and observed hydrographs — Nat_{C1}

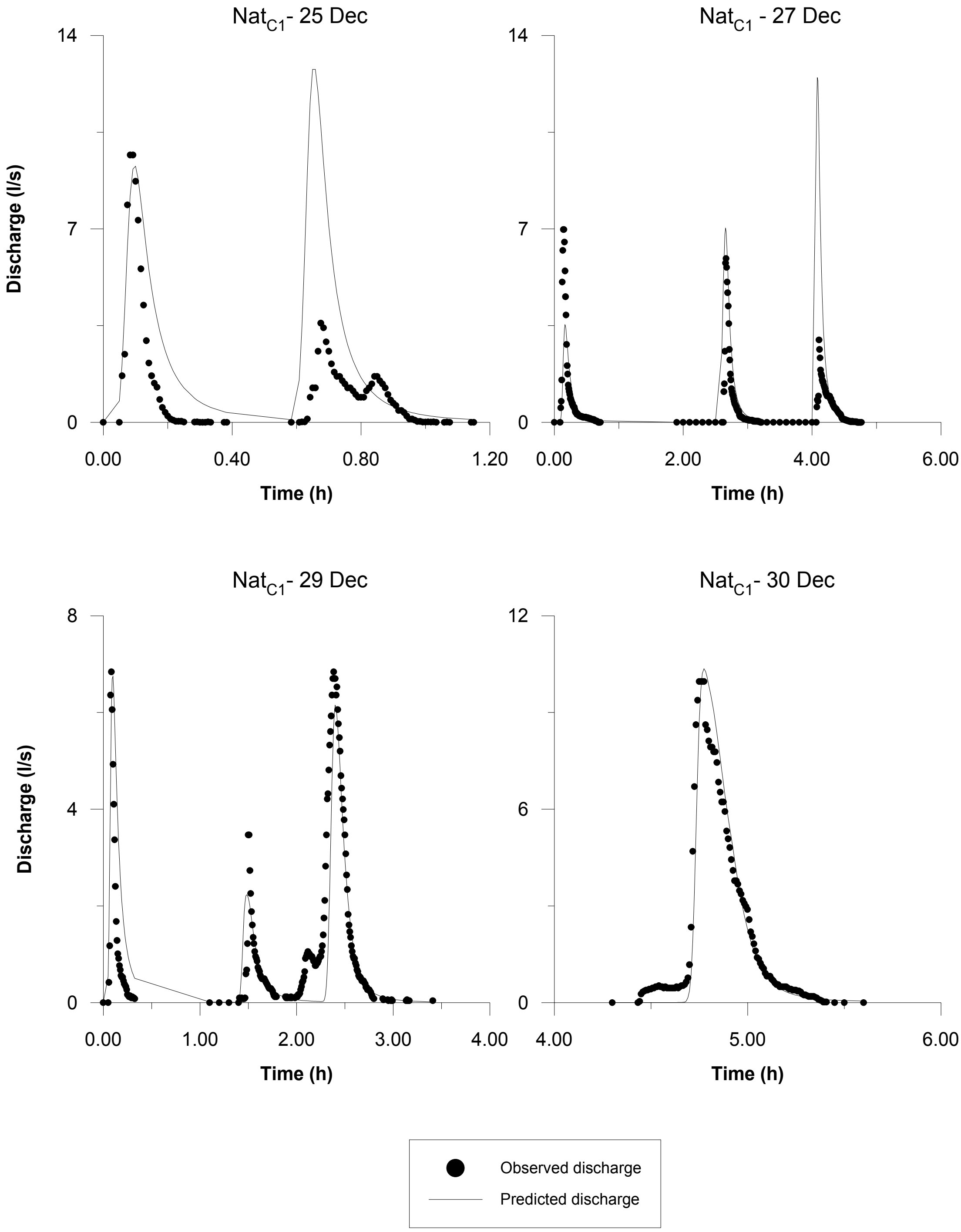

Appendix C.4 — Fitted and observed hydrographs — Nat_{C2}

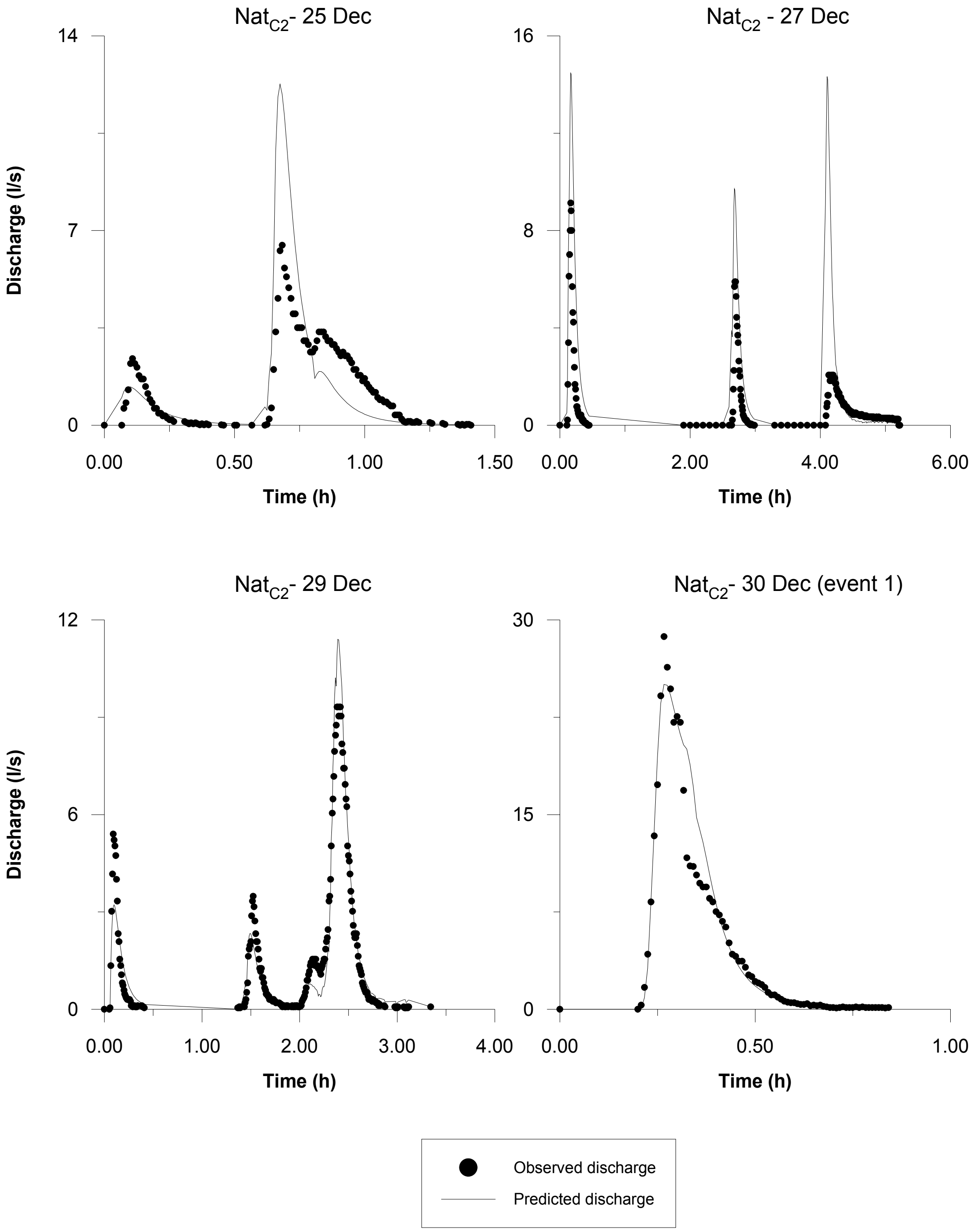

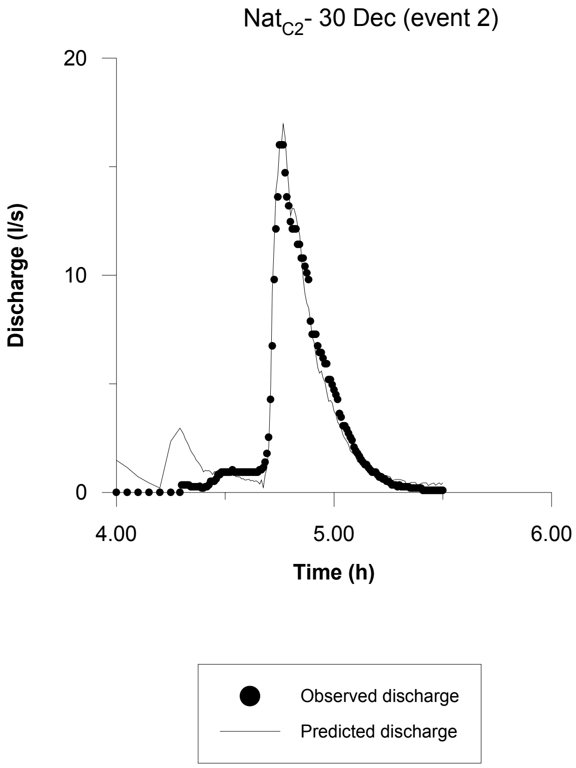
Nat$_{C2}$- 30 Dec (event 2)
20
10
0
4.00
5.00
6.00
Discharge (l/s)
Time (h)
Observed discharge
Predicted discharge

Appendix D — Fitted hydrographs using 'NLFIT' and 'geometric' kinematic wave parameter values — Nat_C

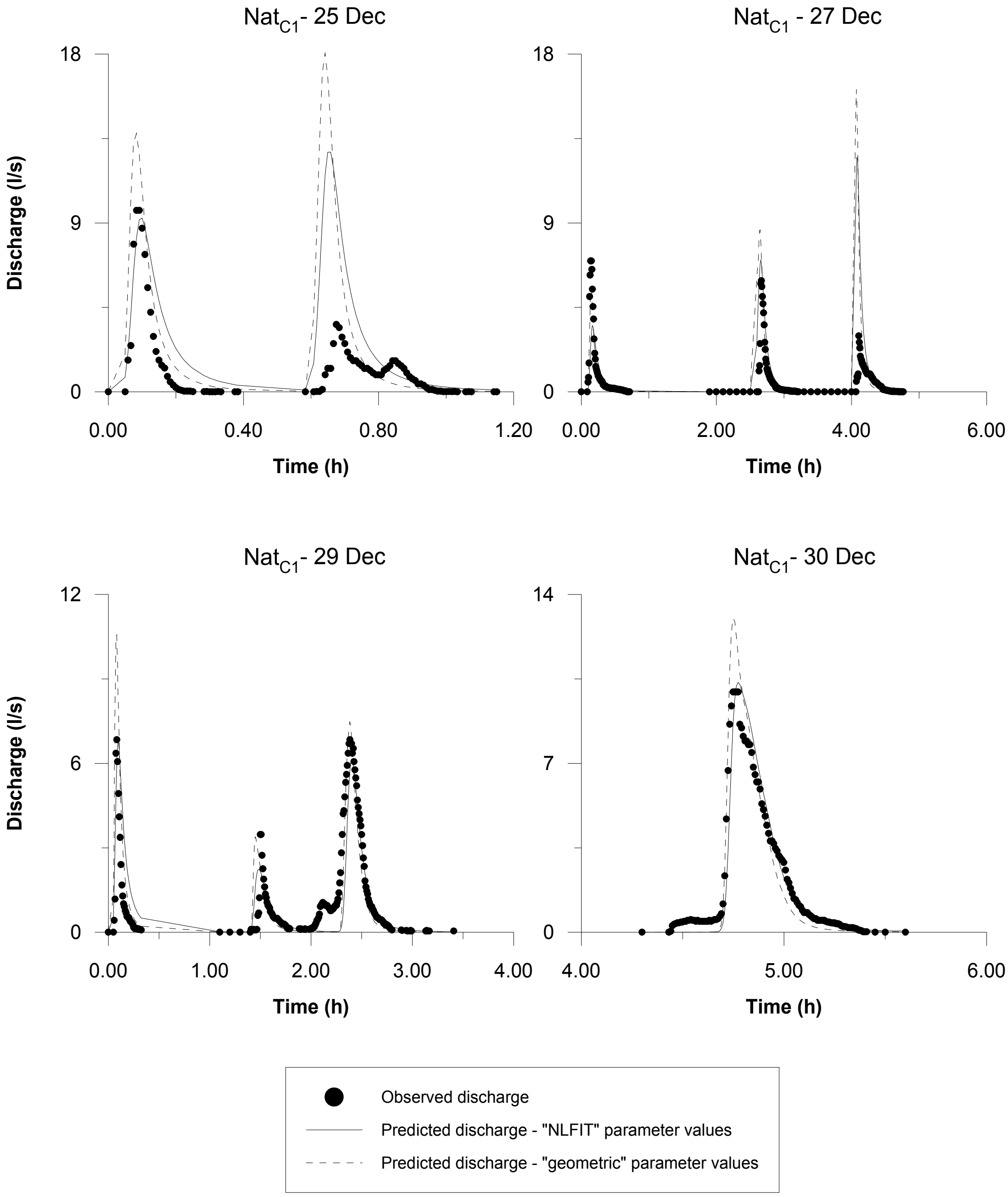

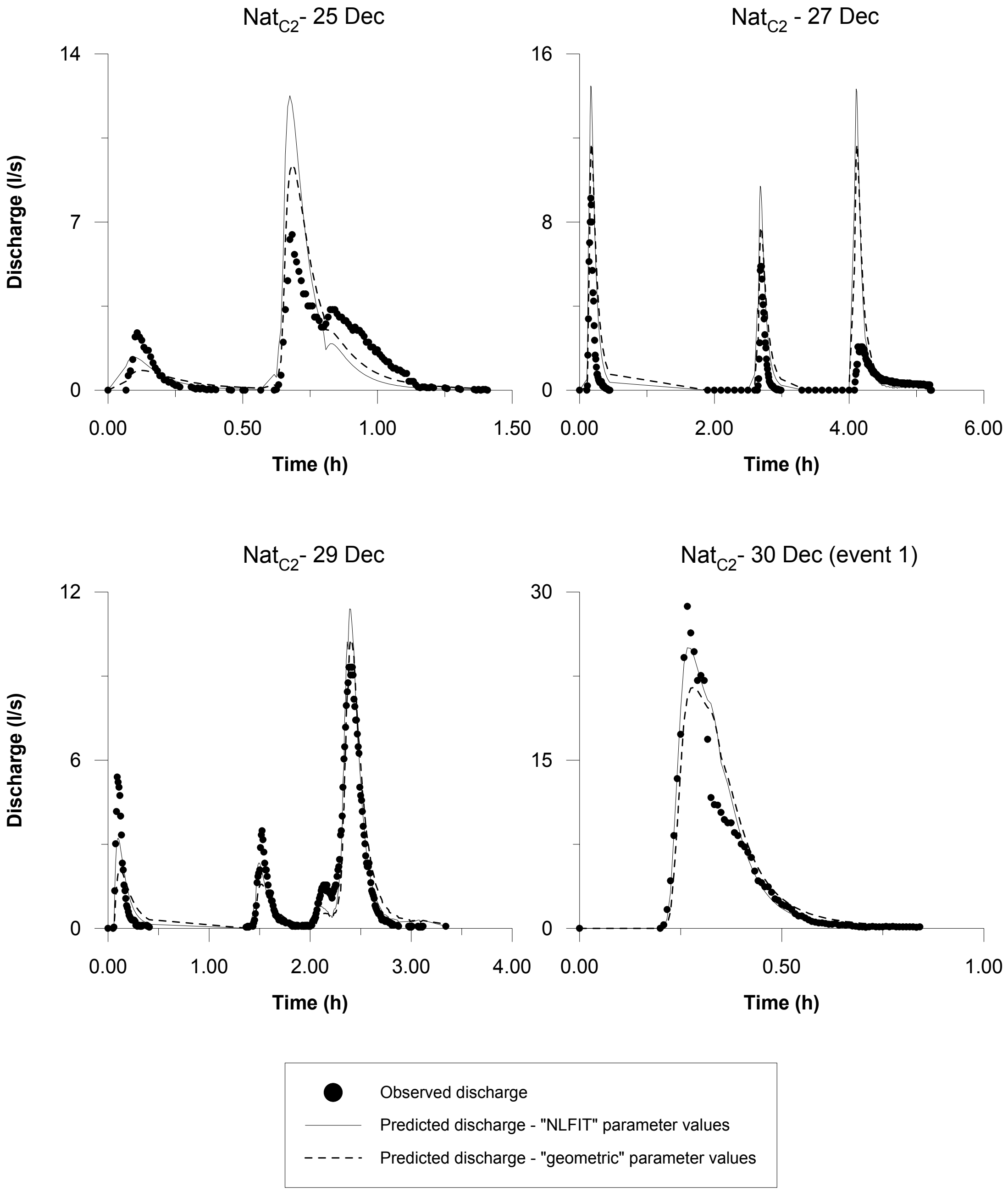
Nat$_{C2}$- 25 Dec
Nat$_{C2}$ - 27 Dec
Nat$_{C2}$- 29 Dec
Nat$_{C2}$- 30 Dec (event 1)
Discharge (l/s)
Time (h)
0
7
14
8
16
6
12
15
30
0.00
0.50
1.00
1.50
2.00
4.00
6.00
3.00
Observed discharge
Predicted discharge - "NLFIT" parameter values
Predicted discharge - "geometric" parameter values

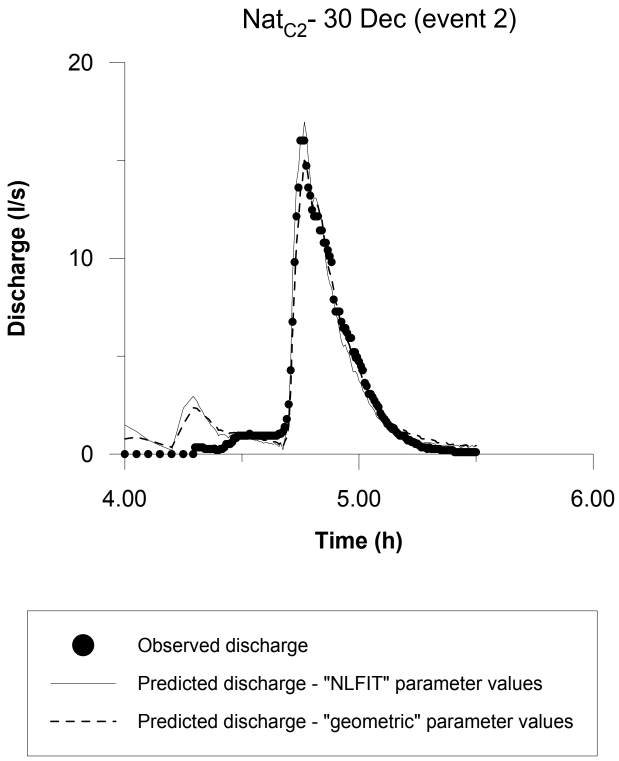
Nat$_{C2}$- 30 Dec (event 2)
20
10
0
Discharge (l/s)
4.00
5.00
6.00
Time (h)
Observed discharge
Predicted discharge - "NLFIT" parameter values
Predicted discharge - "geometric" parameter values

Appendix E — Availability of monitoring data for the rainfall events at Nat_C

Site	Date	Time – start	Time - finish	Rainfall data	Runoff data	Suspended sediment data	Bedload data
Mica	24/12/93	17:25	18:05	X	X	X	X
	25/12/93	17:50	18:15	√	√	X	X
		18:30	19:00	√	√	X	(T)
	27/12/93	11:10	12:00	√	√	(P_s)	X
		13:45	14:25	√	√	√	X
		15:10	16:00	√	√	√	(T)
	29/12/93	18:50	19:15	√	√	X	X
		20:15	20:50	√	√	X	X
		20:50	22:00	√	√	#	(T)
	30/12/93	13:00	14:00	X	X	√	√
		17:20	18:45	√	√	√	√
	31/12/93	17:00	18:00	√	(P_r)	√	√
Quartz	24/12/93	17:25	18:05	√	√	X	X
	25/12/93	17:50	18:25	√	√	X	X
		18:30	19:20	√	√	X	(T)
	27/12/93	11:10	11:40	√	√	√	X
		13:40	14:10	√	√	(P_s)	X
		15:10	16:25	√	√	√	(T)
	29/12/93	18:50	19:15	√	√	X	X
		20:15	20:45	√	√	X	X
		20:45	22:00	√	√	#	(T)
	30/12/93	13:05	14:00	√	√	√	√
		17:00	19:00	√	√	√	√
	31/12/93	17:00	18:00	X	X	X	X

(T) Bedload collected for the whole day

Insufficient no. of samples taken

(P_s) Suspended sediment data predicted using equation 3.23

(P_r) Runoff data predicted using fitted DISTFW model parameter values (table 3.4)

Appendix F — Nat_{C1} monitoring data — 31 Dec